

Biochemical and genetic responses of cuticular mutants

Inaugural-Dissertation

zur

Erlangung des Doktorgrades

der Mathematisch-Naturwissenschaftlichen Fakultät

der Universität zu Köln

vorgelegt von

Derry Frédérique Voisin
(Aus Paris, Frankreich)

Hundt Druck GmbH, Köln

Köln, 2009

**Diese Arbeit wurde am Max-Planck-Institut für Züchtungsforschung
in Köln in der Abteilung Molekulare Pflanzengenetik durchgeführt.**

Tag der mündlichen Prüfung: 13.02.2008

Prüfungsvorsitzender: Prof. Dr. Ulf-Ingo Flügge

Berichterstatter: Prof. Dr. Heinz Saedler
Prof. Dr. Martin Hülskamp
Prof. Dr. Lukas Schreiber

Table of contents

1.	INTRODUCTION	1
1.1.	STEPS IN BIOSYNTHESIS OF CUTICULAR LIPIDS AND KNOWN MUTANTS	3
1.2.	CUTICULAR MUTANTS USED IN THIS STUDY.....	7
1.2.1.	<i>The fiddlehead (fdh) mutant</i>	7
1.2.2.	<i>The lacerata (lcr) mutant</i>	9
1.2.3.	<i>The bodyguard (bdg) mutant</i>	10
1.2.4.	<i>The htm mutant</i>	11
1.3.	CANDIDATE GENES PUTATIVELY INVOLVED IN CUTICLE BIOSYNTHESIS	11
1.3.1.	<i>LEAKO, coding for an epoxide hydrolase</i>	11
1.3.2.	<i>ALDHs, encoding fatty acid aldehyde dehydrogenases</i>	13
1.3.3.	<i>HYD4, an homologue of BDG</i>	14
1.4.	AIM OF THE WORK.....	15
2.	MATERIAL AND METHODS	17
2.1	PLANT LINES	17
2.2	PLANT GROWTH CONDITIONS.....	18
2.2.1.	<i>Greenhouse conditions</i>	18
2.2.2.	<i>Growth chamber</i>	18
2.2.3.	<i>In vitro conditions</i>	18
2.3	BACTERIA STRAINS	19
2.3.1.	<i>Escherichia coli (E.coli)</i>	19
2.3.2.	<i>Agrobacterium tumefaciens (A.tumefaciens)</i>	19
2.4.	BACTERIA GROWTH CONDITIONS	19
2.4.1.	<i>Media composition</i>	19
2.4.2.	<i>Media supplementation for LacZ and antibiotic selection</i>	19
2.5	ELECTRO-COMPETENT BACTERIA TRANSFORMATION	20
2.6	DNA PURIFICATION METHODS	20
2.6.1.	<i>Purification of plant DNA</i>	20
2.6.2.	<i>Confirmation of insertion lines</i>	20
2.7	RNA PURIFICATION FOR LINE CHECKING	21
2.8	EVALUATION OF DNA AND RNA CONCENTRATION AND PURITY	21
2.9	AMPLIFICATION BY PCR AND RT-PCR.....	21
2.10	STAINING WITH TOLUIDINE BLUE SOLUTION.....	22
2.11	CHLOROPHYLL EXTRACTION	22
2.12	SILIQUES OBSERVATION	23
2.13	BOUND LIPID, WAX AND SEED COAT ANALYSES.....	23
2.13.1.	<i>Bound lipid analysis</i>	23
2.13.2.	<i>Wax analysis</i>	24
2.13.3.	<i>Lcr and bdg seeds for seed coat analysis</i>	25
2.13.4.	<i>htm inflorescences for bound lipid analysis and wax analysis</i>	25
2.13.5.	<i>Quantitative and Qualitative analysis by Gas-Chromatography (GC) and GC-Mass Spectrometry (GC-MS) analysis</i>	26
2.13.6.	<i>Reading the runs</i>	27
2.14	ROOT OBSERVATIONS.....	27
2.14.1.	<i>Growth evaluation</i>	27
2.14.2.	<i>Gravitropism experiment</i>	28
2.14.3.	<i>Wave experiment</i>	28
2.14.4.	<i>Water stress experiment</i>	28
2.14.5.	<i>Arabidopsis transformation by floral dipping</i>	29
2.15	<i>HTM PROMOTER AND GENE FUSIONS</i>	29
2.15.1.	<i>Promoter constructs</i>	29

2.15.2.	<i>Protein constructs</i>	30
2.16	MICROSCOPIC OBSERVATIONS.....	31
2.16.1.	<i>Light microscopy</i>	31
2.16.2.	<i>Scanning electron microscopy (SEM)</i>	31
2.16.3.	<i>Fluorescence microscopy</i>	32
2.17	HETEROLOGOUS EXPRESSION OF <i>HTM</i>	33
2.17.1.	<i>Cloning the HTM cDNA in pASK-IBA vectors: Creating a Strep-tagged version of the HTM protein</i>	33
2.17.2.	<i>Complementation assay in bacteria</i>	37
2.18	COMPLEMENTATION OF ARABIDOPSIS <i>FDH</i> MUTANT BY <i>HvFDH</i>	37
2.18.1.	<i>Plant transformation and segregation analysis</i>	37
2.18.2.	<i>Genotyping of plants</i>	38
2.19	MICROARRAY ANALYSIS.....	39
2.19.1.	<i>Plant, growth conditions and hybridization to Affymetrix ATH1 chips</i>	39
2.19.2.	<i>Defining the list of mis-regulated genes in our mutants</i>	40
2.19.3.	<i>Confirmation of our microarray results by semi-quantitative RT-PCR</i>	41
2.20	PHYLOGENIC ANALYSIS.....	41
2.20.1.	<i>BDG and its family</i>	41
2.20.2.	<i>Barley FDH, Antirrhinum FDH and the Arabidopsis FAE family</i>	42
3.	RESULTS	44
3.1.	<i>LACERATA, BODYGUARD AND FIDDLEHEAD</i> MUTANTS.....	44
3.1.1.	<i>Cuticle properties of lcr, bdg and fdh mutants are altered</i>	44
3.1.2.	<i>Under in vitro culture conditions, lcr and bdg show epidermal deficiencies and enhance root growth</i>	45
3.1.3.	<i>The cuticle composition of lcr and fdh leaves is altered</i>	51
3.1.4.	<i>Lcr and bdg mutations have little influence on seed coat composition</i>	55
3.1.5.	<i>Lcr and fdh mutations influence wax composition</i>	60
3.1.6.	<i>The wax deposition is altered in lcr and fdh mutants</i>	64
3.1.7.	<i>Overaccumulation of wax in bdg corresponds to a genetic up-regulation</i>	65
3.1.8.	<i>Bdg, lcr and fdh mutations lead to major changes in gene regulation</i>	67
3.1.9.	<i>Complementation of the Arabidopsis fdh mutant by the barley FDH allele</i>	78
3-2.	<i>HTM (ATXGXXXXX), A PUTATIVE ACYL-TRANSFERASE</i>	80
3-2.1.	<i>The htm mutant</i>	81
3-2.2.	<i>HTM expression in aerial organs</i>	87
3-2.3.	<i>Heterologous expression in E.coli</i>	91
3-2.4.	<i>Heterologous complementation assay in E.coli</i>	92
3.3	INVESTIGATION ON PUTATIVE CUTICULAR GENES.....	93
3.3.1.	<i>Characterisation of insertion lines in the LEAKO gene encoding a putative leukotrien-A4-hydrolase-like protein</i>	93
3.3.2.	<i>Aldehyde-dehydrogenases putatively involved in cuticle synthesis</i>	93
3.3.3.	<i>HYD4, a putative α/β hydrolase-fold enzyme closely related to BDG</i>	95
4.	DISCUSSION	102
4.1	THE <i>FDH, LCR</i> AND <i>BDG</i> MUTANTS.....	102
4.1.1.	<i>A role of the cell wall matrix in the permeability to small hydrophilic molecules</i> ..	102
4.1.2.	<i>Lcr and bdg mutations have an impact on epidermis maintenance</i>	103
4.1.3.	<i>A defective cuticle triggers a compensatory response at the cuticular level</i>	105
4.1.4.	<i>Bdg and lcr mutations do not have a strong influence on seed coat composition</i> ..	108
4.1.5.	<i>A poor cuticular insulation triggers a compensatory response at the transcriptional level</i>	109
4.1.6.	<i>FDH function may be conserved throughout plant evolution</i>	114
4.2	THE <i>HTM</i> MUTANT.....	115
4.2.1.	<i>Expression pattern of HTM</i>	115
4.2.3.	<i>Is HTM directly implicated in the cuticle biosynthesis?</i>	116

4.2.4.	<i>Is HTM an acyltransferase?</i>	118
4.3	INVESTIGATION ON CANDIDATE GENES	120
4.3.1.	<i>The function of the LEAKO gene remains unknown</i>	120
4.3.2.	<i>The putative impact of ALDH5 needs further confirmation.</i>	122
4.3.3.	<i>Is the hyd4-2 insertion responsible for the phenotype of the hyd4-2 mutant?</i>	123
5.	SUMMARY	126
6.	ZUSAMMENFASSUNG	127
7.1	APPENDIX A. LIST OF PRIMERS USED IN THIS STUDY	128
7.2	APPENDIX B. PRC MIXES AND PROGRAMMES.....	132
7.3	APPENDIX C. BOUND LIPID ANALYSIS: WEIGHT-AREA CONVERSION.....	134
7.4	APPENDIX D. MAP OF THE VECTORS USED TO BUILD PROMOTER FUSION CONSTRUCTS.	136
7.5	APPENDIX E. MAP OF THE VECTORS USED TO BUILD PROTEIN FUSION CONSTRUCTS.....	137
7.6	APPENDIX F. CELL WALL BOUND LIPID ANALYSES OF LCR AND FDH MUTANTS SUMMARY TABLE.....	138
7.7	APPENDIX G. LIST OF COMMONLY MIS-REGULATED GENES IN THE THREE CUTICULAR MUTANTS	139
7.8	APPENDIX H. THE ABC TRANSPORTER FAMILY IN ARABIDOPSIS.	141
7.10	APPENDIX I. THE AP2/ERFEB FAMILY IN ARABIDOPSIS.....	142
7.	REFERENCES	143
8.	ACKNOWLEDGMENTS	155
9.	LEBENSLAUF	156
10.	EIDESSTATTLICHE ERKLÄRUNG	157

1. Introduction

As they left water and conquered dry land, plants evolved a protective interface: the cuticle. Cuticle is deposited on the surface of non-woody aerial organs from plants and, is both, a barrier and a sensitive surface. It protects plants against abiotic stresses such as water loss (Kerstiens, 1996; Riederer and Schreiber, 2001) or UV irradiation (Solovchenko and Merzlyak, 2003) and, signals the presence of pathogens (Schweizer et al., 1996b). or herbivores (Kerstiens, 1996) to the plants. In the last decades data illustrating that cuticle is also essential in plant development, maintenance of organ integrity and organ delimitation have accumulated (Lolle et al., 1992; Sieber et al., 2000).

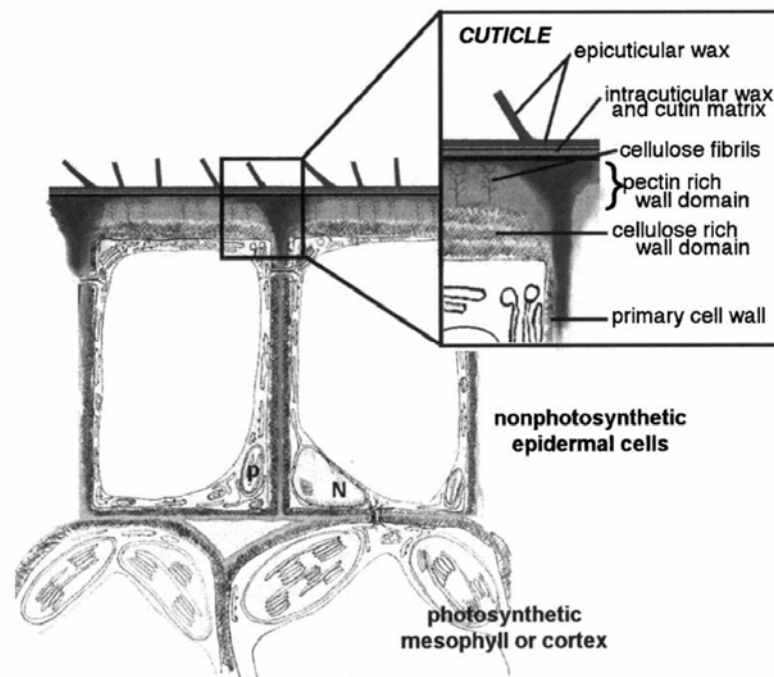


Figure 1. Diagram representing epidermal cells from aerial organs and their outer covering. Cutin and wax are deposited on the surface of the outer cell wall (from (Kunst and Samuels, 2003).

Cuticle comprises cutin and wax, both principally composed of fatty acid derivatives. It also sometimes contains a non hydrolysable fraction called cutan (Heredia, 2003). The cutin biopolymer is cross-linked to the outer cell wall of the epidermal cells; wax which is tangled on its external face (Figure. 1), enhances waterproof properties of the cuticle (Riederer and Schreiber, 2001). The cutin composition has been investigated in different species since 1970s. Kolattukudy and co-workers conducted pioneer biochemical experiments, and by means of gas-chromatography

coupled with mass-spectrometry, determined the composition of cutin polymers synthesized by diverse plant species (Espelie et al., 1979; Kolattukudy, 1980). Based on their results and on chemical principles, the authors suggested the first model of the cutin biosynthetic pathway (Kolattukudy, 1981).

Classically, cutin is mainly composed of aliphatic monomers with 16-18 carbons: C16 and C18 ω -hydroxy fatty acids, and their mid-chain hydroxy or epoxy derivatives. In addition, glycerol and little amount of phenolic compounds are typically found (Heredia, 2003). It is thought that cutin monomers are linked together by ester bonds occurring between their hydroxy and carboxy groups or by intermediating glycerol molecules. Cutan is made of cuticular lipids linked by ether bound and is intermixed with cutin (Villena et al., 1999).

The epicuticular waxes which are embedded in the cutin polyester, can be removed by immersion of plant organs in an apolar organic solvent (Post-Beittenmiller, 1998). The analysis of plant waxes revealed that they mainly consist of very long chain fatty acids (VLCFAs) with a chain length ranging from 20 to 34 carbons and of their derivatives: aldehydes, alkanes, secondary alcohols, ketones, primary alcohols and esters (Kunst and Samuels, 2003). The wax amount depends on the organ, the developmental stage and the environmental conditions: for instance, in *Arabidopsis* of the Landsberg *erecta* ecotype, the wax load deposited on stems is roughly 25 times greater than the leaf wax load (Jenks et al., 1995), and plants grown in dry conditions deposit more wax (Cameron et al., 2006). Depending on the analysed organ, the wax composition may differ: for instance the wax from *Arabidopsis* leaves only contains traces of esters and ketones that are abundant in waxes from stems (Jenks et al., 1995).

The determination of cuticle composition has constituted quite a challenge and allowed in many plant species, including the model plant *Arabidopsis thaliana*, the investigation on its biosynthesis (Croteau and Kolattukudy, 1975; Heredia et al., 2000; Gormann et al., 2004). As a matter of fact, the presence of a regular layer of cutin and wax outside the epidermal cells implicates biosynthesis, exportation of their respective monomers, and, in the case of cutin, also implies polymerisation by

esterification. Biosynthesis, exportation of cuticle materials and setting up of cuticle layer have been the focus of many groups for the last decades.

Recent publications described the cutin composition of the model plant *Arabidopsis thaliana* (Bonaventure et al., 2004; Xiao et al., 2004; Franke et al., 2005), and found that it is not typical. In *A. thaliana*, α,ω -diacids predominate and less mid-chain hydroxy and no epoxy compounds can be found (Bonaventure et al., 2004; Xiao et al., 2004; Franke et al., 2005). Thus, the composition of Arabidopsis cutin is more similar to that of suberin, a biopolymer, for instance, synthesised in roots (Franke et al., 2005), vascular bundles and in response to wounding and pathogen attack (Nawrath, 2002), than to conventional cutin.

1.1. Steps in biosynthesis of cuticular lipids and known mutants

C16 and C18 fatty acids are produced and exported from chloroplasts where the *de novo* biosynthesis of fatty acid takes place (reviewed in (Ohlrogge and Browse, 1995). Subsequent elongation leading to the formation of very-long-chain fatty acids (VLCFA), which have more than 18 carbons, is performed by a plant specific elongation complex, termed elongase (von Wettstein-Knowles, 1982), located in the endoplasmic reticulum (E.R.). Each elongation cycle comprising condensation, reduction, dehydration and another reduction step, leads to the addition of two carbons to the substrate (Fehling and Mukherjee, 1991). VLCFAs produced by elongation of C16 and C18 fatty acids may be channelled towards the cutin or the wax biosynthesis pathways (Figure. 2).

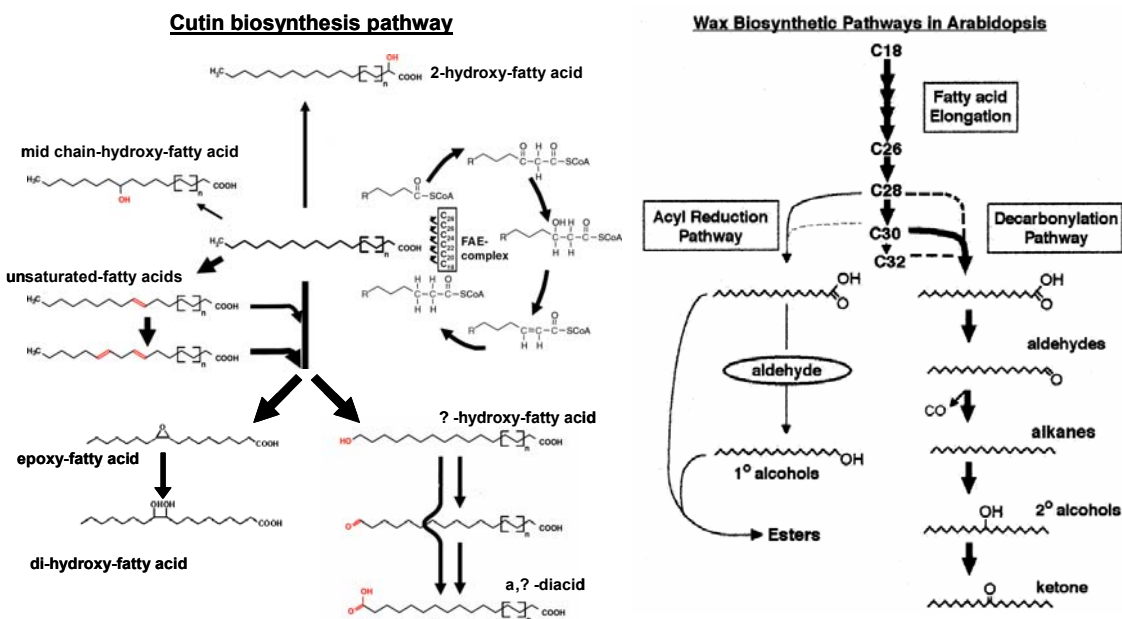


Figure 2. Putative biosynthesis pathways of wax and cutin monomers (adapted from (Franke et al., 2005); (Millar et al., 1999)). FAE: fatty acid elongase complex.

On one hand, C16 and C18 fatty acids can be oxidised to form cutin precursors. Their ω -carbon may first be hydroxylated to form ω -hydroxy fatty acids, and after a second oxidation step, α,ω -diacids may be formed (Figure. 2). Else, fatty acids may be hydroxylated on their second carbon to produce 2-hydroxy fatty acids. The different monomers may also undergo one or more desaturation steps leading to the formation of unsaturated precursors. A share of the various precursors undergo mid-chain hydroxylation leading to the production of mid-chain hydroxy derivatives; in *Arabidopsis* leaves, these compounds are in minor amounts but more present in stem and inflorescence cutin. In other species, where epoxides and mid-chain di-hydroxy monomers are abundant, epoxydation and hydrolisation of epoxide groups must be taking place (Figure. 2).

On the other hand, VLCFAs released by the elongase complex may enter one of the two putative branches of the wax biosynthesis pathway (Kunst and Samuels, 2003). One of them, the acyl reduction pathway leads to the production of primary alcohols and esters. An acylreductase reduces the VLCFAs into VLC primary alcohols, a part of them may subsequently be used as substrates by acyltransferases to synthesise esters. The reduction of VLCFAs leads to the formation of VLC aldehyde intermediates which are not released by the acylreductase but directly processed into

primary alcohols. Aldehydes, finally found in waxes, are the first product of the putative decarbonylation pathway; other acylreductases lead to their production and their release. Some aldehydes are processed by aldehyde dehydrogenases which catalyse the formation of alkanes by cleaving off the aldehyde group of the VLC aldehyde and thus releasing carbon monoxide and alkane molecules with an odd number of carbons. VLC secondary alcohols and ketones derive from the oxidation of alkanes and also have an odd number of carbons.

A key to understand cuticle biosynthesis may reside in mutants with a defective cuticle, hereafter referred to as cuticular mutants. A mutation leading to an impaired cuticle may be manifested by a change in wax or cutin composition, thus revealing the enzymatic function of the disrupted protein (Yephremov and Schreiber, 2005).

Cutin, wax or both can be affected in cuticular mutants. Many *Arabidopsis thaliana* cuticular mutants have now been described and, indeed in some cases, a direct correlation between the mutation and the phenotype could be established. For instance, the *hothead* (*hth*) mutant is characterised by organ fusion in the inflorescences (Krolikowski et al., 2003; Kurdyukov et al., 2006a) and appear to accumulate less α,ω -diacids and more ω -hydroxy fatty acids than wild-type plants (Figure. 2). It follows that HTH is probably able to oxidise ω -hydroxy fatty acids into α,ω -diacids and thus is a ω -alcohol dehydrogenase (Figure.2) (Kurdyukov et al., 2006a). Another example is the (*eceriferum4*) *cer4* mutant in which wax composition is altered (Rowland et al., 2006). Waxes of this mutant contain less primary alcohols (Figure. 2) and the heterologous expression of CER4 in yeast leads to the accumulation of C24 and C26 primary alcohols. CER4 is very likely to encode for an alcohol-forming fatty acyl-coenzyme A reductase (FAR) involved in the acyl reduction pathway of the wax biosynthesis (Rowland et al., 2006). Some cuticular mutants e.g., *eceriferum5* (*cer5/wbc12*) and *desperado* (*dso/wbc11*), are affected in cutin and wax exportation (Pighin et al., 2004; Bird et al., 2007; Panikashvili et al., 2007). *Cer5/wbc12* deposits less wax on its outer surface and *dso/wbc11* less cutin. Inclusions containing bundles of lipidic fibrils are present in the cytoplasm of both mutants (Pighin et al., 2004; Panikashvili et al., 2007). This suggests that CER5/WBC12 and DSO/WBC11 which are membrane transporters of the WBC family, are involved in the export of wax and cutin precursors.

Yet not only cuticle may be affected by a defect in the production or the export of VLCFAs, the composition of other biopolymers such as seed coat, suberin and pollen coat may also be modified and so, provide information about enzymatic functions. As a matter of fact, all biological entity comprising VLCFAs may potentially bear the mark of a biosynthetic, exportation or polymerisation defect, for instance a problem in the elongation of VLCFAs may show in the storage lipid composition of the seeds which contain VLCFAs with a chain length of 20 and 22 (O'Neill et al., 2003).

In plants, β -ketoacyl-CoA synthase of the FATTY ACID ELONGATION (FAE) family catalyse the first step of the elongation process, namely the condensation (Kunst et al., 1992). In Arabidopsis, this multigenic family is composed of 21 members and 11 of them are probably epidermis specific according to microarray data (Suh et al., 2005). FAE1 was the first enzyme of this family to be described: the *FAE1* gene is expressed during seed development and, because of its disruption, storage lipids with a chain longer than C18 are missing in the *fae1* mutant (Kunst et al., 1992; James et al., 1995; Millar and Kunst, 1997; Suh et al., 2005). Among the homologues of the *FAE1* gene, *CUT1/CER6*, *KCS1* and *FDH* are expressed in the epidermis (Millar et al., 1999; Todd et al., 1999; Yephremov et al., 1999). The suppression of the *CUT1* gene leads to a high decrease in wax levels and a there is a shift in monomer composition towards the C22 and C24 compounds (Millar et al., 1999). Thus this enzyme is very likely to catalyse the elongation of C24 fatty acids.

Genes involved in the regulation of cutin and wax biosynthesis rather than directly in the biosynthesis and exportation may also trigger a cuticular phenotype. For instance, the overexpression of the ERF/AP2 transcription factor WIN1/SHN1 leads to the overproduction of wax (Aharoni et al., 2004; Broun et al., 2004) and cutin precursors (Kannangara et al., 2007).

Some genes which function do not seem to be associated with the biosynthesis such as *ALE1* (Tanaka et al., 2001), *CRINKLY4* (Becraft et al., 1996) or *PASTICCINO/PEPINO* (Bellec et al., 2002; Haberer et al., 2002) may also trigger a cuticular phenotype. For instance, mutations in the L1 specific membrane receptor-kinase *CRINKLY4* lead to a loss of cell fate, often to cell fusion and to cell

dedifferentiation and, consequently, to a lack of cuticle both, in maize and *Arabidopsis* (Becraft et al., 1996; Tanaka et al., 2002; Watanabe et al., 2004).

Enzymes involved in cuticle polymerisation are not known, however the heterologous expression of a fungal cutinase, secreted in the extracellular space, in *Arabidopsis thaliana* transgenic plants leads to cuticular damage (Sieber et al., 2000), probably reminiscent of polymerisation absence. These transgenic plants (cutinase expressing: CUTE) and some cuticular mutants have recently been reported more resistant to some pathogens than their WT counterpart (Schnurr et al., 2004; Bessire et al., 2007; Chassot et al., 2007). Although it had been shown earlier that cutin monomers could protect plants against pathogens by activating the production of ethylene and induction of defence related genes (Schweizer et al., 1996a; Schweizer et al., 1996b) this was quite unexpected, puzzling, as cuticle is usually seen as a barrier, the breakdown of which is expected to lead to a defect rather than to an advantage.

1.2. Cuticular mutants used in this study

This work was performed with *Arabidopsis thaliana* mutants.

1.2.1. The *fiddlehead* (*fdh*) mutant

The *fdh* mutant was first identified in the progeny of an EMS-mutagenised population, and it displays ectopic organ fusions between rosette leaves but more frequently affects floral organs and inflorescences (Figure. 3) (Lolle et al., 1992). On leaves of *fdh* mutants, about half of the trichomes are missing; this is probably due to a defect in trichome initiation (Yephremov et al., 1999). In this mutant, organ fusion within flower involves the four whorls, consequently, petals are usually stunted, reaching only 25% of the expected height, and anthers are trapped, the receptive stigma remains out of their reach leading to sterility. Fusion between floral buds does not prevent further elongation of pedicels and stems, and leads to the distortion of the inflorescences (Figure. 3). Fusion involves only epidermal cells and starts after organogenesis when sepals have grown into contact and enclose the floral buds. In the fusion zones, supplementary cells may bridge the organs or, if the organs have grown in parallel, a junction zone lacking the surface characteristics of both joined organs

can be observed. Along the suture zone, the cells do not dedifferentiate but lose their organ specific surface features; when two sepals are involved, only a couple of cell rows are affected (Lolle et al., 1992). It was proposed that upon physical contact of carpels, a messenger, probably water soluble morphogenetic factor(s) is able to fortuitously move through cuticle travel from one organ to the other, leading in response and postgenital fusion (Siegel and Verbeke, 1989). In the fusion zones, in *fdh*, the cuticle layer is still present, no plasmodesmata and no cytoplasmic fusion have been observed. Although ectopic organ fusion in this mutant involves “only” cell wall-to-cell wall “contact” (Lolle et al., 1992), the adhesion between neighbouring organs is strong enough to lead to organ tearing during plant growth (Figure. 4) (Yephremov et al., 1999).

Fdh leaves and non-reproductive shoot organs support pollen germination, mimicking WT pistil, manage to discriminate between pollen grains originating from different species. *Fdh* tissue seems to acquire the possibility to fuse and then to support pollen germination sequentially as pollen tends to germinate better on older *fdh* leaves (Lolle and Cheung, 1993). Although the cuticle is present on the surface of *fdh* aerial organs, the sieving properties of *fdh* tissue are modified: chlorophyll diffuses quicker out of *fdh* leaves than WT leaves; on the surfaces of *fdh* leaves, a somewhat greater quantity of protein could be found (Lolle et al., 1997).

The *FDH* gene was cloned and found to code for β -ketoacyl-CoA synthase with homology to the FAE family (Yephremov et al., 1999; Pruitt et al., 2000). *FDH* is exclusively expressed in the epidermis of young organs (leaves, stem, floral meristems, primordial, petals, stamens, stigma, stigmatic papillae, at the margin of ovules and around the embryo sac) (Yephremov et al., 1999). Spraying with flufenacet, benfuresate and other herbicides of their groups phenocopies the *fdh* mutant (Lechelt-Kunze et al., 2003). These herbicides had previously been linked to a block in the very long chain fatty acid biosynthesis (Kolattukudy and Brown, 1974; Boerger and Matthes, 2002). Not only Arabidopsis responds to these herbicides by organ fusion, but monocots develop “*fdh* like bows” (Lechelt-Kunze et al., 2003). The *Anthirrinum majus* *FDH* gene was able to complement the *Arabidopsis thaliana* *fdh* mutant, and spraying with alachlor (which belongs to the same herbicide group as the flufenacet), triggers the apparition of *fdh* like symptoms on new organs of WT *A. majus* plants

(Efremova et al., 2004). Thus the *Arabidopsis FDH* and *Antirrhinum FDH (AFI)* may be functional equivalents. They share an identical intron-exon pattern, which is unique in the FAE family. During carpel fusion, in *A. majus* and *Arabidopsis*, the down-regulation of the *FDH* gene was observed, probably, to allow cell-cell interactions required during this process. On the other hand the up-regulation of the *FDH* gene occurs in dehiscent anthers in *A. thaliana*. This illustrates the importance of *FDH* in adhesion properties.

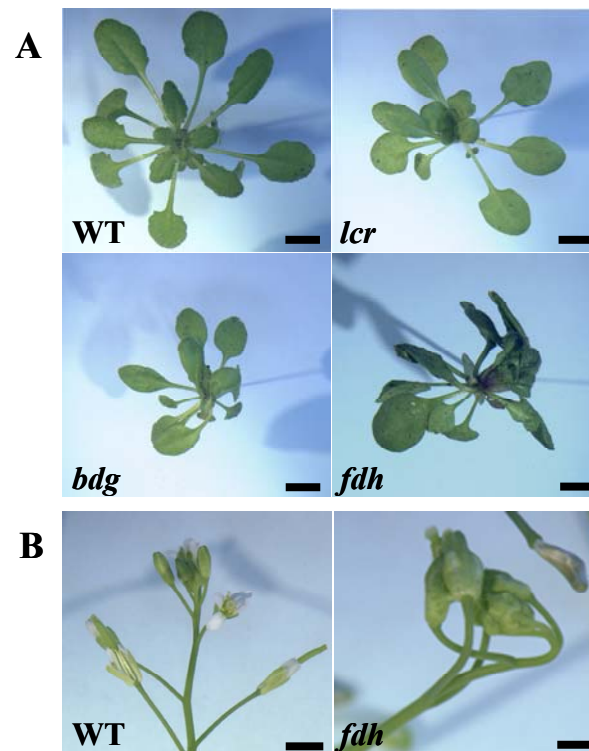


Figure 3. *Lacerata (lcr)*, *bodyguard (bdg)* and *fiddlehaed (fdh)* are cuticular mutants, which develop ectopic organ fusions. (A) WT-Col-0, *lcr*, *bdg* and *lcr* mutants at the rosette stage; plants were five weeks and a half old (grown under short day conditions). (B) WT and *fdh* inflorescences were five weeks old (plants grown under long day conditions). Bar: 2 mm.

1.2.2. The *lacerata (lcr)* mutant

A mutation in the *LACERATA (LCR)* gene has harmful consequences on plant development: mutant plants have reduced growth, deformed leaves, which support pollen germination, show a bushy appearance and a delayed senescence. Trichome development is also affected by the *lcr* mutation, which seems to delay and reduce trichome initiation. A major feature of this mutant is the presence of strong ectopic organ fusion between rosette leaves, that may lead to organ rupture (Figure. 4). Organ fusion in this mutant does not involve cytoplasmic union but allows nutrient diffusion

as detached organs survive for some time after tearing (Figure. 4). The *LCR* gene codes for the CYP86A8 enzyme, a member of the CYP86 clan in the large family of P450s proteins (Benveniste et al., 2006). In vitro assays and sequence homology are supporting the fact that LCR is an ω -fatty acid hydroxylase (Welleesen et al., 2001), which catalyses the hydroxylation of cutin fatty monomers at their ω position (Figure. 2).

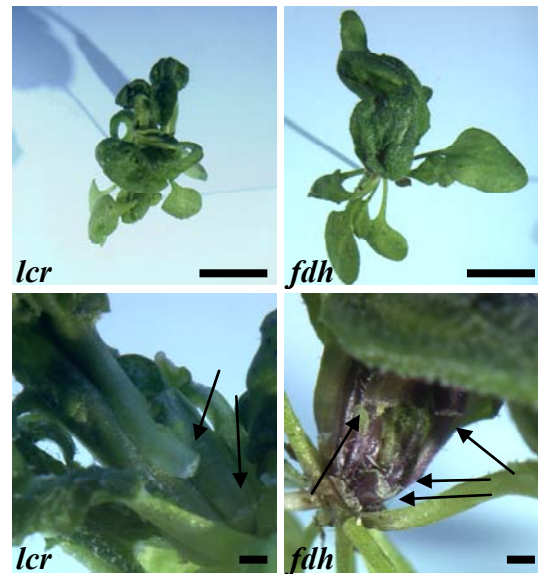


Figure 4. Ectopic organ fusions are strong enough to trigger organ rupture. Cuticle permeability is sufficient to allow irrigation and alimentation of the fully detached organs which remain green. Bar: overview: 1 cm. zoom: 1 mm. Plants were five weeks and half weeks old (grown under short day conditions).

1.2.3. The *bodyguard* (*bdg*) mutant

As I joined the project, the *BODYGUARD* (*BDG*) gene had been cloned in our lab and the analysis of the *bdg* mutant had revealed an overall increase in wax and cutin monomers. This mutant had been noticed for its smaller size and a bushy appearance during a screen of En/Spm transposon-mutagenised *Arabidopsis* plants. Characterised by deformed leaves, which are often joined in a fusion, organ tearing due to organ fusion, *bdg* also displays a trichome phenotype: less mature trichomes can be observed on developing leaves because they tend to progressively die. The increase in cuticle permeability of this mutant had been illustrated by a pollen germination test. Observation of *bdg* tissue under TEM had revealed the presence of a discontinuous cutin covering, inclusion of cutin material in the cell wall, and shown that, in this mutant, the ectopic organ fusion do not implicate cytoplasm union either. *In situ*

hybridisation and immunolocalisation assays had shown that the *BDG* gene is epidermis specific and that the BDG protein is localised to the outer cell wall. *In silico* analyses had revealed that the BDG enzyme belongs to the α/β hydrolase-fold super family and that it has four closely related homologues. Taken together these results suggested that BDG may be involved in the cross-linking of cuticle and cell wall or else in the polymerisation of cutin (Kurdyukov et al., 2006b).

1.2.4. The *htm* mutant

Using toluidine blue as a staining test for permeability increase of the cuticle, Machida and co-workers identified new mutants with a deficient cuticle covering (Tanaka et al., 2004). Toluidine blue is a dye binding to anionic groups in the cell wall that are not accessible in the presence of a wild-type cuticle. However if cuticle is discontinuous, the cell wall constituents are accessible to the dye, which stains tissue dark blue. Among the mutants displaying a dark blue coloration, was the *htm* mutant. Machida and co-workers cloned the *HTM* gene and identified further mutant alleles of this gene. All mutants have similar phenotype (H.Tanaka, personal communication), namely post-genital organ fusion in flowers.

1.3. Candidate genes putatively involved in cuticle biosynthesis

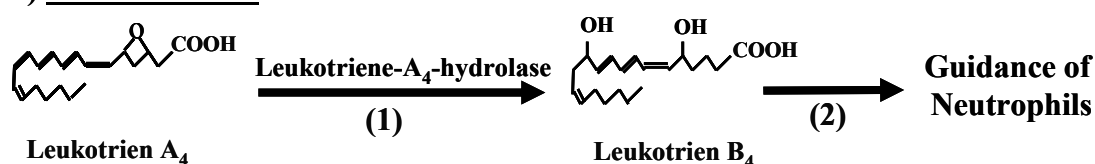
1.3.1. *LEAKO*, coding for an epoxide hydrolase

Epoxy- and mid-chain hydroxyl fatty acids are present in high amounts in cutin from many species, like in *Hedera Helix*, *Clivia miniata*, *Ficus elastica*, for instance (Riederer and Schonherr, 1988; Blee and Schuber, 1993; Graca et al., 2002) Fatty acid components from cutin are linked together by ester bonds occurring between their hydroxy and carboxy groups or involving glycerol (Graca et al., 2002). The cross-linking of the different monomers gives its structure to the cutin (Benitez et al., 2004). When this work started, the cuticle composition of *Arabidopsis thaliana* was not known, we then speculated that in *Arabidopsis*, mid-chain hydroxy groups could take part in the reticulation of the cutin layer, as for instance in *Clivia miniata* and *Ficus elastica* leaves (Schönherr, 2000). In plants, enzymes able to generate mid-chain hydroxy groups are not known whereas in human immune response, the leukotrien-

A₄-hydrolase is able to catalyse the hydrolysis of epoxide rings, forming two mid-chain alcohol functions (Radmark et al., 1984; Shimizu et al., 1984).

During the human immune response, arachidonic acid, a C₂₀ fatty acid, is first released from the plasma membrane of polymorphonuclear leukocytes and then step by step converted into leukotrien-A₄ (LTA₄) (Radmark et al., 1984; Shimizu et al., 1984). This fatty acid derivative is a substrate of a specific soluble lipid hydrolase, the leukotrien-A₄ hydrolase, which converts LTA₄ into leukotrien B₄ (LTB₄), a chemoattractant molecule (Radmark et al., 1984) (Figure. 5). The latter plays an important role in driving the neutrophils during inflammation and hypersensitivity reactions.

a) Role in humans



b) Putative role in plants

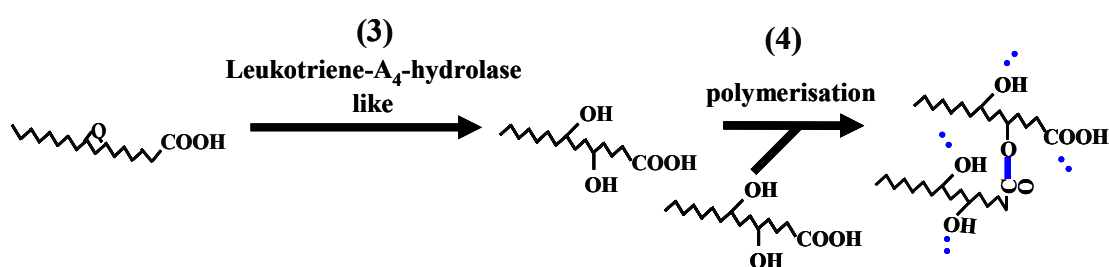


Figure 5. Hydrolysis of epoxide rings in humans and hypothetically in planta. a) the leukotrien-A₄ is activated into leukotrien-B₄ by an epoxide hydrolase, the leukotrien-A₄-hydrolase (1). Leukotrien-B₄ molecules can then attract neutrocytes at the inflammation place and guide them through the immune response process (2). b) Despite the presence of many unsaturations, and consequently the altered folding of the leukotrien-A₄ substrate, a similar process may be catalyzed *in planta* by a homologous enzyme of the human leukotrien-A₄-hydrolase (3). The di-hydroxy monomers could then be linked by esterification, involving a mid-chain hydroxy group and an terminal carboxy group (4). Further polymerisation involving the yet free hydro- and carboxy- groups would then lead to cuticle reticulation. (Dash lines: potential esterification site).

A BLAST against Genbank returned a clear homologue of the human leukotrien-A₄-hydrolase, the At5g13520 gene (34 % of identity). We nicknamed this unique gene *LEAKO*.

1.3.2 *ALDHs*, encoding fatty acid aldehyde dehydrogenases

In *Arabidopsis* cutin, α,ω -diacids are the major compounds (Bonaventure et al., 2004; Franke et al., 2005); they could result from the oxidation of ω -oxo fatty acids, a step which is likely catalyzed by one of the numerous fatty acid aldehyde dehydrogenases ALDHs (Figure. 2). The absence of the aldehyde dehydrogenases involved in this pathway may therefore affect proper cutin formation. However the role of ALDHs in cutin biosynthesis has not been established.

In humans, disruption of the FALDH gene triggers the Sjögren-Larsson syndrome (Rizzo et al., 2001). The latter, among others, causes mental retardation due to the accumulation of long chain alcohols or aldehydes in cells and blood of the patients. Normally these compounds are taken in charge by an enzymatic complex which includes FADH (Figure.6), catalysing the oxidation of ω -oxo-fatty acids.

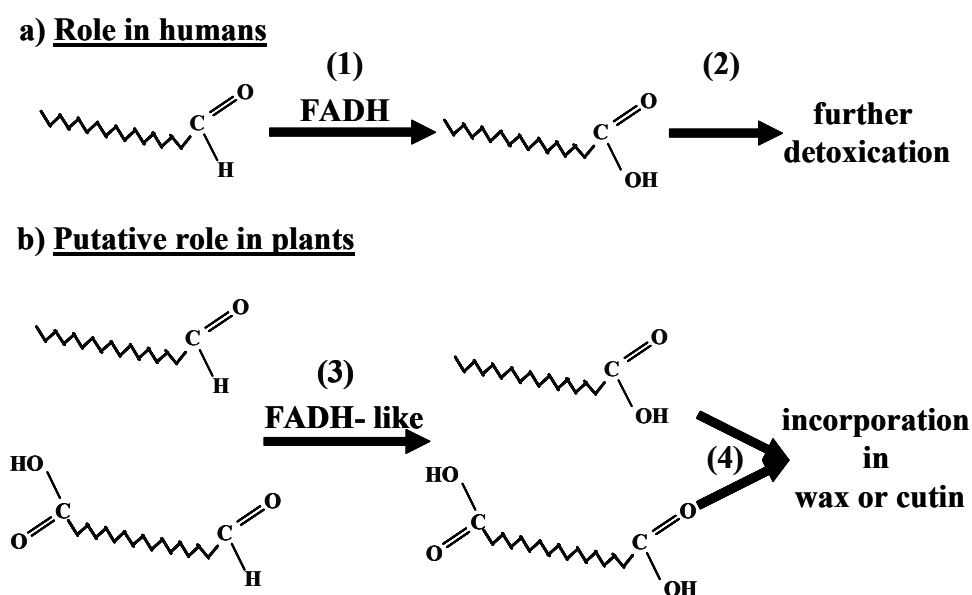


Figure 6. In humans and other animals, liver plays an important role in detoxication. a) The fatty aldehyde dehydrogenase (FADH) contributes to this process by catalyzing the formation of carboxylic acids from, for example, very long chain aldehydes. b) In plant homologue enzymes from the FADH may take part in the production of very long chain fatty acids precursors and components of cutin and wax or of diacids found in cutin.

The sequence of the FADH protein was BLASTed against Genbank, and among the retrieved candidates there were ALDH3 (At4g34240), ALDH4 (At1g44170) and ALDH5 (At4g36250) respectively showing 42%, 46% and 42% identity to FADH (ALDH3A2).

1.3.3 *HYD4*, an homologue of *BDG*

After the recent publication of the *BODYGUARD* (*BDG*) gene (Kurdyukov et al., 2006b), we decided to investigate on its closely related genes; they might share similar functions, localisation and so have similar effects on plant development. They may also have preponderant roles in plant development. The En/Spm transposon population generated in *A. thaliana* (Col-0) by Wisman and co-workers (Baumann et al., 1998) was screened for insertions in the closely related genes to *BDG* (A. Yephremov, unpublished data). These genes were nicknamed “*HYD*” as *BDG* belongs to the α/β hydrolase-fold super family. The *BDG* protein has, a signal peptide, leading to the secretion of *BDG* in the extracellular space, and two domains including a hydrolase/acyltransferase domain which may confer cutin polymerase function to *BDG*. The four *HYD*-homologous enzymes respectively share an amino acid identity of 82%, 64%, 45% and 40% with *BDG* α/β hydrolase-fold domain (Kurdyukov et al., 2006b).

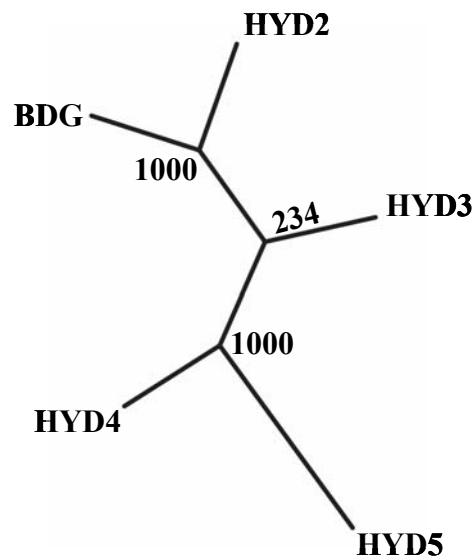


Figure 7. Phylogenetic relationships between *BDG* and the four *HYD* proteins. Predicted protein sequences available from TAIR were used to build this tree (1000 repetitions; <http://power.nhri.org.tw/power/home.htm>). Numbers displayed near by the forks indicate the frequency at which the embranchment occurred.

At that time a putative effect on seed germination (low percentage or absence of germination) had been observed in mutants carrying an insertion in the *HYD4* gene (At5g17780), which product shows 45% identity to *BDG* α/β hydrolase-fold domain; however no ectopic organ fusion had been reported.

1.4. Aim of the work

The main aim of this work was to understand the molecular functions of cuticular genes by investigating the chemical composition of cuticular lipids in the loss-of-function *lcr*, *fdh* and *bdg* mutants and by characterizing their transcriptomes. This included the analysis of biochemical and transcriptome responses, which may be critical in maintaining cuticular homeostasis and necessary to ensure survival of plants.

The second aim of the research was to biochemically characterise the cuticular *htm* mutant and to study the expression pattern of the *HTM* gene and the localisation of the HTM protein.

The third aim of the work was to examine the cuticular phenotypes of the novel mutants identified in the mutant screen or by reverse genetics.

In this work, two different approaches were taken to gather more information about cuticle biosynthesis in *Arabidopsis thaliana*: by analysing further the effects of the *lcr*, *bdg*, *fdh* and *htm* mutations (forward genetic) and by characterising insertion lines in candidate genes putatively involved in cuticle biosynthesis (reverse genetic).

2. Material and methods

2.1 Plant lines

Source	collection	Name of the line	Gene	Mutation	Nickname of the line
Lab		<i>bodyguard (bdg)</i>	At1g64670	Deletion	<i>bdg</i>
Lab		<i>lacerata (lcr)</i>	At2g45970	Truncated Transposon	<i>lcr</i>
Lab		<i>fiddlehead (fdh)</i>	At2g26250	Transposon footprint	<i>fdh</i>
H.Tanaka		<i>htm</i>	AtXgXXXXX	Substitution (xxxx)	<i>htm</i>
SALK Institute ¹	SALK Institute ¹	SALK_069038	At5g17780	T-DNA insertion	hyd4-1
NASC ⁴	GABI-KAT ²	711C08	At5g17780	T-DNA insertion	hyd4-2
RIKEN ³	RIKEN ³	52-0951	At5g17780	Ds-transposon insertion	hyd4-3
RIKEN ³	RIKEN ³	12-3258	At5g17780	Ds-transposon insertion	hyd4-4
NASC ⁴	JIC ⁵	SM_319056	At5g17780	Spm-transposon insertion	hyd4-5
NASC ⁴	JIC ⁵	SM_319060	At5g17780	Spm-transposon insertion	hyd4-6
SALK Institute ¹	SALK Institute ¹	SALK_117791	At5g13520	T-DNA insertion	leako-1
NASC ⁴	Singenta	SAIL_636_D12	At5g13520	T-DNA insertion	leako-2
SALK Institute ¹	SALK Institute ¹	SALK_091250	At4g36250	T-DNA insertion	aldh5-1

Table 1. Plant lines, characteristics and origins. At = Arabidopsis thaliana.

¹ <http://signal.salk.edu/>

² <http://www.gabi-kat.de/db/> (Rosso et al., 2003)

³ <http://www.brc.riken.go.jp/lab/epd/catalog/transposon.html>

⁴ <http://seeds.nottingham.ac.uk/Nasc/action.lasso?-response=/Nasc/information/ordering.lasso>

2.2 Plant Growth conditions

In order to have a reliable control, for instance for bound lipid analysis, chlorophyll extraction or toluidine blue staining, WT and mutant plants were grown side by side.

2.2.1. Greenhouse conditions

Seeds were sown on soil (Minitray). After synchronization (five days at 4°C), plants were grown under short day conditions (8 h day/ 16h night) for four to 11 weeks depending on the experiment and then under long day conditions to induce flowering. As indicated in the Result part, plants were sometimes directly grown under long day conditions after synchronisation.

2.2.2. Growth chamber

As indicated when required, after sowing and synchronisation, plants were sometimes grown in growth chamber (8 h day/ 16h night; 20°C/18°C).

2.2.3. In vitro conditions

Seeds were surface-sterilized by applying a 70 % ethanol solution for 10 min and a 10 % bleach solution for 15 min. After washing them four times with sterile water, seeds were kept in the dark, at 4 °C, to synchronize their germination.

After sterilisation and synchronization, seeds were either transferred directly into 500 ml glass pots containing about 70 mL of solid ½ MS (Duchefa Biochemie) media supplemented with sugar (1/2 MS + 3% sucrose; pH 5,8; 0,7% agar; Roth) or on round plates (1/2 MS + 3% sucrose; pH 5,8; 0,7% agar; Roth).

After germination on round plates, as their roots were about 1 cm long, seedlings were transferred onto vertical plates (1/2 MS + 3% sucrose; pH 5,8; 0,84% agar (Roth)), to allow the observation of their roots. With a concentration of 0,84% agar the media does not slip at the bottom of the vertical plates.

Plants were grown under long day condition (16h light /8h dark; 21°C).

2.3 **Bacteria strains**

2.3.1. Escherichia coli (E.coli)

- DH10B: F⁻, mcrAD (mrr-hsdRMS-mcrBC) F80*lacZ*DM15, *DlacX74*, *deoR*, *recA1*, *endA1*, *araD139*, D (*ara*, *leu*) 7607, *galU*, *galK*, I min *rps1*, *nupG*.

The two following *E.coli* K12 strains were obtained from Prof. David S. Stephens (Emory University; USA)

- JC200: *plsC*⁺, *met*⁺, *tet*^S, *thr-1* *ara-14* Δ (*gal-att* λ) *hisG4* *rpsL136* *xyl-5* *mlt-1* *lacY1* *tsx-78* *eda-50* *rfbD1* *thi-1*.

- JC201: derives from the JC200 strain but is *plsC*.

Due to its mutation in the *plsC* gene encoding a acyl-glycerol-3-phosphate acyltransferase, the JC201 cells are thermosensitive. They grow normally at 28-30°C but cannot grow at 42°C (Coleman, 1990).

2.3.2. Agrobacterium tumefaciens (A.tumefaciens)

-GV3101 (Koncz and Schell, 1986): its genomic DNA contains a resistance gene to Rifampicin and its helper plasmid (pMP90) encodes a resistance gene to Gentamycin.

2.4. **Bacteria growth conditions**

2.4.1. Media composition

LB (Luria-Bertani Medium): for 1L: 10g of Tripton/Pepton (Roth), 5g of Yeast Extract (BactoYeast Extract; Difco), 10g of NaCl (Merck). For plates, add 15g of agar per litre of media (Bactoagar; Difco).

YEB: 5g of meat extract (Merck), 1g of yeast extract (BactoYeast Extract; Difco), 5g of Tripton/Pepton (Roth), 2ml of MgSO₄ 1M (Merck), 5g of sucrose (Merck). For plates, add 15g of agar per litre of media (Bactoagar; Difco).

2.4.2. Media supplementation for LacZ and antibiotic selection

When “blue-white selection” was required, the LB media was supplemented with Xgal (5-Bromo-4-chloro-3-indolyl β -D-galactopyranoside; Roth; final concentration:

60µg/ml) + IPTG (Isopropyl β-D-1-thiogalactopyranoside; Roth; final concentration: 7,5µmol/ml).

When required, the media were supplemented with the adapted antibiotics. The end concentrations in medium are indicated in the table.

Antibiotic	<i>E.coli</i>	<i>A.tumefaciens</i>
Ampicillin (DUCHEFA)	100 µg/ml	//////////
Kanamycin (MERCK)	25 µg/ml	25 µg/ml
Cloramphenicol (SIGMA)	34 µg/ml	//////////
Carbenicillin (SIGMA)	//////////	50µg/ml
Gentamycin (DUCHEFA)	//////////	25µg/ml
Rifampicin (DUCHEFA)	//////////	100 µg/ml

Table 2. List of antibiotics used in this study and their final concentration in media.

2.5 Electro-competent bacteria transformation

E. coli and *A. tumefaciens* electro- competent cells were prepared as essentially described in (Sambrook and Russell, 2001): only the overnight culture was grown at 18°C and resuspended in 7% DMSO instead of GYT medium.

When needed *E.coli* electro-competent cells were transformed by applying 1500 kV using an Eppendorf Electroporator 2510. For the transformation, of *A. tumefaciens* cells, 1800kV were applied using the same electroporator.

2.6 DNA purification methods

2.6.1. Purification of plant DNA

In order to purify plant DNA, we used the DNeasy Plant Mini Kit (QIAGEN).

2.6.2. Confirmation of insertion lines

Six to ten plants per line were chosen randomly and their genomic DNA was purified. Using a T-DNA left border primer and gene specific ones, we respectively amplified each DNA. In parallel we amplified WT DNA as control.

2.7 RNA purification for line checking

Generally young rosette leaves from five of the previously characterized plants were individually harvested and ground. RNA was purified using the RNeasy Plant Mini Kit and the RNase-Free DNase Kit from Qiagen. RNA was eluted from filter by adding twice 40 μ l of RNase-free water onto the membrane and centrifuging. Samples were frozen at -20°C . To prepare samples for microarray hybridisation, we also used the RNeasy Plant Mini Kit and the RNase-Free DNase Kit from Qiagen but each individual sample contained leaf tissue from 15 independent plants (see Microarray Analysis).

2.8 Evaluation of DNA and RNA concentration and purity

Prior to PCR, the concentration of the DNA templates was estimated by comparing 2 or 5 μ l of each sample to a scale of Lambda DNA (Fermentas). Alternatively a NanoDrop Spectrophotometer ND-1000 (Peqlab Biotechnologie GmbH) was used to perform the measurements.

Prior to RT-PCR, the concentration of each RNA sample was estimated as follows: 1 μ l RNA + 7 μ l RNase free water+ 2 μ l loading buffer were loaded on a 1,5% agarose gel, along with a sample of known concentration. A picture of the gel was taken, and for a more accurate RNA quantification, the gel was scanned using a Typhoon 8600 (Amersham Biosciences).

2.9 Amplification by PCR and RT-PCR

Primers were usually ordered from SIGMA-GENOSYS, except for the cloning of the *HTM* gene in pASK-IBA vectors. The primers, being particularly long, were ordered from MWG (Germany). See **Appendix A**.

After quantification, DNA template was amplified using either a home-made Taq polymerase (Pluthero, 1993) or a high fidelity kit (Expand High Fidelity PCR System from ROCHE), when the PCR product would be used further for cloning.

After quantification, the target mRNA was retrotranscribed into cDNA from 500 ng of total RNA and was then amplified. Both, the retrotranscription reaction and the PCR amplification, were done using the One Step RT-PCR Kit from QIAGEN.

PCR and semi-quantitative RT-PCR reactions were performed usually in a volume of 25µl. A Peltier Thermal Cycler (PTC-225; BioRad) was used to perform the RT reactions and the amplifications.

Mix and PCR programmes: see **Appendix B**

2.10 Staining with toluidine blue solution

Toluidine blue is a hydrophilic dye and by consequence does not stick to the cuticle, a hydrophobic matrix; but where no cuticle is present; water is free to get in contact with the epidermal cell wall, hence the staining.

Mutant and WT plants were grown in greenhouse or on plates. Seeds, siliques, inflorescences or leaf material from WT and mutant plants were stained for 2 min using a fresh and filtrated solution of toluidine blue (0,05% w/v dist.water) (adapted from (Tanaka et al., 2004)). The organs were immersed in the staining solution at room temperature without any shaking, and were rinsed with tap water prior to each picture session. Pictures of the samples were taken using a Leica WILD420 microscope.

2.11 Chlorophyll extraction

Plants were grown in the greenhouse under short day conditions (8 hour light/ 16 hours dark) for 7-8 weeks. About 500 mg of rosette leaves was harvested from approximately 100 plants which were divided in six independent samples. In the case of mutants showing leaf fusion, representative samples were composed of fused leaves, a plant showing strong fusion, and fully grown leaves. Samples were weighed prior to the addition of ethanol (80%). The extraction was conducted at RT (22,5 °C) in a rotating water bath (18 rpm). Samples (1 ml) were taken after 10, 20, 40, 60 and 80 min of extraction. In order to determine the total amount of chlorophyll present, samples were finally boiled at 90 °C for 15 min. They were cooled down by burying in ice for 20 min before the final sample was taken. Optical densities were measured

at 647, 664 and 750 nm using an UVIKON 810/820 photometer (adapted from Lolle et al. 1997). The two first ODs are the absorption maxima of the chlorophyll and the last one, 750nm, was measured to constitute the baseline.

2.12 Siliques observation

Siliques were fixed to microscope slides with double sided sticky tape, opened along the replums and seed contents were observed using a Leica MZ FLIII microscope.

2.13 Bound lipid, wax and seed coat analyses

2.13.1. Bound lipid analysis

The composition in bound lipid of *lcr* and *fdh* leaves was analysed twice for each mutant. Plants were grown for 10-11 weeks into short day conditions prior to tissue harvest.

Tissue harvest and extract preparation

Approximately 30 leaves from different developing stages were harvested to constitute a sample. In order to increase the sample representativeness, each sample included tissue from at least 15 plants (normally from between 15-25 plants). WT leaves were then quickly placed in a transparent plastic cover and scanned (Epson Perfection 1640SU) to allow the estimation of their area. Leaves were then cut into pieces and extracted into 25 ml chloroform: methanol (1:1) for seven days to remove soluble lipids. The solvent was changed on daily basis and when finally removed, the samples were left to air dry for a couple of days. The leaf residues were weighed on a Sartorius M21S balance to measure their dry weight. At least five samples were prepared per plant type.

Depolymerisation and derivatisation

These steps were done according to (Franke et al., 2005).

Approximately 50 mg of dried tissue were depolymerised and transesterified for 2h at 80°C by adding 6 ml of 1 M MeOH-HCl (Supelco; 3M). The hydrolysis products were then recovered using hexane: after 2h of hydrolysis, 6 ml of hexane, 1 ml of a saturated NaCl solution and 100 µl of C32 acid standard (20µg of dotriacontan;

Fluka) were added. The samples were mixed by inversion and the organic phase transferred into a new tube. The samples were then extracted three more times with 4 ml hexane. The content of the organic phase were then dried under N₂-flux, recovered in app. 100µl of hexane and transferred in a “glass Eppendorf tube” for the derivatisation. To the content of each sample 20 µl of pyridine (Fluka) and 20µl BSTFA (N,O-bis-Trimethylsilyltrifluoroacetamide; Macherey-Nagel) were added. The samples were strongly vortexed and incubated for 50 min at 70°C. The samples were finally transferred into GC vials for chromatography runs.

2.13.2. Wax analysis

The composition in wax monomers was analysed once for *lcr* and *fdh* mutants. Plants were grown for seven weeks under short day conditions prior to tissue harvest.

Tissue harvest and extract preparation

A sample was composed by leaves from different developing stages. Ten rosettes leaves from ten different WT plants were harvested to constitute a sample. As the mutant leaves are smaller, about 12 leaves were harvested from the mutants. Leaves were carefully dipped into 6 ml chloroform for 10s. WT leaves were scanned to allow the estimation of their area (see bound lipid analysis). The wax extracts were kept in the fridge until the analysis.

To estimate the dry weight of the leaf material used for wax extraction, the soluble lipids of the leaves were removed. As for the preparation of leaf residue for bound lipid analysis, leaves were cut into pieces and extracted into 8 ml of chloroform:methanol (1:1) for seven days (see above). Afterwards, the leaf residues were weighed on a Epson Perfection 1640SU balance.

Derivatisation

This step was done as described in (Franke et al., 2005)

Twenty µl of C24 internal standard (4 µg of tetracosan; Fluka) were added to each wax extracts, the samples were dried under N₂-flux and transferred into “glass Eppendorf tubes” for the derivatisation (see bound lipid analysis).

2.13.3. Lcr and bdg seeds for seed coat analysis

Getting rid of the storage lipids

About 10mg of mature Arabidopsis seeds were ground using an agate mortar and pestle deep frozen in liquid nitrogen. Seeds were recovered in app. 5 ml of chloroform: methanol (1:1) and put to roll on a horizontal shaker (RM5 V-30 CAT; Labortechnik Fröbel GmbH) at 48°C (21 rpm) for 7 days. Solvent was changed on daily bases; tubes were centrifuged 2 min at 943 g (2000rpm) to sediment the seed particles and allow us to pipetted the solvent away (Heraeus Separattech Varifuge3.OR). After the last removal, the samples were left opened for 2-3 days to evaporate the solvent.

Depolymerisation and derivatisation

As in the bound lipid analysis, the residues were depolymerised and transesterified by acid-catalyzed transmethylolation (Franke et al., 2005).

However, instead of 6 ml of 1M MeHCl (Supelco; 3M), only 1 ml was used in this case. After 2h at 80°C, the hydrolysis products were also recovered using hexane: 1ml of hexane, 1 ml of a saturated NaCl solution and 100 µl of C32 acid standard (20µg of dotriacontan; Fluka) were added. The samples were then proceeded as for bound lipid analysis. Only the organic contents of the samples were not extracted three additional times with 6 ml hexane but with one.

2.13.4. htm inflorescences for bound lipid analysis and wax analysis

Plants were ten weeks old (seven week short days and three weeks long days) when the tissue was harvested.

Tissue harvest and extract preparation

Five independent samples were prepared for each experiment and per plant type.

- For wax analysis

About 0,6 g (fresh weigh) of inflorescences were weighed and, using a metal mesh from a kitchen sieve (pores =0,75 mm *1 mm), immersed into 5 ml of chloroform for approximately 15 s. After removal of the tissue, the beaker and the mesh were rinsed

with 1ml of chloroform each, bringing the volume to about 7 ml. The wax extracts were pipetted into other glass vials to discard pollen grains. The extracts were stored in the fridge until the analysis.

- For bound lipid analysis

After the wax extraction, tissue was transferred into 15 ml of chloroform: methanol (1:1), cut into small pieces to extract soluble compounds. The solvent was changed eight times and then the samples were let to dry.

Further preparation (see corresponding protocols for more detail)

- For wax analysis:

Four μg of C24 (tetracosan; Fluka) were added to each sample as internal standard.

- For bound lipid Analysis:

Total amount of dried tissue was weighed and approximately 26 mg of tissue (dry weigh) were processed further. Compare to the protocol for analysis of bound lipids from leaf tissue (see above), volumes from the different solutions added in the next steps were divided by two. As internal standard, 10 μg of C32 (dotriacontan; Fluka) were added to each sample.

2.13.5. Quantitative and Qualitative analysis by Gas-Chromatography (GC) and GC-Mass Spectrometry (GC-MS) analysis

To quantify their contents, the samples were run on a GC (GC-FID Agilent Technologies 6890N or HP_5890) equipped with a flame ionisation detector. To identify their components, a sample per plant type was run on a Agilent Technologies 6890N GC combined with a quadrupole mass-selective detector 5973N (Agilent Technologies). The monomers were identified according to their EI-MS spectra (70eV, m/z 50-700). Helium was used as carrier gas (2 ml min^{-1}).

The extracted samples for bound lipid analysis and for seed coat analysis were run according to the “SUBERIN” method and the wax extracts were run according to the “WACSH” method.

The SUBERIN method (Franke et al., 2005) can be broken down into the following steps: injection at 50°C into the column (DB-1, 30 m *0,32 mm, 0,1µm (J&W)); after 2 min at 50°C, the temperature is then modified as follows: 10°C⁻¹ to 150°C, 1 min at 150°C, 3°C min⁻¹ to 310°C, 30 min at 310°C.

The WACSH method (Kurdyukov et al., 2006b) consists in the following steps: injection in a GC capillary (DB-1, 30 m *0,32 mm, 0,1 µm (J&W)) at a column temperature of 50°C; after 2 min at 50°C, the temperature is raised stepwise: 40°C min⁻¹ to 200°C, 2 min at 200°C, 3 °C min⁻¹ to 310°C, 30 min at 310°C.

2.13.6. Reading the runs

The compounds were identified according to their fractioning patterns on the GC-MS runs, by comparison with the content of available databases. The compounds were quantified according to their peak area compared to the area of the internal standard on GC chromatograms. These steps were performed using the HPGC ChemStation Rev.A.07.01 [682] programme to read and to integrate the GC chromatograms and the Enhanced ChemStation G170AA programme (Version A.03.00) to interpret the GC-MS runs. Further calculations were done in Microsoft Excel 2003 and statistical analysis were done using the Statistica package (6.0; Statsoft).

The area of the scanned leaves was estimated using the Adobe Photoshop (7.0) program. *Lcr* and *fdh* leaves are often misshaped and fused which prevent us from measuring their surface by scanning. To estimate the area of the mutant leaves we used the linear regression between the measured WT weight and areas (see **Appendix C**).

2.14 Root observations

2.14.1. Growth evaluation

Periodically, during the first week of vertical growth, the position of the root tip was checked and marked. The number of secondary roots was evaluated by eye on daily basis during this period. The measurements were stopped when some of the roots reached the bottom of the plates. Plates were then scanned (Epson Perfection 1640SU)

and, using the Scion Image programme (Scioncorp), the length of the marked sections were evaluated.

Afterwards, plants were removed from the plates in order to evaluate their growth by weighing. To detach them from the agar, plates were opened and tap water was poured onto the surface of the plates. The plates were then placed on a shaker moving slowly for about 2 h at room temperature. Each plate contained four WT and four mutant plants; the four of each kind were pooled – after separation of their roots and aerial parts- and allowed to dry (four days at 55°C) in pre-tarred balance trays. Plants were weighed using a Sartorius Analytic A120 S balance.

2.14.2. Gravitropism experiment

After germination and transfer onto vertical plates seedlings were grown during a day in long day lighting (16h light /8h dark; 21°C). The plates were then transferred in the dark and grown in the same orientation for two more days. The plates were then rotated by 90° and the plants were grown one more day before scanning the plates (adapted from (Marchant et al., 1999)).

2.14.3. Wave experiment

After germination, the seedlings were transferred to 9 cm square plates containing 1,5 % (w/v) agar. This high agar concentration prevents the roots from penetrating the agar and provides a permanent “obstacle-touching stimulus”. After four days of vertical growth, the plates were tilted backwards (45 ° from the vertical). After two days of growth in this position the plates were brought to a new angle (70° from the vertical). Finally the plates were brought back to the vertical and grown further. Plates were scanned and marked periodically (adapted from (Okada and Shimura, 1990)).

2.14.4. Water stress experiment

Seedlings were allowed to germinate on horizontal plates for a week and, when the roots were about 1,5 cm long, the seedlings were transferred to vertical plates containing various PEG (Av. Mol. Wt. 8000) concentrations, namely 5%, 7,5% and 10% (w/v) (SIGMA) (adapted from (Eapen et al., 2003)).

Root growth was monitored as described before. The measurements were stopped when the root tips of plants grown in control plates without PEG touched the bottom of the plates.

Plants were grown further to observe the effect of PEG on plant development. After two weeks in presence of PEG, the plates were scanned to report root extension, plant developmental stage, and state. As no measurement of root length or number of secondary roots was easy to perform, roots were weighed.

2.14.5. Arabidopsis transformation by floral dipping

To a 500 ml *A. tumefaciens* culture, 25g of sucrose and 100µl of silwet (SILWET L-77 OSi Specialities INC.) were added. The 2,5L Erlenmeyer were whirled manually in order to disperse the Silwet and to dissolve the sugar. Most of the “transformation mixture” was poured into a 400-ml beaker, and Arabidopsis plants bearing young floral buds were dipped 1 min in the transformation mixture. Plants were then kept overnight in a closed bag and in a horizontal position (adapted from (Jakoby et al., 2006)).

2.15 HTM promoter and gene fusions

2.15.1. Promoter constructs

Reporter constructs based on the native promoter were made. First, 2110 bp upstream of the ATG from the *HTM* gene were amplified with the D038-D039 primers. The amplification was performed using Expand High Fidelity polymerase (ROCHE) (see **Appendix B**). The PCR fragments were then cloned into the pGEM-T vector (Promega) and transformed in *Escherichia coli* (DH10B). Transformation mix was plated on selective medium (LB ampicillin, Xgal, IPTG). DNA from a few white clones was extracted (QIAprep Spin Miniprep kits; QIAGEN) and sequenced by the ADIS service (MPIZ).

A promoter fragment containing no mutation was selected and cut out from the pGem-T vector using *HindIII* - *XbaI* enzymes (NEB). The *HindIII* site was present in the template sequence upstream the D039 primer annealing site, whereas the *XbaI* site

was introduced by the D038 primer. After gel extraction (QIAGEN) and cleaning using Microcon (Millipore; Microcon YM-100) the fragment was ligated (~ 8µl insert + vector, 1 µl 10x for T4 DNA ligase buffer Fermentas + 0,9 µl ligase (SIGMA; T4 DNA ligase), 12 °C, overnight) into binary vectors carrying one of the reporter genes (GFP, DsRED or GUS). These binary vectors were prepared in the lab and derive from the GPTV-BAR vector (Becker et al., 1992) (see **Appendix D** for maps). One µl of each ligation mix was used to transform *E.coli* by electroporation. Transformation mixes were plated on selective media (LB kanamycin) and a few colonies were checked by colony-PCR (see **Appendix B**).

A positive clone for each vector type was grown, its plasmid DNA was purified and used to transform *A. tumefaciens* (GVC301). A few microlitres of the transformation mix were plated under selective conditions (YEB-kanamycin- gentamycin-rifampicin) and, after 2 days of incubation, the colonies were tested by PCR (see **Appendix B**). The transformations in *A. tumefaciens* were successful and liquid cultures grown from those plates were used to transform *Arabidopsis thaliana* (Col-0) by floral dipping (Jakoby et al., 2006); see above).

Seeds from those transformants were harvested and germinated on soil. After germination, plants were selected by spraying them three times with a 0,1% BASTA solution (AgrEvo; every third day).

Prior to cutting, organs were embedded in 5% low melting agarose (Biozym agarose) containing 0,01% SILWET (SILWET L-77 OSi Specialities INC.) (Efremova et al., 2004). The sections were 100µm or 150µm thick and done using a vibratome series 1000 (Ted Pella Inc.).

2.15.2. Protein constructs

The 5295 bp-long genomic region comprising the *HTM* gene and promoter was amplified using the D039-D040 primer pair and Expand High Fidelity polymerase (ROCHE). The D039 primer introduces a *Bsi*WI restriction site and the D040 primer introduces a *Xma*I restriction site. The amplification products were subcloned in pGEM-T vector (PROMEGA) in order to generate compatible ends by restriction.

The insert was then cut out from the pGEM-T vector using the *XmaI-BsiWI* enzymes (from NEB; two-step digestion: 5U, 2µg DNA digested for 3h30 hours by each enzyme) and the destination vectors were opened by *XmaI-BsiWI*. The genomic fragment was then ligated in frame with the GFP, GFP-StreptagII, StreptagII or DsRED reporter elements carried by one of the pBct derivatives (see **Appendix D**). These plasmids were prepared by A.Yephremov. Thus, the reporter elements are at the C-terminal of the HTM protein.

Instead of sequencing the app. 6kb-long constructs, we selected 20 positive clones per construct type, grew minicultures and performed plasmid extraction (QIAGEN Spin Mini-prep kit). Using an aliquot of each of the 20 minipreps, a “plasmid mix” was prepared by reporter category and used to transform *A. tumefaciens*. Colonies were checked by PCR and 20 positive clones were picked to inoculate a liquid culture per reporter category. These liquid cultures were used to transform *Arabidopsis thaliana* (Col-0) by floral dipping (Jakoby et al., 2006); see above).

2.16 Microscopic observations

2.16.1. Light microscopy

Observations were done using either a Leica MZ FLIII or a Leica WILD420 stereomicroscope.

WT and *bdg* roots were observed in natural stage or after staining with a 0,05 % toluidine blue to enhance the contrast.

2.16.2. Scanning electron microscopy (SEM)

Two and half week olds leaves from WT, *bdg* and *lcr* grown under tissue culture conditions were collected. Fresh plant material was glued onto a sample holder and deep-frozen instantaneously by plunging it into liquid nitrogen slush at -180°C. Under vacuum conditions, the sample was then transferred into the cryochamber. Ice crystals present on the surface of the sample were sublimated at -89°C before sample coating. The frozen tissue was then coated with a thin layer of gold. The examination of the

samples was conducted at -175°C using a Zeiss DMS940 scanning electron microscope.

Using the same instrument, a petiole from four weeks old WT, *bdg* and *lcr* leaves from plants grown under tissue culture conditions were observed by scanning electron microscopy. The mutant tissue showed deformations (bulges) visible by eye.

Rosette leaves from 6-7 week-old plants grown under short day conditions were prepared for cryo-SEM; the samples were deep frozen and sputtered with palladium with a K1250X cryo-transfer unit from Emitech. Their surface was observed using a Zeiss SEM SUPRA 40VP microscope cooled down at -140°C with liquid nitrogen.

After eight weeks of growth in short days and four weeks of growth in long days, the 4th or 5th internodes from *lcr*, *bdg* and *fdh* stems were also observed using a Zeiss SEM SUPRA 40VP after deep freezing and sputtering with a K1250X cryo-transfer unit from Emitech

2.16.3. Fluorescence microscopy

To document the expression pattern of the *HTM* gene, different organs from transgenic plants expressing one of the reporter constructs were examined using a Zeiss LSM510 Meta confocal microscope or a Leica TCS SP2 AOBS confocal microscope. For the Zeiss microscope, an argon laser was used to excite the GFP molecules at a wave length of 488 nm and the fluorescent emission was observed between 500-530 nm. A HeNe laser was used to excite the DsRED molecules at a wave length of 546 nm and the emission of fluorescence was observed between 565-615 nm. For the Leica microscope, the GFP molecules were excited at 488 nm and their fluorescence observed between 493-530 nm and the DsRED proteins were excited at 561 nm and their fluorescence was observed between 560-620 nm. Images presented here were taken with the Zeiss microscope.

Siliques and inflorescences from transgenic plants expressing the *HTM::DsRED* protein construct were also observed using a Leica stereo-microscope MZ-FL-III equipped with a D546/10 excitation filter and a D600/40 barrier filter. The later excludes chlorophyll auto-fluorescence.

2.17 Heterologous expression of *HTM*

2.17.1. Cloning the *HTM* cDNA in pASK-IBA vectors: Creating a Strep-tagged version of the *HTM* protein

The *HTM* cDNA was provided by the RIKEN stock centre (<http://www.brc.riken.go.jp/lab/epd/catalog/cdnaclone.html>) and amplified using the Expand High Fidelity PCR System (ROCHE) and the suitable primer pairs. The PCR products were first subcloned into pGEM-T (Promega) and cut out with *BsmBI* enzyme (NEB; 2 µg of DNA were digested by 5U of *BsmBI* for 5h). The pASK-IBA_2C, 3C and 5C vectors were opened using the *BsaI* restriction enzyme (NEB; 2 µg of DNA were digested by 5U of *BsaI* for 5h30).

The pASK-IBA vectors encode a chloramphenicol resistance gene and allow the production of a tagged version of the protein of interest using Anhydrotetracycline (AHT) as inducer and not IPTG as classically done (see <http://www.iba-go.com/>). The recombinant protein will be tagged with the StrepTagII peptide in N-terminus (N-term) or C-terminus (C-term) depending on the plasmid used for its production.

The pASK-IBA_2C allows the tagging of the protein in C-term and the transfer of the tagged protein into the periplasm from the host. The pASK-IBA_3C allows as well the production of a protein tagged in C-term but not its exportation to the periplasm. Finally the pASK-IBA_5C allows the cytoplasmic production of a recombinant protein but tagged in its N-term.

After ligation (150 ng vector + 250-300 ng insert in a final volume of 10 µl; o.n. at 12°C; (SIGMA; T4 DNA ligase)), competent *E.coli* DH10B cells were transformed with 1µl of each ligation mix. The transformants were selected on LB plates supplemented with chloramphenicol and colonies checked by PCR. Over-night cultures were grown (37°C and 250 rpm) and their plasmid was extracted using the Spin Mini-prep kit from QIAGEN. Two clones per plasmid type were sequenced by the ADIS service (MPIZ). A clone bearing no mutation for each plasmid type was then used further for protein expression.

Induction of protein expression

An over-night culture (37°C, 250 rpm) was inoculated per plasmid type and, next day, a 100ml pre-induction culture was inoculated with 2ml of each overnight culture. After 2h of growth at 37°C (200 rpm), the pre-induction cultures had reached a O.D._{600 nm} of about 0,6 and were ready for induction (see Manual: Expression and purification of proteins using Strep-tag and/or 6x Histidine; <http://www.iba-go.com/download.html>).

Prior to induction, 5 ml were taken of each culture to constitute a negative control and grown in parallel of the induced cultures. To induce the protein production 9,5 µl of anhydrotetracycline (end concentration in media: 200 ng/ml) were added into each pre-induction culture.

As recommended by the manufacturer, we first induced the production of the protein for 3h at 30°C, which gave good results. To improve the quantity of soluble protein, we then tested three other production conditions: after the addition of AHT, the cultures were either grown at 18°C for 3h or o.n., or grown at 30°C, o.n..

To discriminate between the efficiency of the different conditions of induction, an aliquot (1ml) of each culture and respective negative controls was taken and centrifuged at the end of the induction period. The rest of the cultures were centrifuged (15 min at 1600 g in an Avanti J-25I centrifuge; Beckman) and the cell pellets were frozen (-20°C).

Protein extraction

Soluble and insoluble fractions were analysed by SDS-PAGE. An aliquot of each fraction per culture and corresponding negative control was run on a denaturing 10% acrylamide gel (acrylamide/ bisacrylamide; 29:1). Two gels loaded with the same samples were run in parallel (40 mA) and after migration one was used for Commassie staining and the other for western blotting.

Running buffer (Sambrook and Russell, 2001):

Tris-Glycine-SDS (1X): tris-base 25mM, glycine 250 mM (pH=8,3) and 0,1% SDS (w/v).

Coomassie staining (Sambrook and Russell, 2001):

The gel was fixed for 10-15 min in 25% (v/v) isopropanol-10% (v/v) acetic acid, stained for 10-15 min in Coomassie solution (0,03% (w/v) R250 Brilliant blue in 10% acetic acid) and gradually destained in a 10% (v/v) acetic acid solution.

The protein transfer was performed using an Amersham Biosciences_TE77PWR transfer apparatus and done according to (Sambrook and Russell, 2001). The proteins were transferred from the gel onto a nitrocellulose membrane (Amersham Hybond™ ECL™; 0,45µm pore size) in approximately 30 min at 45 mA (0,8mA/cm²). The proteins were transferred from gels onto membranes under semi-dry conditions.

Transfer buffer (Sambrook and Russell, 2001): Tris-Glycine-SDS (1X): tris-base 48 mM, glycine 39 mM and 0,037% SDS (w/v), methanol 20%.

Prior to the detection, we checked that the transfer had occurred by Ponceau staining. Done according to (Sambrook and Russell, 2001): the membrane was stained with 0,5% Ponceau red solution (v/v in acetic acid 1%; v/v) for 1min. Excess of staining was removed using distilled water. Finally, most of the coloration was removed before proceeding with the Strep-tag HRP Detection Kit.

We checked the presence of our protein using the Strep-tag HRP Detection Kit from IBA (according to the manufacturer instructions). This kit is based on the detection of the strep-tagII tagged protein by a Strep-Tactin complex fused to the horse radish peroxydase (HRP). First, the membrane is washed and blocked, second it is incubated with the enzyme conjugate (Strep-Tactin HRP fusion). Afterwards, the presence of the Strep-Tactin HRP complexes, and thus of the recombinant protein, is revealed using a chromogene solution (colorimetric detection). The HRP catalyses the transformation of a colourless substrate into a coloured product. The use of this kit saves a lot of time as there is only one blocking step of 30 min and only one labelling time of 30 min. This kit also makes the detection easier as the colour can be directly read on the membrane.

From this experiment, we concluded that growing the cultures at 18°C for 3h leads, in our case, to the production of more soluble protein. We therefore proceeded further with the pellet of these cultures.

Protein purification

At the end of the induction period, the cultures were centrifuged and the medium removed. Five ml of Buffer W (100mM Tris/HCl pH8, 150 mM NaCl, 1 mM EDTA; see Manual: Expression and purification of proteins using Strep-tag and/or 6x Histidine; <http://www.iba-go.com/download.html>) were added to the cell pellets from the 100ml and the samples were frozen at -20°C for more app. 1h. The pellets were thawed quickly and centrifuged 15 min at 4°C at ~ 1600 g (4000 rpm) (Beckman Avanti J-25I) in order to sediment cell debris and protein aggregates.

The tagged-*HTM* protein was purified using a gravity flow Strep-Tactin column of 1ml bed (Sepharose). The purification (see short protocol for Strep-tagII purification; <http://www.iba-go.com/download.html>) was done at room temperature: five wash fractions and six elution fractions were retrieved and the elution of the tagged protein was followed by measuring at O.D._{280 nm} using a NanoDrop Spectrophotometer ND-1000 (Peqlab Biotechnologie GmbH).

An aliquot of the fractions containing some protein were run on a denaturing 10% acrylamide gel (acrylamide/ bisacrylamide; 29:1). After electrophoresis, a Coomassie staining and a Western blot were done. Protein bands from the gel stained with the Coomassie solution, matching the position of the bands revealed by the HRP conjugate on the Western membrane, were sent to the MALDI for confirmation of their nature.

Protein sequencing

This work was performed and described by Thomas Colby.

The sample was analyzed by LC-MS-MS/MS using a Q-Tof2 (Micromass/Waters) mass spectrometer coupled to a Waters CapLC (with nano-flow splitter) equipped with a 75micron x 150mm Atlantis dC18 Nanoease column with a Symmetry C18

pre-column in forward-flush configuration. Peptides were eluted with 15-minute gradient from 10-50% acetonitrile (0.1% formic acid) which was followed by column cleaning and re-equilibration phases.

Eluted peptides were measured in survey-scan mode with a capillary voltage of 1.6 kV and a cone voltage of 45V and a m/z collection range of 400-1600 Da and 1 second frames. Multiply-charged precursor ions of sufficient intensity were fragmented in an argon collision cell under mass-dependent collision energy. Daughter-ion spectra were collected over the range 50-1800 Da with 1.9 second frames.

Peakfiles from the processed spectra were submitted to MASCOT MS/MS search with a peptide mass error tolerance of 0.4 Da and a Fragment mass tolerance of 0.4 Da. The Mascot score of 670 on a total of 19 peptides covering 34% of the sequence made the identification unequivocal.

2.17.2. Complementation assay in bacteria

Electro-competent cells of the *E.coli* JC 200 and JC 201 were transformed with the pASK-IBA 3C carrying the *HTM* cDNA. Positive clones were selected on LB chloramphenicol medium (30°C). Some positive clones were replicated twice, and half of the plates were placed at permissive (30°C) and restrictive (42°C) temperatures.

We also established the bacteria growth curve in liquid media following the OD increase (Eppendorf BioPhotometer) at both temperatures and performed the complementation test in these conditions too.

2.18 Complementation of Arabidopsis *fdh* mutant by *HvFDH*

2.18.1. Plant transformation and segregation analysis

The promoter of the *Arabidopsis thaliana* *FDH*, from the base -660 till the base -16 before the ATG, and the cDNA of the barley (*Hordeum vulgare*) *FDH* gene have been introduced in a binary vector comportsing a carbenicilline and a BASTA resistance gene (cloning by Jafar Jabbari Sheikh; Klaus Oldach's group; University of Adelaide, Australia).

The received plasmid was introduced in *A. tumefaciens*, some colonies were tested by PCR and two positive clones were grown to produce more plasmid. Plasmid DNA was prepared using a QIAprep Spin Miniprep Kit, and 0,5 µg were digested by 5 U of EcoR1, 2,5 U Sal1, 2,5 U Pvu1 (NEB) for 5h at 37°C separately. We proceeded further with a colony containing a plasmid showing the expected restriction pattern.

Plants were grown under long day conditions (16 h day /8 h night). *Arabidopsis thaliana* Col-0 and *fdh* heterozygous plants (genotyped by tetra-primer ARMS-PCR; see below) were transformed by floral dipping (see above; (Jakoby et al., 2006). Transformants were bagged individually.

The progeny from 53 transformants (42 heterozygous *fdh* and 9 WT Columbia plants) were sown and sprayed with a 0,1% BASTA solution (see above). Progeny of *FDH* heterozygous and of “*HTM* reporter” plants were used as negative and positive controls respectively.

BASTA resistant plants were examined at the rosette, young flower and silique stages. Only then, to avoid any stress to the plants, tissue was harvested for genotyping.

The observations were done visually and under the microscope (Leica WILD420). Pictures were also taken with a digital camera (Nikon E8400).

2.18.2. Genotyping of plants

Genomic DNA was purified according to the 96 DNA protocol (Michaels and Amasino, 2001) to genotype plants prior to transformation. Genomic DNA from the BASTA resistant plants was purified using a DNeasy Plant Mini Kit from QIAGEN.

For genotyping, plant DNA was amplified by a multiplex PCR allowing the distinction between WT, heterozygous and homozygous mutant plants (Figure. 8; primer design and PCR optimisation by J. Sheikh (University of Adelaide, Australia) based on (Ye et al., 2001): $T_{\text{annealing}}=60^{\circ}\text{C}$ and elongation time=40s.

The results of the PCR and of the visual observations, done on the BASTA resistant plants, were compared. We concluded that some plants with a WT appearance had a

mutant genotype (see Results). We confirmed this result by sequencing four WT-looking like plants found mutant by PCR. As a control, the PCR product from a WT Columbia, a *fdh* mutant and that of a survivor, genotypically and phenotypically mutant, was also sequenced (ADIS; MPIZ). The D155-*AtFDH3* and D156-*AtFDHR3* were used for sequencing.

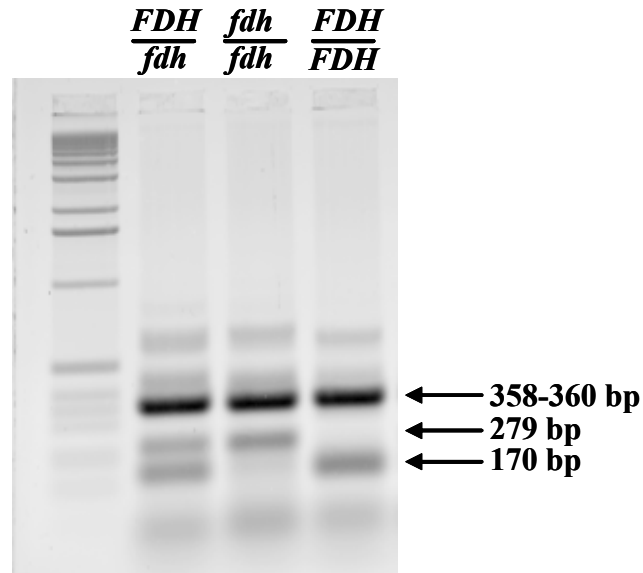


Figure 8. Distinguishing between *FDH* and *fdh* alleles by ARMS-PCR. The primer pair D155-D156 amplifies the 358 bp region containing the transposon foot-print; mutant gives a 360 bp product. Both, D156-D166 and D155-D157 generate allele specific products: the first pair amplifies the mutant allele (239 bp) and the second the WT allele (170 bp) respectively.

2.19 Microarray analysis

2.19.1. Plant, growth conditions and hybridization to Affymetrix ATH1 chips

Mutants (*bdg*, *lcr*, *fdh*) and WT (Col-0) were grown side by side under short day conditions (8 h day/ 16h night; 20°C/18°C). Plants were five weeks and a half when tissue was harvested. Four independent samples were prepared per plant type. Each sample contains tissue from 15 plants. Young deformed and/or fused leaves (2mm to 1cm) were chosen to compose the samples. Total RNA was purified using the RNeasy Plant Mini Kit (QIAGEN) according to the manufacturer instructions. The RNA samples were sent to the Integrated Functional Genomics (IFG) platform of the Westfalian-Wilhelms-University (Muenster, Germany; <http://ifg-izkf.uni-muenster.de/Genomik/>) for quality checking, concentration optimisation and hybridisation on Affymetrix ATH1 arrays. For each plant type, we have three

biological replicates and no technical replicates. Two samples per plant type were sent first for hybridisation and later, a third sample per genotype was hybridised.

2.19.2. Defining the list of mis-regulated genes in our mutants

Using the Microarray Suite 5.0 programme of the Affymetrix package, samples were scaled to an overall fluorescence intensity of 500 to allow their comparison. Each mutant dataset was compared to each WT dataset, and thus signal log ratios (slr) were calculated (MAS5 statistical algorithm; Statistical algorithms description document, technical report; Affymetrix 2002). The results comprising Affymetrix gene ID, slr, detection signal, Absence/Presence (A/P) call, change status and the p-value associated to the detection of a intensity change were exported into Microsoft Excel (2003). Genes were filtered out if they did match the following criteria:

- Their signal log ratios should be equal or higher than 1 or equal and lower than -1;
- Their A/P calls were checked for coherence (i.e. if “a signal” is called PRESENT with a detection intensity of 250 in one case, it should not be called ABSENT or MISCELLANEOUS with a detection intensity of 249 or lower in the other samples);
- A gene should at least be called PRESENT twice either in the mutant or in the WT samples;
- If a gene had more than three NC (NON CHANGE) among its nine change statuses, the gene was excluded of the list.

As for the confirmation of our microarray results, the list of the candidate genes for RT-PCR had been established according to the data obtained on two replicates (see Results), we had to slightly decrease the stringency of our selection criteria and also include genes which among their nine slr values had one value between -1 and 0 or 0 and 1. Genes fulfilling this criterion and all the others are among the list of mis-regulated genes in our mutants.

Programme settings in
Microarray Suite (5.0)

Scaling factor	500
Alpha1	0,05
Alpha2	0,065
Tau	0,015
Gamma 1L	0,0045
Gamma 1H	0,0045
Gamma 2L	0,006
Gamma 2H	0,006
perturbation	1,1

We also performed a Bayesian T-test and calculated False Discovery Rates (FDR), based on the p-values calculated in the T-test (<http://cybert.microarray.ics.uci.edu/>; (Allison et al., 2002). The corresponding data and the list of previously sorted mis-regulated genes were compiled.

Cybert and PPDE settings

For the estimation of Bayesian Standard Deviation, a sliding window of 101 and a confidence value of nine were chosen. The p-log transformed values were used as input and three β iterations were done for the PPDE calculation. Low-Value Handling was left to zero.

During the procedure, we used the Merge macro from the FiRe package (<http://www.unifr.ch/plantbio/FiRe/main.html#mozTocId845754>; (Garcion and Metraux, 2006) to merge tables and the Compare Three Lists macro from the FiRe package to draw the Venn Diagrams.

Locus Identifier corresponding to the array elements were retrieved from the TAIR database (<http://www.arabidopsis.org/index.jsp>; [Microarray Elements](#); version of the 02.05.2007)

2.19.3. Confirmation of our microarray results by semi-quantitative RT-PCR

The list of the candidate genes was established according the data obtained on two replicates. The profile of accumulation of each gene was established and using a number of amplification cycles in the linear phase of accumulation, the change in regulation between mutant and WT was checked (primer list and number of amplification cycles; (see **Appendix A**).

2.20 Phylogenic analysis

2.20.1. BDG and its family

The predicted sequences from the BDG and the four HYD proteins were used to build an un-rooted tree. The calculations were performed on the Phylogenetic WE6 repeater

platform (<http://power.nhri.org.tw/power/home>) using default settings (pair wise alignment: “slow and accurate option”; Gonnet matrix) and the Neighbor-joining as a clustering method (1000 bootstraps).

2.20.2. Barley FDH, Antirrhinum FDH and the Arabidopsis FAE family

This tree was built using the predicted protein sequences encoded by the 21 elongases from the *Arabidopsis thaliana* FAE family, AFI from *Antirrhinum majus*, FDH from *Gossypium hirsutum* plus hvFDH from *Hordeum vulgare* (barley). The calculations were performed on the Phylogenetic WE6 repeater platform (<http://power.nhri.org.tw/power/home>) as described above.

3. Results

3.1. Lacerata, bodyguard and fiddlehead mutants

3.1.1. Cuticle properties of *lcr*, *bdg* and *fdh* mutants are altered

In a screen for mutants with increased cuticle permeability, Machida and co-workers described the use of toluidine blue as a dye which stains organs when their cuticle is not properly formed (Tanaka et al., 2004). This water-soluble molecule adheres to hydrophilic surfaces rich in anionic groups present, for instance, in plant cell wall. In presence of a normal cuticle no staining can be observed; however, in presence of a defective cuticle, this dye can probably access the underlying cell wall materials, leading to tissue staining. We applied this method to leaves of our mutants and observed a patchy staining, highlighting the irregular impermeability of their cuticle (Figure. 9_A). Leaf coloration did not differ between fused or unfused rosette leaves.

To further illustrate the modification in cuticle permeability of our mutants, we performed chlorophyll leaching assay (Lolle et al., 1997). As described by Lolle and co-workers, intact rosette leaves were immersed in 80% ethanol, solvent samples were taken regularly and their absorption measured at 647 and 664 nm (absorption maxima of the chlorophyll). In this experiment, we used leaves from *fdh* as control; our results for this mutant are similar to the data from Pruitt and co-workers (Lolle et al., 1997). Rosette leaves from the respective mutants release their chlorophyll content faster than WT. Thus, this result (Figure. 9_B) also suggests that the cuticle of these mutants is weakened. To study if there is a relation between cuticle permeability and the engagement in ectopic organ fusion we prepared two different types of *lcr* samples. The first type only contained leaves that were not joined in a fusion (sample of type N), the second contained both, leaves joined in a fusion and leaves not joined in a fusion (sample type J+N). The sample of type N loses its chlorophyll pigments quicker than the WT control but slower than the sample of type J+N. This last element of comparison shows that higher permeability may be linked to fusion.

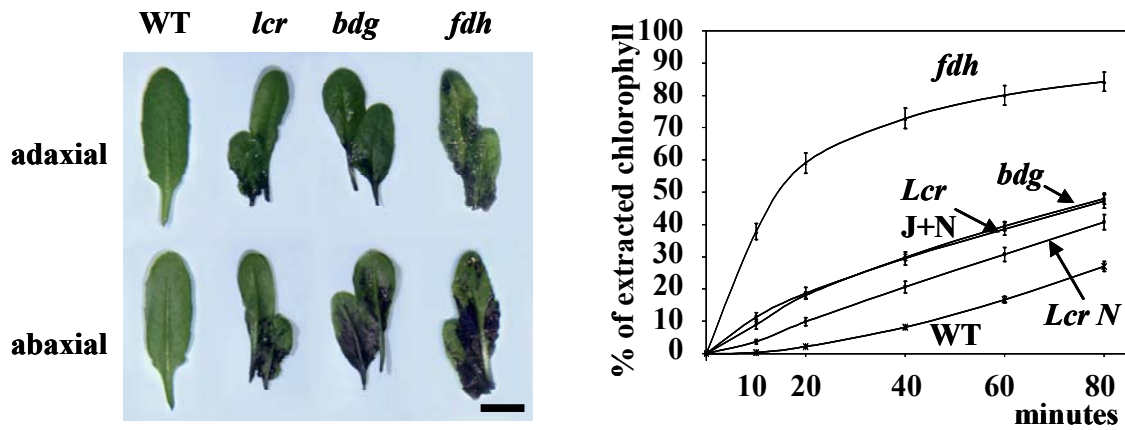


Figure 9. The effect of an impaired cuticle shown by toluidine blue staining and chlorophyll leaching. (A) WT and mutant leaves after 2 min immersion in a 0,05% toluidine blue solution and destaining in water. WT leaves remain unstained whereas mutant leaves display a patchy coloration. (B) Chlorophyll extraction from representative rosette leaves of *bdg* and *lcr* mutants. *Fdh* was used as a control, the samples of type N contained only *lcr* leaves not engaged in a fusion and, the sample of type J+N contained leaves joined in a fusion and leaves not joined in a fusion. At least six repetitions per plant type were made. Average \pm standard error (s.e.) are presented here. Plants were seven-eight weeks old (short day conditions).

3.1.2. Under *in vitro* culture conditions, *lcr* and *bdg* show epidermal deficiencies and enhance root growth

When grown under greenhouse conditions, many cuticular mutants show a wide range of phenotypes (post-genital organ fusion, leaf deformation,...) and are generally smaller than their WT counterparts. An overall increase in cutin monomers per leaf area was shown in WT plants grown under water deprivation and in the *bdg* mutant (Faust, 2006; Kurdyukov et al., 2006b). Therefore, one cannot exclude that the open-air growth conditions, which are suitable to WT growth, are actually deleterious to the cuticular mutants, which may not be able to maintain water balance. The progressive death of trichomes, which after a while lie flat on the epidermis of *bdg* leaves, may be for instance one of the effects of the dehydration (Kurdyukov et al., 2006b).

As it is not possible to propagate *fdh* mutants by selfing (the *fdh* mutant is sterile) and not always easy to distinguish *fdh* mutants from WT or heterozygous plants at early developmental stages, therefore only *bdg* and *lcr* were considered for further characterisation under *in vitro* culture conditions.

To this end, plants were grown on hormone-free MS media. Although plants could develop under high humidity and were thus free from any dehydration stress,

trichomes in *bdg* still collapse in a progressive way (Figure. 10_C_D_E). Apart from trichome degeneration, the presence of tears in the epidermis was observed on the surface of young, misshaped or WT-looking leaves of *bdg* (Figure. 10_F_G_H_I). Under *in vitro* culture conditions, neither *bdg* nor *lcr* seedlings showed growth retardation; they even thrived better than WT plants (Figure. 11). They, however, still displayed leaf deformation (Figure. 10_B), leaf fusion and early appearance of axillary apical meristem (Figure. 10_A).

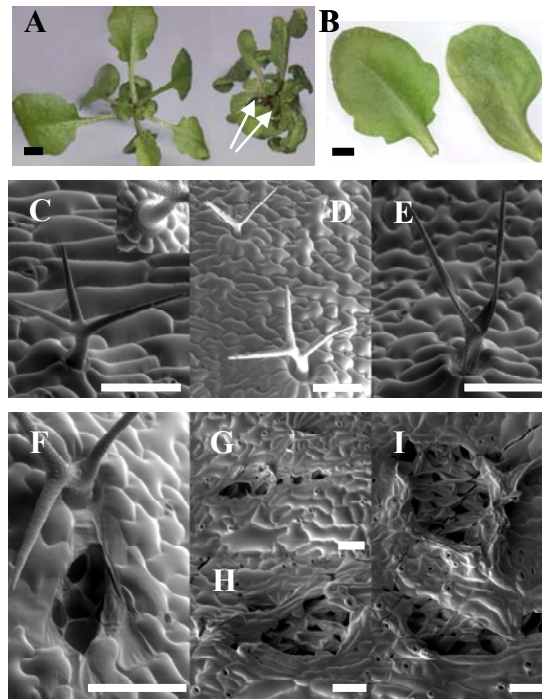


Figure 10. Leaf and trichome phenotype of *bdg* when grown under *in vitro* culture conditions. (A) Three weeks and a half old WT and *bdg* plants. *Bdg* leaves are misshaped, showing short and thick petioles and deformed limbs (see also B). Early in the vegetative phase, before any shoot has grown, a second meristem sometimes forms on *bdg* (or *lcr*) plants (arrows). (B) Two weeks and a half old representative WT and *bdg* leaves. (C)(D)(E) Collapsing trichomes observed on the adaxial side of *bdg* leaves. The base of a WT trichome is shown in the inset (C). Different phases of trichome death could be observed on the surface of *bdg* leaves. In *bdg*, trichome bases do not remain bulbous; they progressively loose contact with the subsidiary cells. Trichomes often become flat, and collapse. (F) to (I). Ruptures in the epidermis were observed on the surface of *bdg* leaves. As the leaves grow, the tears enlarge, and expose larger area of mesophyll (G). Bar: (A)(B) 2 mm; (C) to (I) 100 μ m.

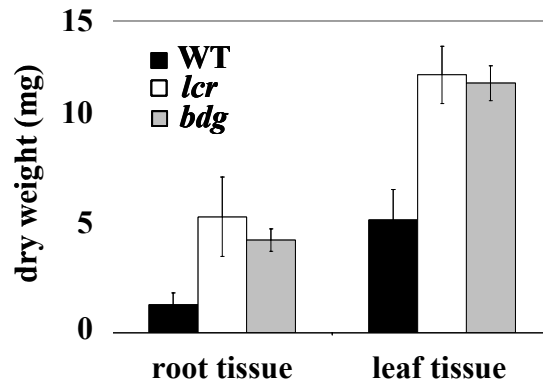
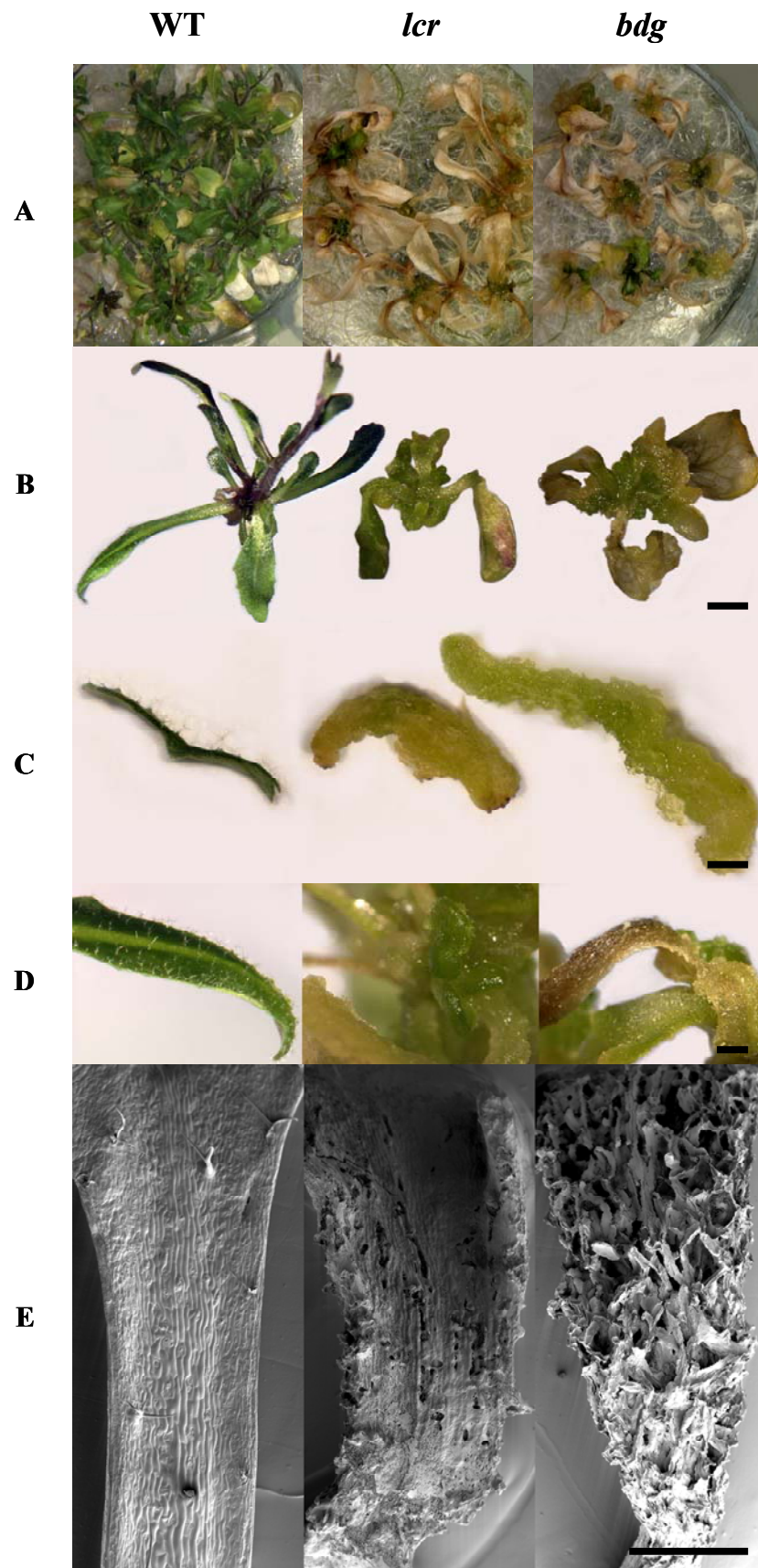


Figure 11. Plant biomass of *lcr* and *bdg* mutants under *in vitro* culture conditions. After germination, plants were grown for a week on vertical plates. Root and aerial organs of the plants were dried for three days at 60°C before weighing. Weight means and standard deviations presented here are based on 32 WT plants, 16 *lcr* and 16 *bdg* plants.

When grown under 100% relative humidity, WT and seedlings from both mutants at first developed slightly translucent leaves. WT plants seemed to adapt to the environment but mutants progressively developed glossy and vitrified leaves. Outgrowths tended to develop on the petiole from succulent leaves (Figure. 12_B_C_D); and, while after approximately four weeks WT plants bolted, most mutant plants had degenerated into a callus-like structure (*bdg*: 30 out of 33; *lcr*: 20/27) or kept producing leaves and showed fusion (Figure. 12_A_B). This is reminiscent of cutinase-expressing plants (CUTE plants) which show callus-like bulges at the tearing points (Sieber et al., 2000). We confirmed this observation and, furthermore, found that when grown under slightly more humid greenhouse conditions (tray partially covered), regeneration of roots or full plantlets could take place on CUTE plants (Figure. 13). Some of the *bdg* or *lcr* plants, among the ones showing fusion, did bolt and develop reddish shoots. A petiole from a succulent leaf of each mutant was observed under SEM. As only one petiole per mutant was observed, no conclusion about the degree of epidermal damage can be drawn, yet the epidermal defect was obvious in both mutants, the epidermis could even be absent in *bdg* (Figure. 12_E). Although the petioles still had the expected shape, their covering was impaired, exposing their mesophyll tissue. We also conducted a toluidine blue staining on three-week old plants grown under *in vitro* growth conditions: petioles, fusion zones and abaxial leaf sides were mostly stained (data not shown).



←Figure 12. Callusing of *bdg* and *lcr* mutants under *in vitro* culture conditions. (A) After four weeks of growth under *in vitro* culture conditions, most WT plants have bolted whereas most of the *lcr* and *bdg* plants have degenerated. (B) A representative four weeks old WT,

lcr and *bdg* plant. Most mutants display a callus-like structure in the shoot apex. Two older leaves had been removed from the *lcr* sample before taking images. Older leaves have lost most of their pigmentation and younger organs have a succulent appearance. Bulges are visible on the surface of the petioles. (C) Transversal cut through a WT, *lcr* and *bdg* rosette leaf. Mutant organs are thicker. Absence of trichomes and of a clear epidermal delimitation. (D) Close up on a WT leaf, a *lcr* shoot meristem from which young succulent leaf-like organs emerge, and of a leaf petiole of *bdg*. Notice the presence of bulges on the surface of mutant organs. (E) SEM pictures showing the surface of a petiole from each plant type. Both mutant samples displayed bulges visible by eye. A discontinuous epidermal cell layer covers *lcr* petiole whereas no epidermis is present on the surface of *bdg* sample. Bar: (B) 5 mm (C) to (E) 1 mm.

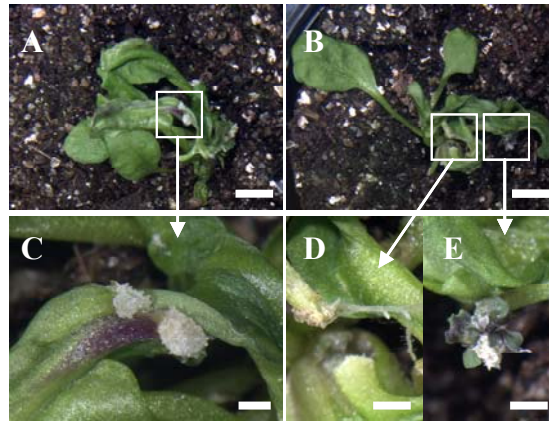


Figure 13. Features of CUTE plants. Plants were five weeks old. (A) (B) All CUTE plants show organ fusion and some of them leaf or petiole tearing (25/63). Notice the presence of white bulges at the place of recent organ rupture in (A) and in (C). (B) In 8% of the cases (2/25 plants displaying callus-like structures), roots, leaves or complete mini plants develop on these callus-like structures. Bar: (A) (B) 5 mm (C) to (E) 1 mm.

Both, *bdg* (Kurdyukov et al., 2006b) and *lcr* (A. Yephremov, unpublished data), genes are expressed in roots where no cutin is synthesised. As a first approach to understand their importance in root development, we grew plants on vertical plates and found that both mutants appear to be as sensitive to gravitropism as the WT control (see Methods). We also observed that the perception of obstacles (hard agar surface) by the mutant roots does not seem to be altered, as the wavy pattern of their main root was not different from the WT pattern (see Methods). With respect to root growth and root morphology, no difference could be found in the length of the main roots between mutants and WT (Figure. 14_A_B). However the growth of secondary roots seemed to be initiated earlier in both mutants which, developed more secondary roots than the WT (Figure. 14_A_C).

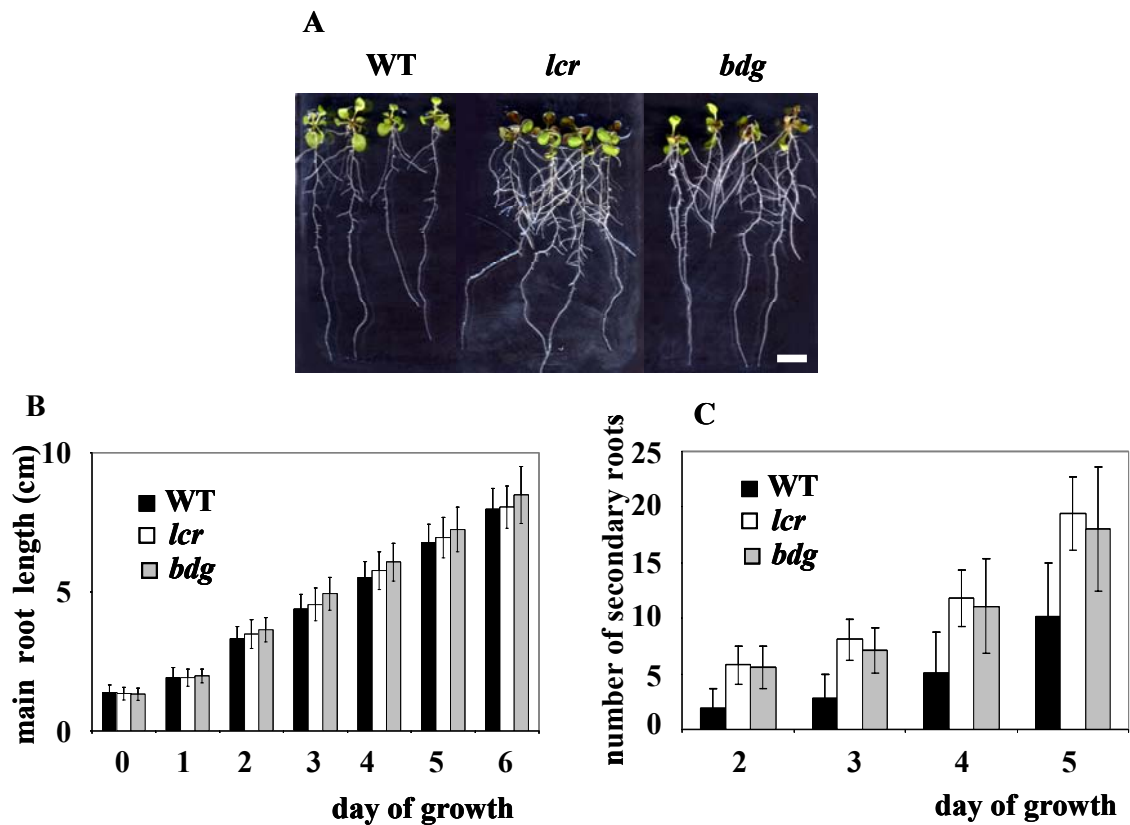


Figure 14. Effects of the *bdg* and *lcr* mutations on root growth. (A) Wild type Columbia, *bdg* and *lcr* plants were grown on vertical plates for a week. The mutants have developed more secondary roots. (B) The length of the main root was recorded on daily bases until 6 days of growth on vertical plates. The graph shows averages and standard deviations based on 16 *bdg*, 15 *lcr* and 32 WT plants. (C) The number of secondary roots was recorded during five days of growth on vertical plates. Averages and standard deviations are shown for 16 *bdg*, 15 *lcr* and 32 WT plants. Bar: (A) 1 cm.

As mutants seemed to be sensitive to water deprivation, some polyethylene glycol (PEG) was added to the media (Eapen et al., 2003). PEG binds water molecules, thus reducing the water potential of the media, without inducing hypertonic stress. But mutants still grew more secondary roots than WT in the presence of various PEG concentrations (Figure. 15_A). Therefore, no effect directly imputable to dehydration by lack of root expansion could be detected. The mutants still tend to grow better in these conditions too (Figure. 15_B)

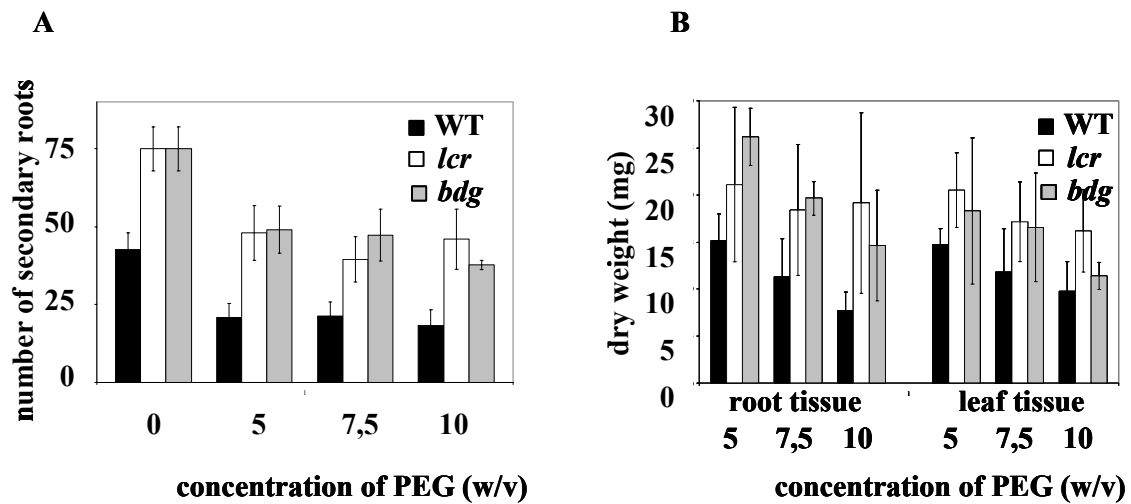


Figure 15. Growth and root development of *bdg* and *lcr* on media containing PEG. (A) Graph showing the number of secondary roots in WT, *bdg* and *lcr* when grown in presence of various PEG concentrations. (B) Weight data for roots and aerial organs from WT and mutants grown in presence of various PEG concentrations for two weeks. Averages and standard deviations are shown, based on at least three plants except for *lcr* “10% PEG” where only data from two plants were included.

Growing *bdg* and *lcr* plants under *in vitro* culture conditions allowed us to confirm the characteristic features of these mutants like leaf fusion and enhance branching and also, to verify that trichome death in *bdg* does not depend on environmental conditions. The repercussion of both, *bdg* and *lcr* mutations, on root development seem to indicate that they affect the hormonal equilibrium of the whole plant. Both proteins may be, through their effect in cutin synthesis, involved in signalling.

3.1.3. The cutin composition of *lcr* and *fdh* leaves is altered

After removing the soluble lipids, we analysed the cell wall bound lipid composition in *lcr* and *fdh* leaves by GC and GC-MS (see Methods). The cell wall bound lipid composition of *lcr* and *fdh* was analysed twice per mutant. Each experiment series included at least five replicates per plant type (see Methods and see **Appendix F for Summary table**). As cuticle composition is influenced by the environment (Faust, 2006) mutants and WT controls have to be grown in parallel.

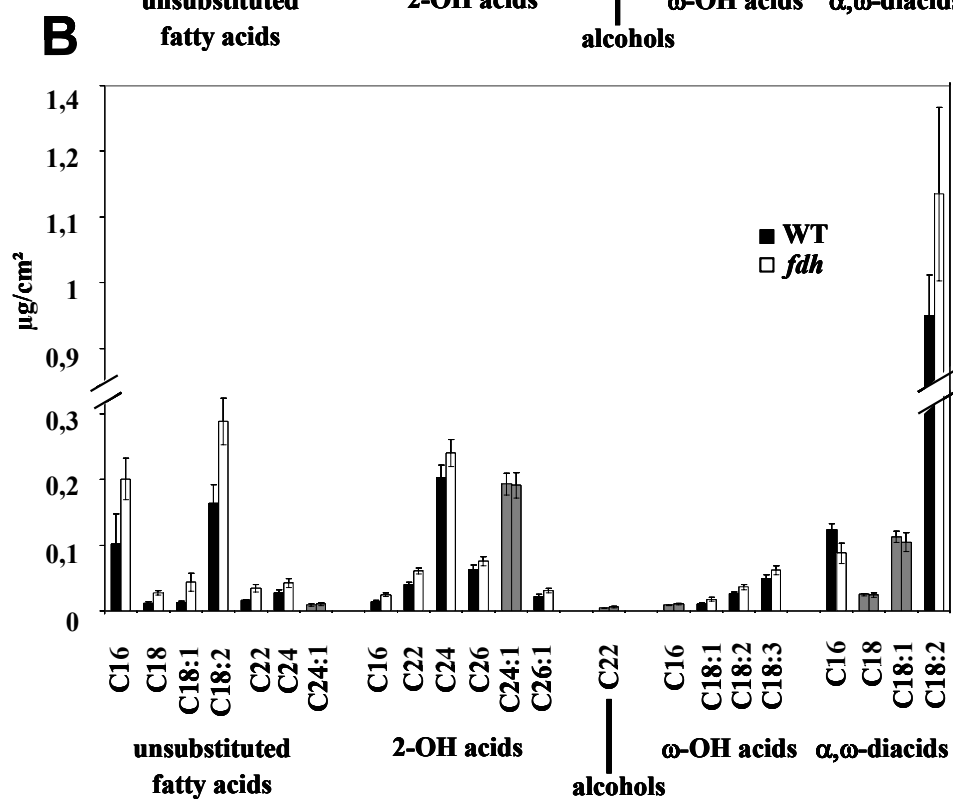
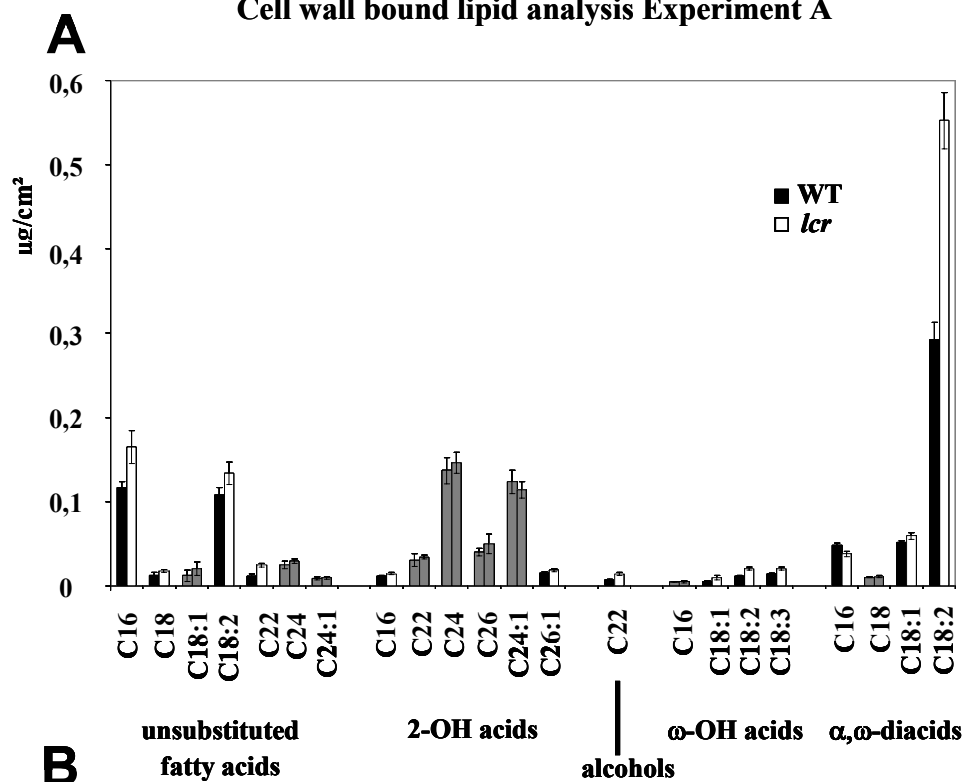
First, *lcr* and WT were sown, two weeks later *fdh* and WT were put on soil. Then, to facilitate the direct comparison between the mutants and to understand how much of the changes in bound lipid composition is due to the respective mutations, *lcr*, *fdh* and

WT control plants were sown in parallel and analysed a second time. The first set of analyses is grouped in experiment A; the second analysis referred to as experiment B.

There are two ways to analyse cutin: the first one consists in the isolation of pure cutin by enzymatic digestion to separate it from the cell wall (Franke et al., 2005). This is quite laborious to do with *Arabidopsis* leaves which cuticle is about 20 nm thick, therefore another method was optimised. This method consists in removing all soluble lipids from leaf pieces by extracting them in chloroform-methanol. After a week or so, of extraction, only cell wall bound lipids are left (Franke et al., 2005). The composition of isolated cutin and cell wall bound lipid residues are similar; monomers belonging to the following functional categories were identified by both methods: very long chain unsubstituted fatty acids, very long chain alcohols, 2-hydroxy acids, ω -hydroxy fatty acids and α,ω -diacids (Franke et al., 2005). However shorter very long chain fatty acids (16-18 unsaturated monomers) and 2-hydroxy acids were found more abundant in the cell wall bound lipids than in the cutin. We therefore decided to sort the monomers identified by cell wall bound lipid analysis into two groups. Thereafter, “typical cutin compounds” refers to very long chain unsubstituted fatty acids (chain lengths of C22, C24), very long chain alcohols, ω -hydroxy fatty acids, and α,ω -diacids; the expression “cutin concomitant compounds” refers to shorter very long chain unsubstituted fatty acids and 2-hydroxy acids.

In experiment A and B, both mutants show a global increase in typical cutin compounds: 60% and 70% for *lcr* and 15% and 30% for *fdh*. The decrease in C16 α,ω -diacid is, in weight, more than compensated by an increase in C18:2 α,ω -diacid, the most abundant cutin monomer (Figure. 16).

Cell wall bound lipid analysis Experiment A



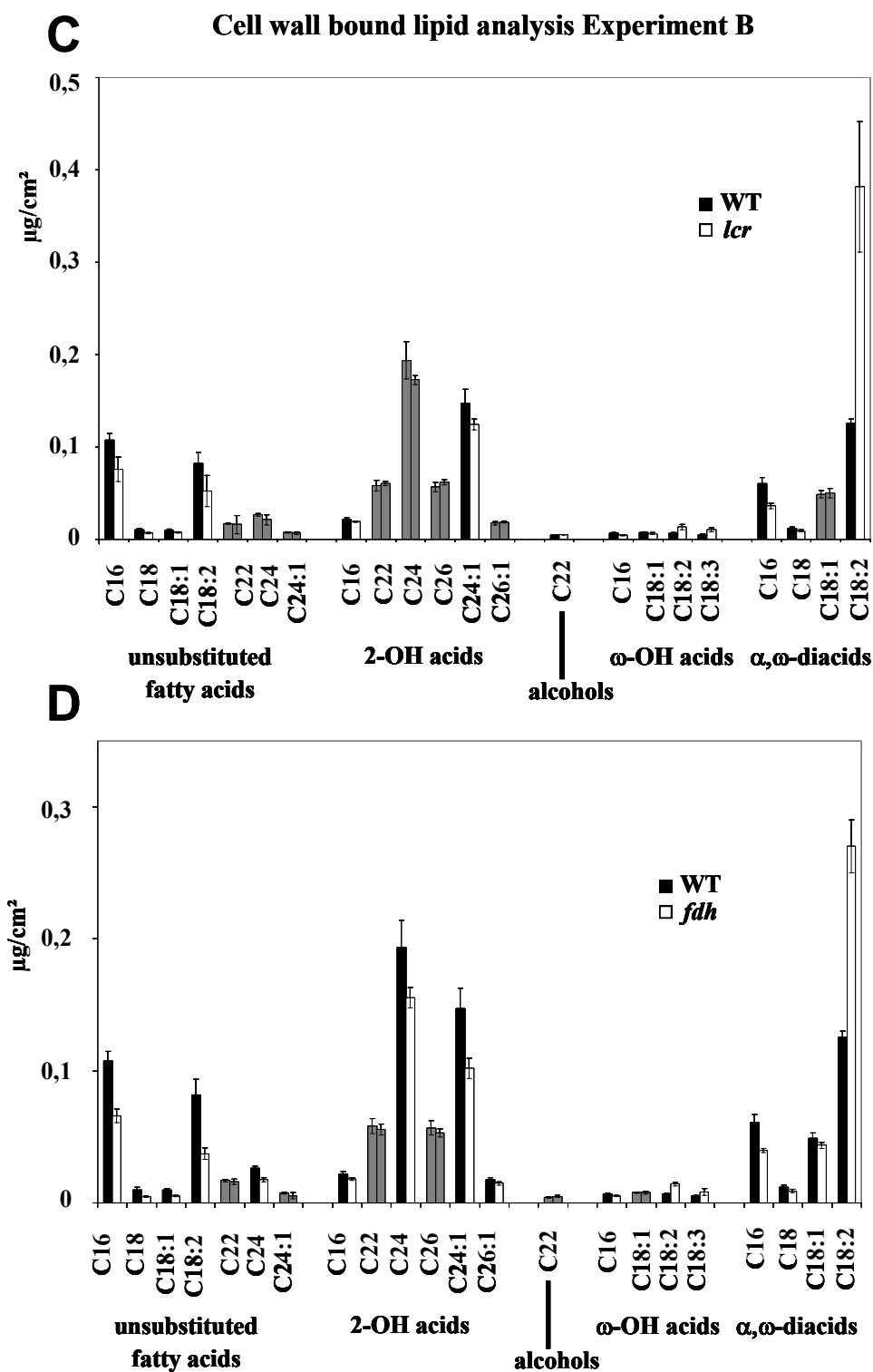


Figure 16. Analysis of cell wall bound lipid from *fdh* and *lcr* mutants. Experiment A (A,B) and B. (C,D) Mean values and standard deviations are plotted on the graphs. When statistically (Mann-Whitney U test; $<0,05$) the difference between WT and mutant amounts were found not significant, the bars are filled with grey. 2-OH acids: 2-hydroxy fatty acids; ω -OH acids: ω -hydroxy fatty acids.

As a matter of fact the amount of C18:2 α,ω -diacid seems to be highly variable. In experiment A, mutants and respective WT controls were sown two weeks apart and the amount of C18:2 α,ω -diacid detected in *fdh*'s WT control ($\sim 0,9 \mu\text{g}/\text{cm}^2$) is three

times higher than in that of *lcr* ($\sim 0,3 \mu\text{g}/\text{cm}^2$) (Figure. 16; A,B). In experiment B, all plants were sown at a time, so there is only one WT control, the amount of C18:2 α,ω -diacid present in WT bound lipids only reached about $0,1 \mu\text{g}/\text{cm}^2$ this time (Figure. 16; C,D). This represents appreciatively a third or a tenth of what was detected in experiment A. The amount of this monomer may be fine tuned according to the environmental conditions. In any case, the amount of C18:2 α,ω -diacid detected in the mutants is higher than in the WT plants. It is nearly always twice higher in the mutants except for *fdh* in the experiment A (Figure. 16 B); in this case the WT accumulated a remarkably high amount of C18:2 α,ω -diacid ($\sim 0,9 \mu\text{g}/\text{cm}^2$) and *fdh* only showed about a tenth increase ($\sim 1,1 \mu\text{g}/\text{cm}^2$). The WT amounts in other monomers were quite similar from an experiment to the other.

The differences observed between the WT and the mutants in typical cutin compounds were reproducible (Figure. 16); this holds particularly true for the very long chain alcohols, the ω -hydroxy fatty acids and the α,ω -diacids. As far as unsubstituted VLCFA (22-24 carbons) are concerned, this mostly remains true as well except for the variation of C24 acid content in *fdh* (Figure. 16). We observed a significant overaccumulation of most of the monomers (Figure. 16), but no modification in the general monomer repartition. The changes in detected shorter chain unsubstituted acids and 2-hydroxy acids appear to be more environmentally related, as they are not consistent between the two rounds of experiments but are similar in both mutants within an experiment (Figure. 16).

Effects of *lcr* and *fdh* on the composition of cell wall bound lipids are comparable. That was quite unexpected as *LCR* and *FDH* have distinct functions (Yephremov et al., 1999; Wellesen et al., 2001).

3.1.4. *Lcr* and *bdg* mutations have little influence on seed coat composition

As *BDG* and *LCR* are expressed during ovule development and as we could observe a defect in seed covering during seed development by toluidine blue staining (Figure. 17), we decided to analyse the seed coat composition of both mutants. As seeds are protected during their development, we may be able to shade off most of the

environmental effects and only observe the effects of the respective mutations. *Bdg* and *lcr* mutations may also have distinct effects on the composition of this polymer.

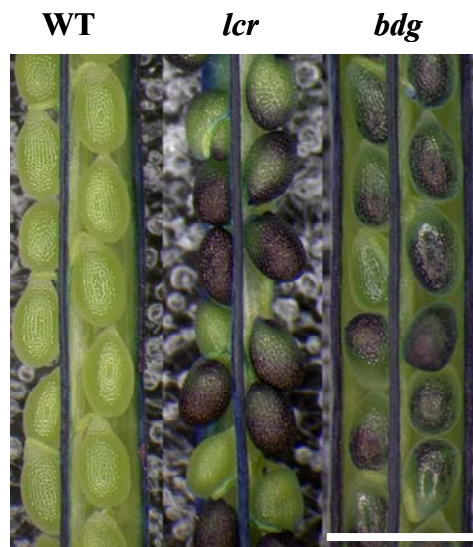
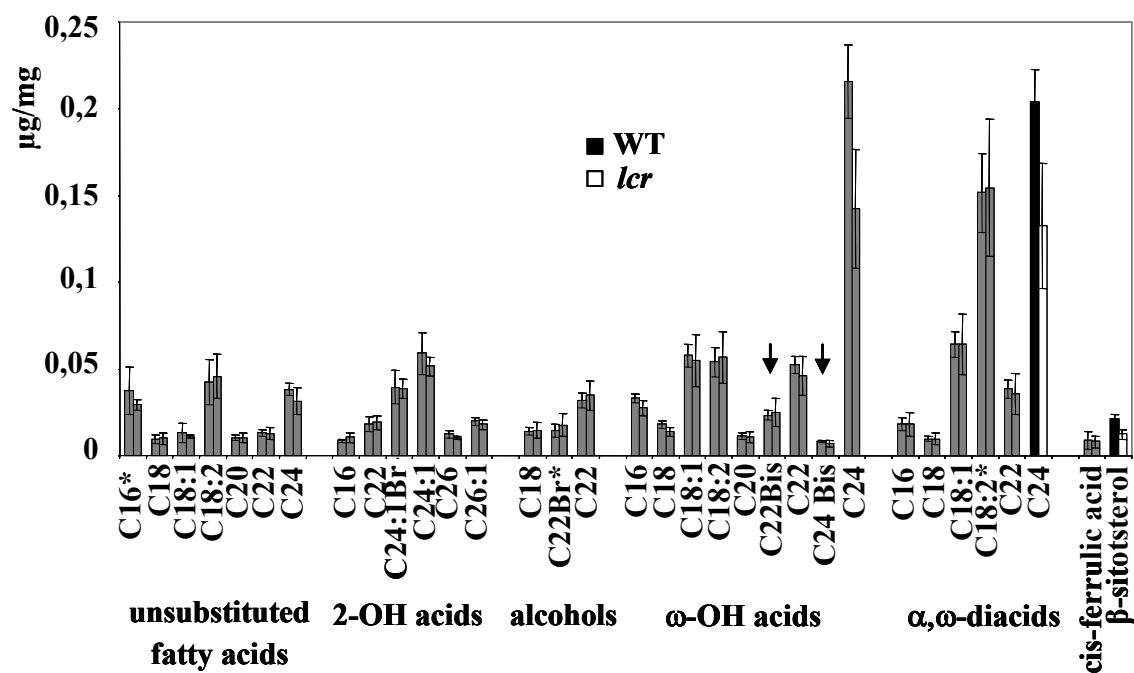
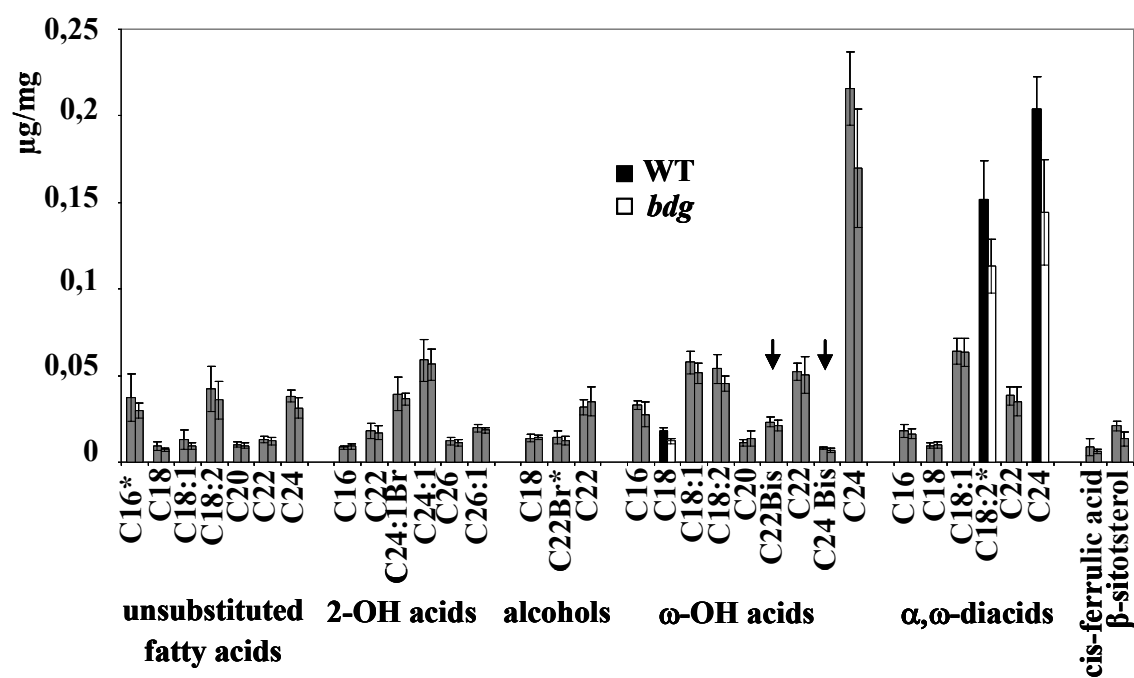


Figure 17. Toluidine blue staining of *lcr* and *bdg* developing seeds. WT, *lcr* and *bdg* ripening seeds after 2 min of immersion in a 0,05% toluidine blue solution. Whereas WT seeds remain unstained, both, *bdg* and *lcr* seeds, are stained. Bar: 1mm.

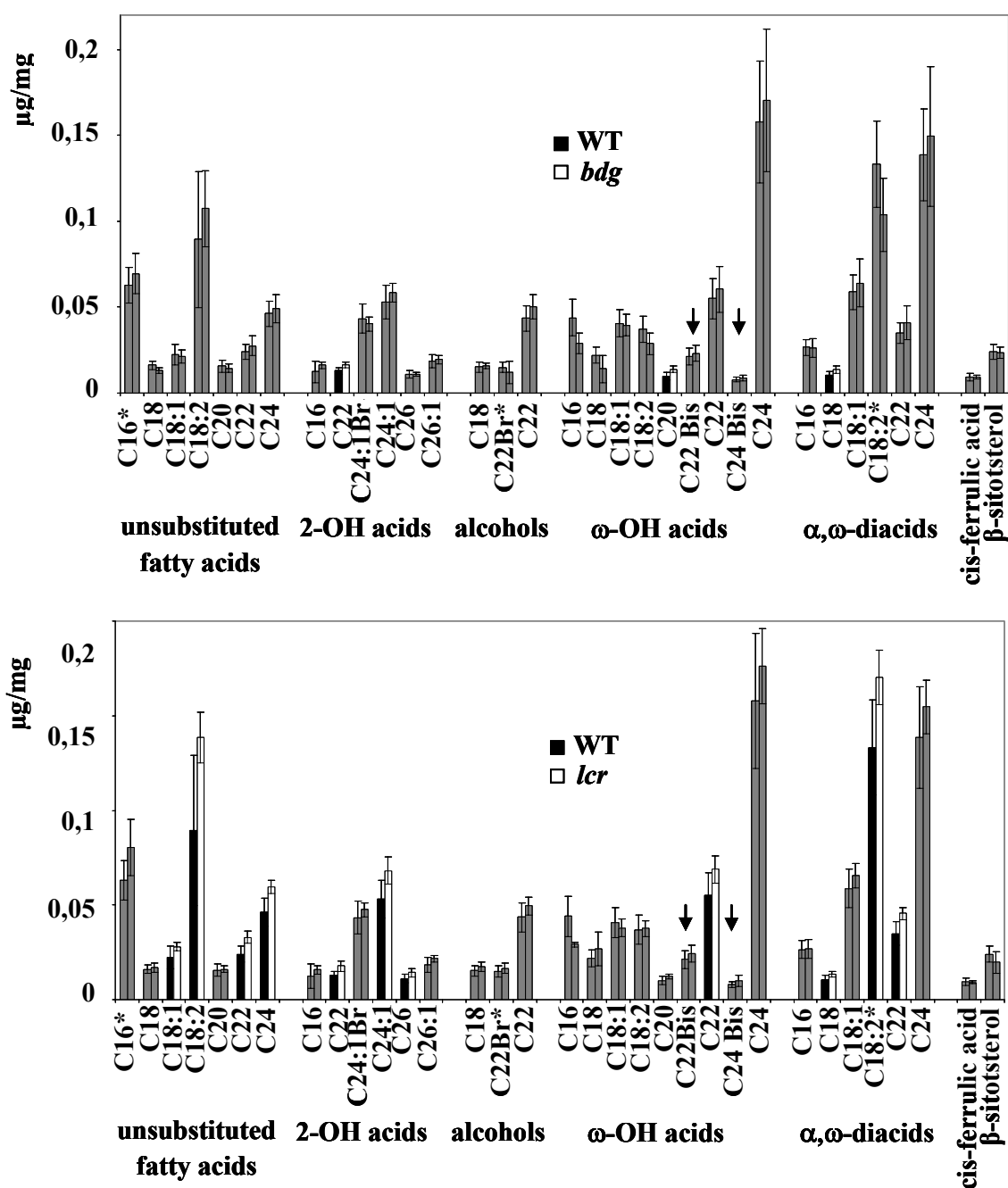
When we became interested in the seed coat composition of our cuticular mutants, no extraction method was available. So we developed a new extraction method: we started from 10 mg of WT seeds and tested if storage lipids could be efficiently removed from intact seeds. Storage lipids are the most abundant lipids in seeds and would mask the seed coat monomers. As after a day of extraction, intact seeds had only released 1% of their total content of storage lipids, we cracked the seeds, using an agate mortar and pestle deep-frozen in liquid nitrogen. We recovered the cracked seeds in chloroform: methanol (1:1) (see Methods) and extracted the soluble lipids, mostly storage lipids in this case, for seven days changing the solvent four times. The amount of extracted storage lipids steeply decreased: after a day of extraction: about 95% of storage lipids were present in the solvent. After seven days of extraction and four solvent changes, only traces of storage lipids were left (0,17 %; 0,5 $\mu\text{g}/\text{mg}$ seed) and we could preliminary determine the composition of the WT Columbia seed coat. Because the amounts of storage lipid left and that of seed coat monomers were in similar ranges, from then on we thus included more solvent changes. In the next experiments, instead of filtering to change the solvent we centrifuged to minimise particle loss (see Methods). We then applied this method to *lcr* and *bdg* seeds.

Most of the changes in seed coat composition of the *lcr* and *bdg* mutants were found to be not statistically different according to the Mann-Wihtney U statistical test ($p < 0,05$) (Figure. 18). This may indeed be attributed to the protection offered by the silique during seed development. This analysis was done twice per mutant, on two independent seed sets. To constitute the samples used the experiment A, seeds from 20-30 *bdg*, *lcr* and WT plants had been respectively pulled together, and four samples taken from the respective pools. Each sample from the experiment B was composed of seeds from three independent plants.

Seed coat analysis Experiment A



Seed coat analysis Experiment B



In experiment A, both mutants tend to accumulate less C24 ω -hydroxy-fatty acid than the WT control, and a clear decrease is observed in C24 α,ω -diacid. *Bdg* seed coat also showed a reduction in C18:2 α,ω -diacid (Figure. 18). In experiment B, these differences were not observed: levels of C24 ω -hydroxy fatty acid and of C24 α,ω -diacid in *bdg* and *lcr* were similar to that of WT, and this time *bdg* did not show a significant decrease C18:2 α,ω -diacid (Figure. 18). The comparison of both series of experiments revealed that the level of C24 ω -hydroxy fatty acid in the mutants was similar in both experiments but that of the WT control was much higher in the first than in the second series (Figure. 18), dropping from about 22 $\mu\text{g}/\text{mg}$ seed to 18 $\mu\text{g}/\text{mg}$ seed.

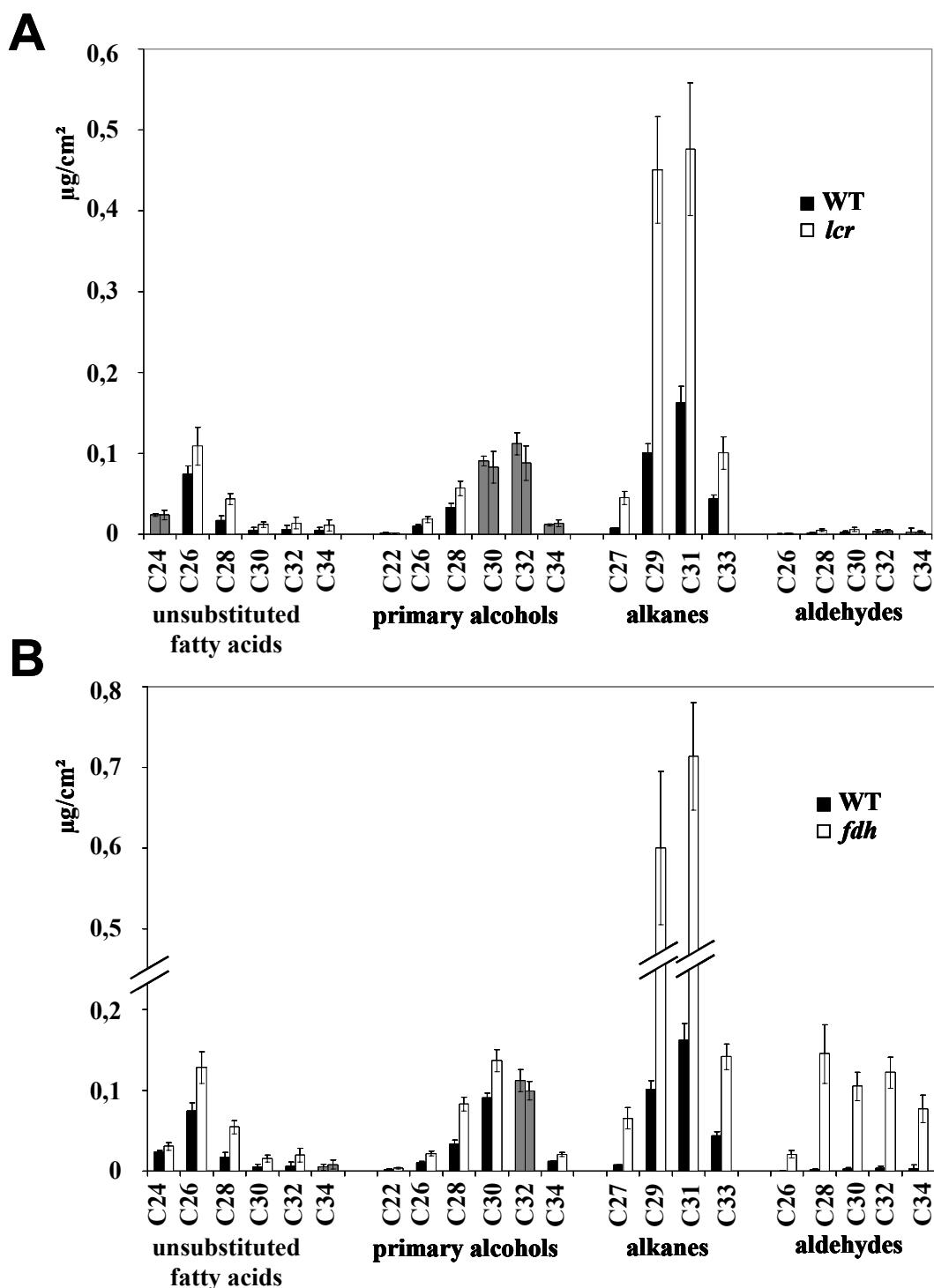
An overaccumulation of seed coat monomers was observed neither in *lcr* nor in *bdg*, this may be because of silique protection and weak environment impact or else, because both mutations do not really or directly influence the seed coat composition.

3.1.5. *Lcr* and *fdh* mutations influence wax composition

Bdg accumulates more wax than WT plants (Kurdyukov et al., 2006b) and, in this mutant, the wax biosynthesis pathway is upregulated (Kurdyukov et al., 2006b); see Microarray). As the microarray data also revealed the up-regulation of genes involved in the wax biosynthesis in *lcr* and *fdh* (see Microarray), we checked whether this up-regulation is also accompanied by a greater wax accumulation in these mutants.

Wax load from *lcr* and *fdh* leaves were analysed by GC and GC-MS (see Methods; (Kurdyukov et al., 2006b). The wax analysis had already been performed on the *lcr* mutant (R. Franke, personal communication), results obtained in both experiments are very similar.

In average, wild-type leaves had a wax load of $0,72 \pm 0,07 \mu\text{g}/\text{cm}^2$, *fdh* leaves a wax load of $2,66 \pm 0,25 \mu\text{g}/\text{cm}^2$, and *lcr* leaves $1,57 \pm 0,25 \mu\text{g}/\text{cm}^2$. In average, this represents a 3,7 and a 2,2 fold increase in wax per cm^2 in *fdh* and in *lcr* mutants, respectively. This is mainly due to a greater accumulation of alkanes in both mutants and, in the case of *fdh*, also due to the massive accumulation of aldehydes (Figure. 19).



←Figure 19. Influence of the *lcr* (A) and *fdh* (B) mutations on the wax composition in their leaves. Mean values of at least five replicates, each containing a leaf from at least ten independent plants, and standard deviations are plotted on the graphs. When statistically (Mann-Wihtney U test; $p < 0,05$) no significant difference was found between WT and mutant, the bars are filled with grey.

Most of the monomers accumulate in both mutants; the most abundant monomers namely the alkanes show the strongest increase in *lcr* (4 fold per cm^2). The *fdh* waxes also have a greater amounts of alkanes (5,7 fold), however this is not the only massive

accumulation observed in this mutant: a drastic increase in the aldehydes amounts (46,3 fold) is observed in this mutant.

Polycyclic alcohols, namely brassinosterol, β -sitosterol, campesterol and cholesterol, were also identified in mutant and WT waxes. As the aliphatic monomers, they were found to accumulate more in both mutants: globally *fdh* waxes contains three times more polycyclic alcohols per cm² and *lcr* twice more (data not shown). In relative amounts, however there is no much of a difference: when included in the calculations, the polycyclic alcohol group represents app. 11% of the wax monomers in the WT, about 9 % in *fdh* and about 11% in *lcr* (data not shown).

In proportion, unsubstituted acids and primary alcohols are less abundant in both mutants and the alkane share of both mutants is greater. In *lcr* there are proportionally less aldehydes than in the WT, and in *fdh* much more (Figure. 20).

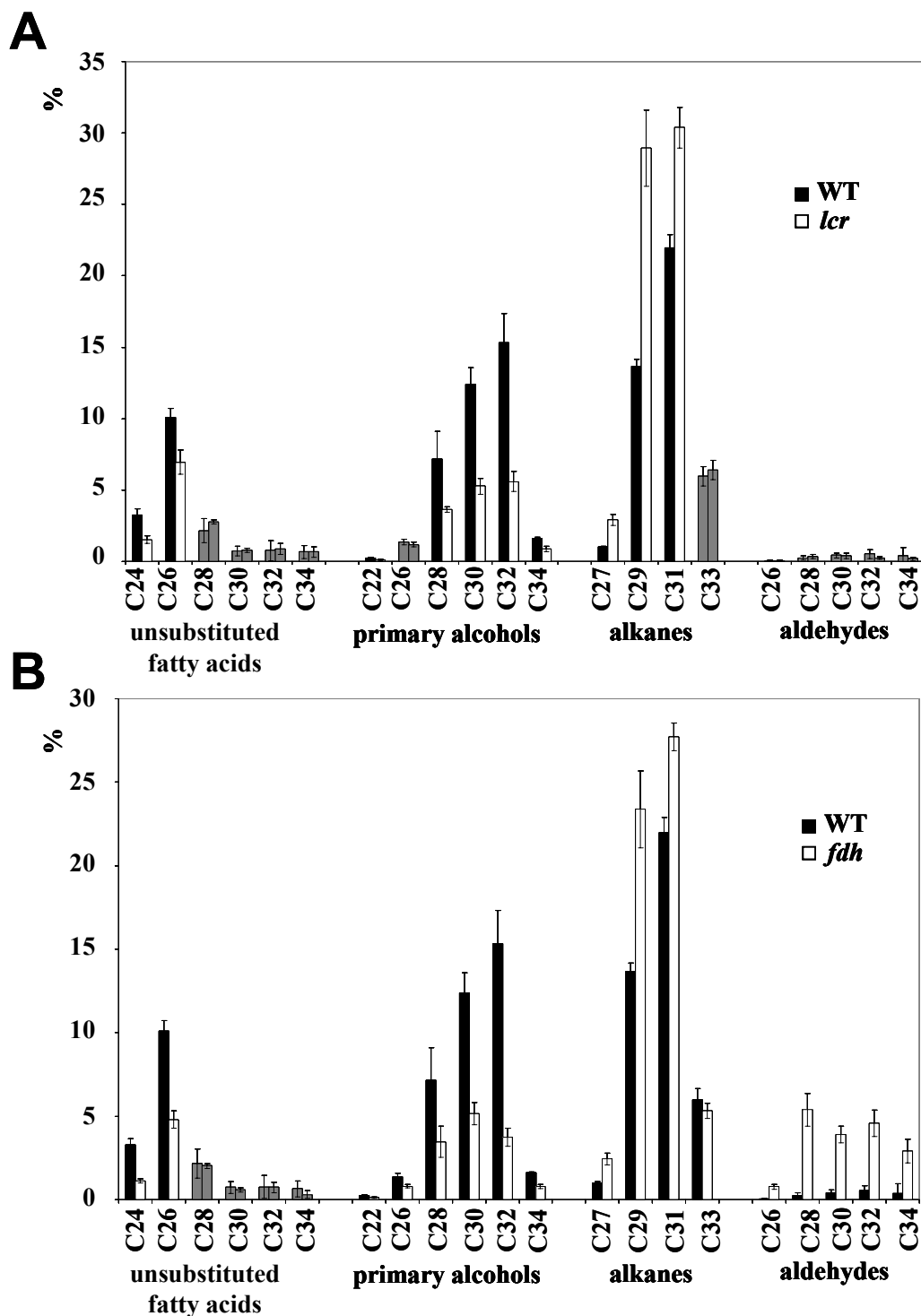


Figure 20. Wax composition of WT, *lcr* (A) and *fdh* (B) leaves. Amount of each monomer is expressed as a percentage of the total amount of aliphatic monomers. When WT and mutant amounts were not found statistically (Mann-Whitney U test; $p < 0.05$), bars are filled with grey.

In summary, *fdh* and *lcr* mutations affect wax composition, leading to an increase in wax load per square centimetre and to disequilibrium between the compound categories. The former suggest these mutants may try to overload their epidermal

surface with wax, to cope with the deficiency of their outermost coating, and the latter suggest that the mutants try to adjust the hydrophobic properties of their waxes.

3.1.6. The wax deposition is altered in *lcr* and *fdh* mutants

As the wax deposition and crystal shapes have been reported to be influenced by wax composition (Jetter and Riederer, 1994; Rashotte and Feldmann, 1998), we examined mutant leaves under SEM (Figure. 21). Crystals are usually absent from the surface of *Arabidopsis* leaves; here the wax overproduction in the mutants can be correlated to the visible presence of wax on the surface of leaves, particularly in the case of *lcr* and *fdh*.

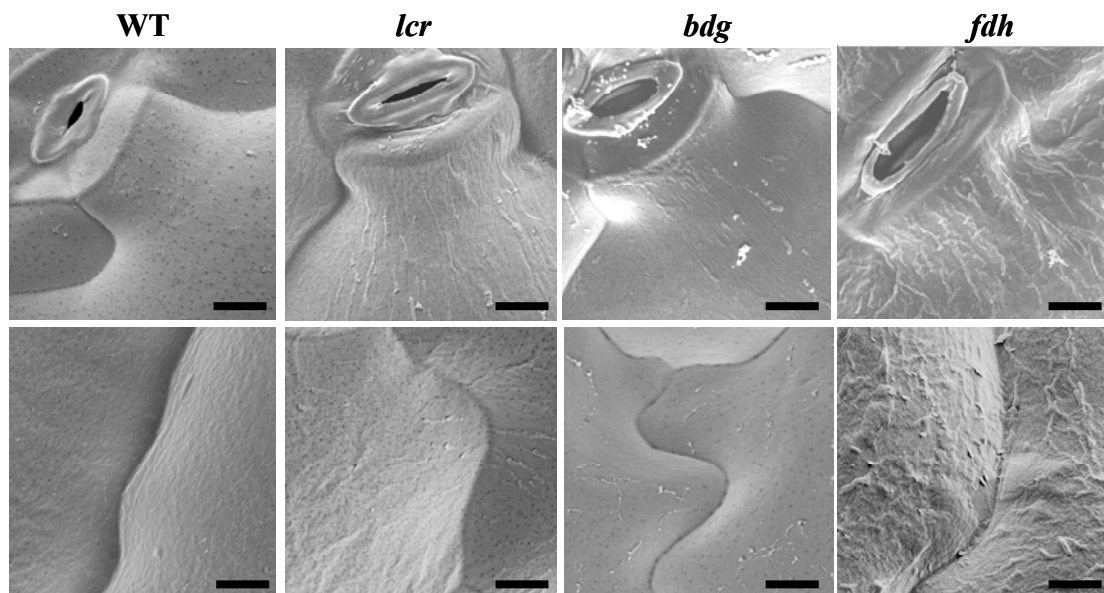


Figure 21. Scanning electron micrographs of the adaxial side of WT, *lcr*, *bdg* and *fdh* rosette leaves. At least four rosette leaves per plant type was observed under SEM. The surface of WT leaves is smooth whereas the surface of *fdh* leaves is covered by “wax flows” from which thin plate-like crystals often emerge. Less wax flows are visible in *lcr* which appears to have an irregular wax covering. In the case of *bdg* only rare wax flows can be found on the leaf surface. Plants were seven weeks old (short day conditions). Bar: 5 µm.

On the surface of *bdg* leaves, crystals are only rarely seen. The uniform wax overaccumulation in this mutant (Kurdyukov et al., 2006b) may just lead to an increase in thickness of the uniform wax layer present on the leaf surface and not to the formation of visible crystal structures. However no conclusion can be drawn about crystal shape from the observation of *fdh* leaves. As wax is more abundantly deposited on stems, stem is a privileged tissue for observation of wax crystals; assuming that the mutations would affect the wax composition of the stems in the same way that they do in leaves, we observed stems under SEM (Figure. 22). The

abundance in wax crystals was similar in WT and mutants, yet the three mutants were found to deposit more crystals shaped like horizontal plates than ropes or dendrites on the surfaces of their stems (Figure. 22). Thus, the increase in aldehyde observed in *fdh* does not seem to be the cause of this change.

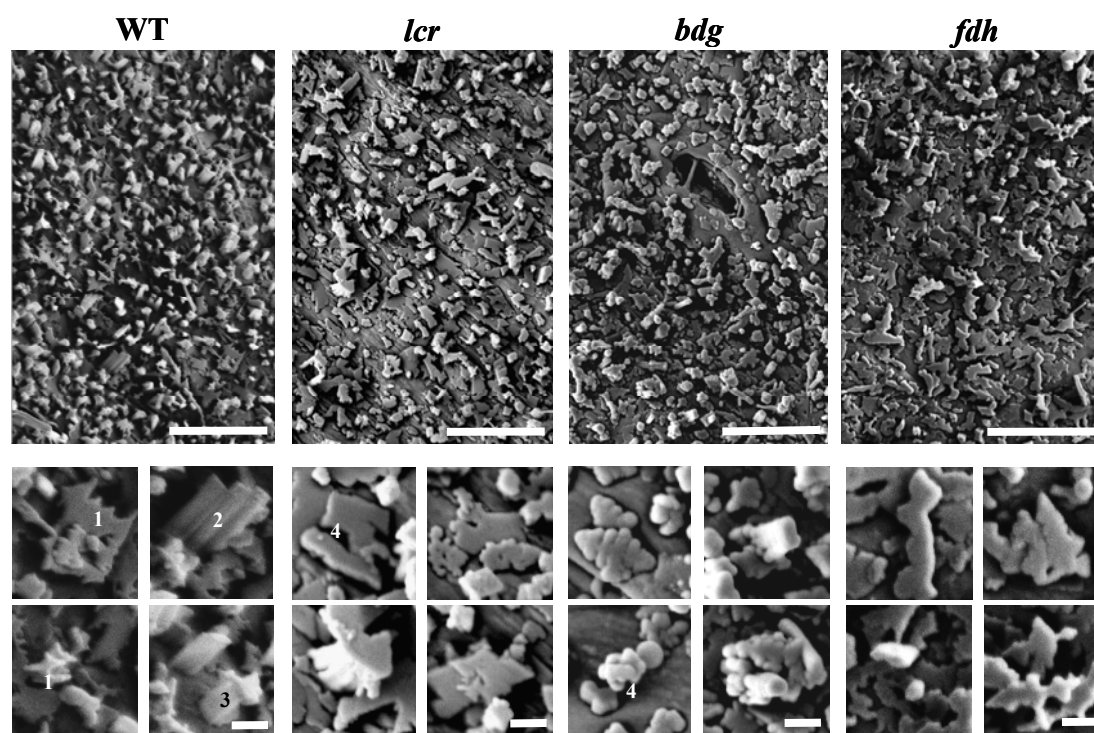


Figure 22. Scanning electron micrographs of the stem surface of WT, *lcr*, *bdg* and *fdh* stems. Two stems (4th or 5th internode) were observed per plant type. WT waxes mostly contain dendrites (1), ropes (2) and umbrellas (3) whereas mutant samples mainly display horizontal plates (4). Plants were 12 weeks old (first eight weeks short day then four weeks long day). Bar: overview: 5 μ m and zoom: 1 μ m.

3.1.7. Overaccumulation of wax in *bdg* corresponds to a genetic up-regulation

That *bdg* accumulates wax components and particularly more alkanes, led us to check whether this was correlated with the up-regulation of the *CER1*, *WAX2* and *WIN1/SHN1* genes.

Overexpression of the *WIN1/SHN1* (At1g15360) ethylene response factor-type transcription factor leads to wax accumulation in *Arabidopsis* leaves and stem (Aharoni et al., 2004; Broun et al., 2004) and modification of cutin composition (Kannangara et al., 2007). The overexpression of *WIN1/SHN1* also leads to the activation of several genes involved in the wax biosynthesis, among them *CER1* (At1g02205) (Broun et al., 2004), coding for a putative aldehyde decarbonylase (Aarts et al., 1995) or a protein involved in alkane exportation (Broun et al., 2004).

The WAX2 (At5g57800) protein may be involved in wax biosynthesis as the *wax2* mutant deposits less product from the putative decarboxylation pathway (Chen et al., 2003). The precise function of this protein, showing 32% of identity to CER1, remains unknown.

By semi-quantitative RT-PCR, we showed that in the *bdg* mutant the *CER1* transcript significantly accumulates to greater amounts, that *WIN1/SHN1* mRNA has the tendency to be more present and that the level of *WAX2* transcript is not modified (Kurdyukov et al., 2006b).

We analysed the transcriptom of *lcr*, *bdg* and *fdh* mutants using Affymetrix ATH1 chips. And, according to our microarray data and the semi quantitative RT-PCR done to confirm them, we found that the *WAX2* transcript is significantly more present in the three mutants and that of *CER1* was only slightly more abundant (Figure. 23 and Figure. 24). We did not recheck the level of *WIN1/SHN1* by RT-PCR as from our microarray data set it was clearly not found significantly changed; the expression level of this gene was found below the detection level in both WT and mutants.

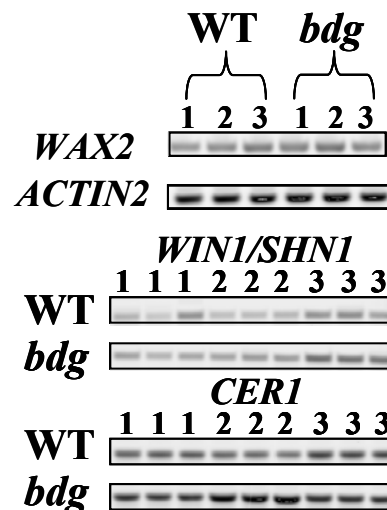


Figure 23. Modification of the expression level of genes implicated in wax biosynthesis in *bdg*. The quantity of each transcript was estimated by semi-quantitative RT-PCR (after optimisation of number of cycle; see Methods). In this case the *ACTIN2* (At3g18780) and the *CER1* (At1g02205) transcripts were amplified for 24 cycles. Three independent WT and three independent *bdg* samples were used as templates, once in the case of the *WAX2* and *actin2* genes, and three times (technical replicates) for the *WIN1* and *CER1* genes.

The fact that the genes involved in wax biosynthesis are highly environmentally and physiologically regulated may explain this apparent contradiction, both, the plant age (eight VS five weeks and a half), leaf size (0,5-1 cm VS 0,2-1 cm), and the environmental conditions (greenhouse VS growth chamber) may all have contributed to this discrepancy. However, both results point out that in the *bdg* mutant transcripts from the wax biosynthesis and particularly, the putative decarbonylation pathway, accumulate to higher levels.

The increase in wax deposition may be linked to the higher level of transcripts from the decarbonylation pathway, achieved by transcript stabilisation or gene upregulation, or linked to modification of the catalytic properties of the respective enzymes. The latter may be boosted by increase of substrate availability, quicker product channelling, or may also undergo secondary modifications.

3.1.8. *Bdg*, *lcr* and *fdh* mutations lead to major changes in gene regulation

The results of our biochemical analysis suggest that *bdg*, *lcr* and *fdh* mutants, appear to compensate the absence of a completely functional cuticle by, for instance, accumulating more cutin and wax monomers. Using microarrays, we analysed the transcriptional changes taking place in gene expression in these three mutants, to see whether a parallel can be drawn between physical accumulation of cuticle compounds and mis-regulation of genes which potentially could contribute to these changes. This microarray analysis may also shed light on secondary phenotypes of cuticular mutants and pinpoint effects of each mutation.

A method for handling of microarray data

Total RNA from three wild-type Col0 samples and three samples of each mutant (*lcr*, *bdg* and *fdh*) were hybridised to ATH1 Affimetrix microchips (see Methods). We first sorted out the genes and defined the list of candidates for RT-PCR confirmation according to the results obtained for two replicates, sent first. The inclusion of the results from the third replicate allowed us to establish a sorting method for our genes and to narrow down the list of mis-expressed genes in our mutants (data not shown).

Considering the results from the two first replicates, we only included genes showing a consistent mis-regulation greater than a 2 fold increase or decrease, in a mutant, in the list of putatively mis-regulated genes. However after the incorporation of the results from the third replicate, it became clear that this method was too stringent, because some genes found mis-regulated by RT-PCR (Figure. 24) had not been included in the list of putatively mis-regulated genes (data not shown). We therefore decreased the stringency of our criteria by including genes, which once showed a change smaller than a 2 fold increase or decrease. Thus, combining our RT-PCR results and data sorted with MicroarraySuite, we defined a representative sorting method (see Methods) for microarray results.

Validation of microarray data

We first checked whether the transcripts from the mutated genes were respectively less abundant in the mutants. The level of *FDH* transcript is consistently lower in the *fdh* mutant (Yephremov et al., 1999), and the *FDH* gene is found among the consistently downregulated genes in our microarray data.

The mRNA from *LCR* and *BDG* only showed a tendency to be less abundant, both genes are absent from the list of consistently downregulated genes from their respective mutant. The presence of the mutations may not significantly influence the stability of their respective mRNA. We also observed that a mutation in one of these three genes does not affect the expression of the other two.

Then we chose 12 genes among the putatively upregulated genes in the three mutants for confirmation by RT-PCR. We also included *CERI* as it was shown to be up-regulated in *bdg* before (Figure. 23; (Kurdyukov et al., 2006b). Two third of the candidates are potentially involved in lipid biosynthesis or trafficking, the others respectively encode a palmitoyl-protein thioesterase (named *PPT1*), an extensin (*XTH8*) and two *ERF/AP2* transcription factors.

We first optimised the number of cycles of amplification for each gene on WT total RNA, and then performed the semi-quantitative RT-PCR on the RNA samples sent for microarray hybridisation (Figure. 24).

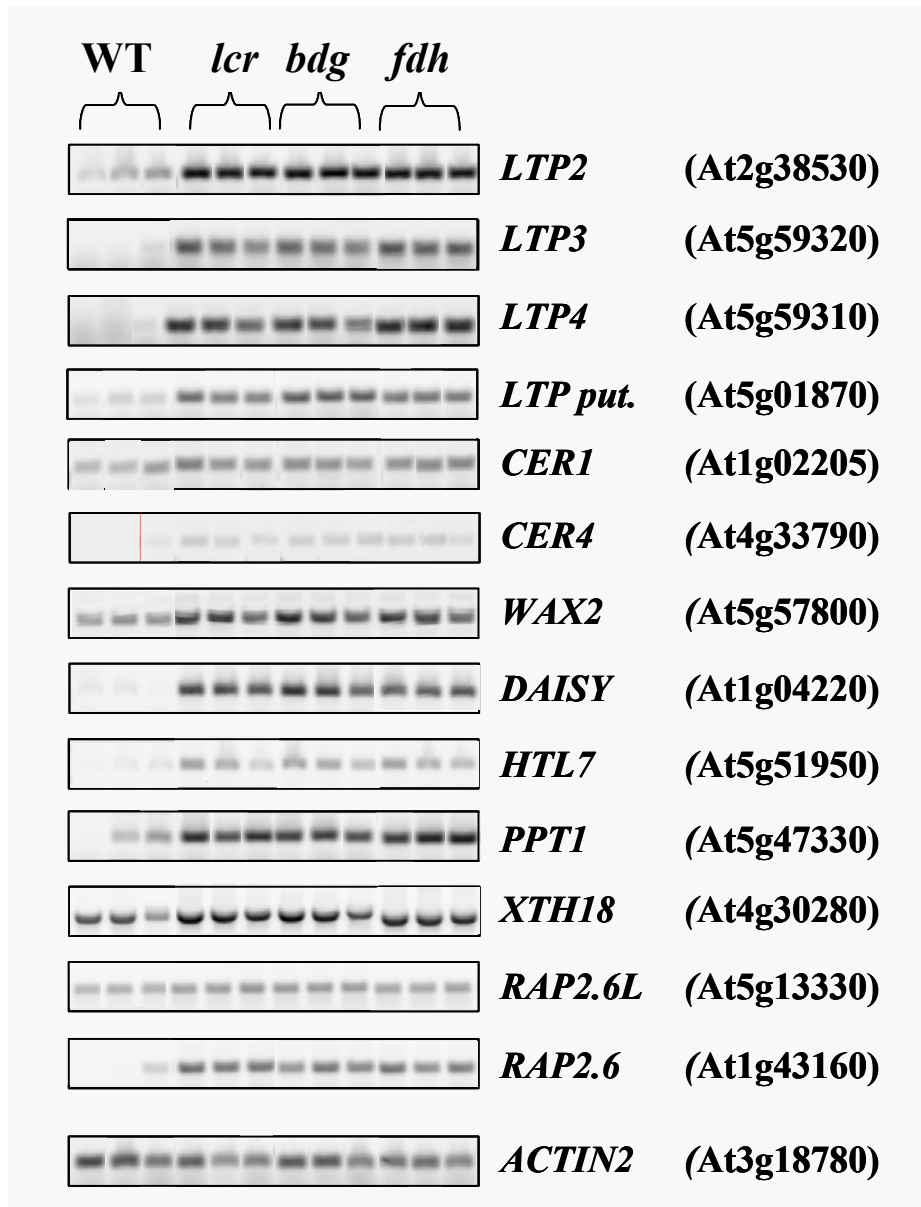


Figure 24. Confirmation of the microarray data by semi-quantitative RT-PCR. Twelve candidates among the most up-regulated genes were chosen for data confirmation by semi-quantitative RT-PCR. *CER1* (At1g02205) was also included as it was previously found to be induced in the *bdg* mutant (Kurdyukov et al., 2006b) *ACTIN2* (At3g18780) was amplified as control. In this experiment, the *ACTIN2* (At3g18780) and the *CER1* (At1g02205) transcripts were amplified for 22 cycles.

The transcript of all the candidate genes was found more present in the mutant samples. The mRNA of the *CER1* gene, which was not in the list of commonly mis-regulated genes, was found slightly more abundant in the mutants. In conclusion the RT-PCR results match well the microarray data which could then be further analysed.

General repartition of the consistently mis-regulated genes

According to applied criteria, more genes were found to be mis-regulated in *fdh* (333) than in *lcr* (158) or *bdg* (80). Some of the genes were mis-regulated in all three mutants, only in two or in one of them (Figure. 25). The majority of consistently mis-regulated genes is potentially epidermis specific according to the microarray data from Beisson and co-workers who compared the transcriptome of epidermis from *Arabidopsis* stems to that of whole stems (Suh et al., 2005). Relatively few mis-regulated genes were downregulated: 27 in *fdh*, 5 in *lcr*, and 8 in *bdg*. Only one gene from the set of consistently mis-regulated genes was differentially mis-regulated between the mutants: At1g01470 was found to be upregulated in *lcr* and *fdh* but downregulated in *bdg*. At1g01470 encodes the late embryogenesis abundant protein14 (LEA14) also known as light stressed-regulated 3 (LSR3). This protein is involved in response to wounding and stress by high light intensity (Dunaeva and Adamska, 2001) and may be epidermis specific according to microarray data (Suh et al., 2005). The members of the multigenic family encoding the LEA proteins are usually expressed to protect tissues from desiccation damage and are abundantly expressed in the embryo at the end of seed development (Blackman et al., 1995; Delseny et al., 2001).

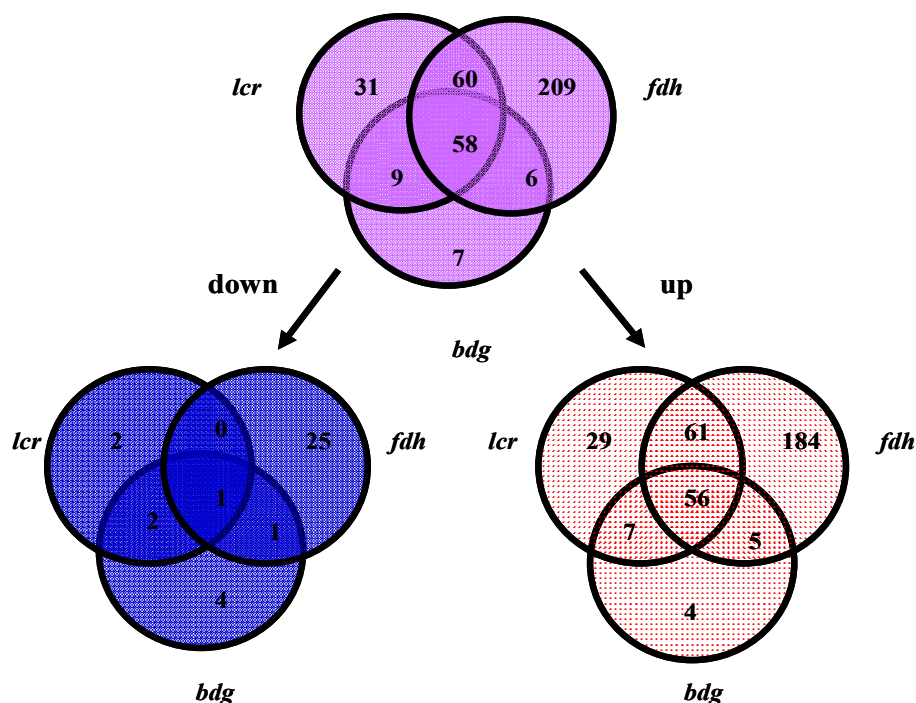


Figure 25. Venn diagrams showing the repartition of mis-regulated genes by the *lcr*, *bdg* and *fdh* mutants. In violet, mis-regulated genes; in blue, downregulated genes; in red, upregulated genes.

The effect of the *lcr*, *fdh* and *bdg* mutations on the expression of closely related genes

As *LCR*, *FDH* and *BDG* belong to multigenic families in Arabidopsis, the upregulation of a gene of their same families constitute the most straightforward way to compensate the mutations.

The disruption of the *LCR*, *BDG* and *FDH* genes triggers the up-regulation of At1g04220, a beta-ketoacyl-CoA synthase from the fatty acid elongase (FAE) family. A 12 to 16 fold upregulation is observed in the mutants. This beta-ketoacyl-CoA synthase may be epidermis specific (Suh et al., 2005), is active when expressed in yeast, and could elongate C16 and C18 endogenous fatty acids to form C22, C24 and C26 acids (Trenkamp et al., 2004). The activity of this enzyme was recently described *in planta*, it was named DAISY (R. Franke, personal communication).

In the case of *fdh*, the expression of two other elongases is altered: *CUT1/CER6* (At1g68530) and At2g28630 were also found up regulated, however to a lesser level than *DAISY*; 2,4 and 3,4 fold respectively. The suppression of *CUT1/CER6* gene leads to a sharp reduction in both decarboxylation and acyl reduction pathways from the wax biosynthesis, giving the plants a waxless appearance (Millar et al., 1999). *CUT1/CER6* is epidermis-specific and its silencing blocks the production of wax compounds with a chain length longer than to 24 carbons (Millar et al., 1999).

The disruption *LCR*, *BDG* and *FDH* genes did not trigger a significant mis-regulation of any member of the CYP86 family, to which *LCR* belongs, except for the *LCR* gene in the *lcr* mutant. However *lcr* and *fdh* mutations trigger the upregulation of the *CYP94C1* gene (At2g27690) by 15 and 13 fold, respectively. In *bdg*, the increase in transcript level was not found significant; the quantity of *CYP94C1* RNA remaining below the detection level. This cytochrome P450 enzyme was recently shown to be able to catalyse the formation of α,ω -diacids *in vitro* using C12 to C18 acids as substrate (Kandel et al., 2007). According to the data from Beisson and co-workers, this gene is probably not epidermis specific (Suh et al., 2005). *Lcr* and *fdh* mutations may therefore promote its expression in epidermis.

The *fdh* mutation triggers the upregulation by 2,8 times of *HYD2* (At5g41900) which is amongst the closest homologues of *BDG* (Figure. 7) and is likely epidermis specific

(Suh et al., 2005). This gene is not on the list of consistently misregulated genes for the two other mutants but still shows an upregulation tendency.

As expected the disruption of these three cuticular genes, particularly *lcr* and *fdh*, triggers the induction of a member of their family.

The range of commonly upregulated genes in the three mutants

According to the microarray data obtained on stem peels by Beisson and co-workers, most genes from the commonly upregulated category (39/56) are probably epidermis specific (Suh et al., 2005)(see **Appendix G for list of commonly misregulated genes**).

Among the 56 commonly upregulated genes from these mutants, there are genes that were reported to act in lipids metabolism (14/56), some of them are cuticular genes. *WAX2/YRE/FLP1* (At5g57800) function is related to wax biosynthesis (Chen et al., 2003). *CER4* (At4g33790) encodes an alcohol-forming fatty acyl-CoA (FAR) responsible for the production of primary alcohols during wax biosynthesis (Rowland et al., 2006). The transcripts of some homologues of known cuticular genes were found in much higher amounts in the mutants: that of the DAISY elongase (see above) and of *HOTHEAD-LIKE7* (At5g51950; *HTL7*; (Krolkowski et al., 2003), for instance. The latter is homologous to the epidermis specific *ACE/HTH* gene, which encodes for a fatty acid ω -hydroxylase. Cutin from *ace/hth* mutant contains more ω -hydroxy-fatty acids and less α,ω -diacids (Kurdyukov et al., 2006a).

In our analysis the At2g04570 gene, coding for a putative lipase of the GDSL family, was found up-regulated. This protein may catalyse the formation of alcohols from esters and its mRNA was found more present in *WIN1*-HA plants, over expressing the *WIN1/SHN1* gene (Kannangara et al., 2007). As observed by Broun and co-workers, this GDSL protein shares some similarity with EXL1-3, the member of a group of extracellular lipases, involved in the formation of pollen coat (Mayfield et al., 2001). Apart from these genes that appear to be involved in cuticular lipid synthesis, five genes coding for lipid transfer proteins (LTPs), were induced in the *lcr*, *bdg* and *fdh* mutants. Proteins of this large multigenic family are likely to be involved in lipid transport: *in vitro* assays show that they are able to bind fatty acids and to transfer

phospholipids between membranes (Douliez et al., 2000). The expression of the *LTP3* (At5g59320) and *LTP4* (At5g59310) genes is upregulated by abscisic acid (ABA) (Arondel et al., 2000), and their product was localised to the cell wall (Kader, 1996). Both genes are expressed in flowers; *LTP3* is also expressed during seed development and *LTP4*, in siliques. *LTP2* (At2g38530) is localised in the plasma membrane and may transfer phospholipids to the plasma membrane (Dunkley et al., 2006). The application of *LTP2* from barley on tobacco leaves protects the later against the pathogen *Pseudomonas syringae* (pv. tabaci 153) (Molina and GarciaOlmedo, 1997). The expression of two genes encoding putative LTPs, namely At5g01870 and At3g22600, were also strongly enhanced in our mutants. At5g01870 is similar to *LTP6* and present in endomembrane whereas the putative LTP-protease inhibitor At3g22600 maybe attached to the external face of the plasma membrane by a glycosylphosphatidylinositol (GPI) anchor (Eisenhaber et al., 2003). *Arabidopsis* transgenic plants overexpressing At4g12470, At4g12480 or At4g12490, three members of the *LTP* family, are resistant to *Botrytis cinerea* (Chassot et al., 2007).

Transcripts from nine genes potentially associated with cell wall maintenance and remodelling were also found among the commonly upregulated genes. Four of them code for structural elements of the cell wall, namely two hydroxyproline rich proteins (At5g09530 and At2g16630) and two glycine rich proteins (At4g21620 and At3g20470). The transcript of the *GPR5* gene (At3g20470) was also found in greater abundance in *bdg*, *lcr* and *fdh*. The glycine rich protein *GPR5* may be another structural element of the cell wall or the protein may be anchored to the plasma membrane (Sachettomartins et al., 1995). The expression of the *GPR5* gene is restricted to the epidermis of aerial organs and plays a role during the initiation of lateral shoots (Sachettomartins et al., 1995). The activity of this gene is precisely tuned during ovule-seed development: first expressed in all embryonic cells, it is only detected in the protoderm from the torpedo stage on (Magioli et al., 2001). Sachetto-Martins and co-workers found that the *GPR5* gene is expressed at a high level in cells undergoing dedifferentiation prior to somatic embryogenesis. Later, the expression of *GRP5* in the protoderm may be necessary to strengthen the epidermal cell wall thus delimitating growth. The *XTH18* (At4g30280), *XTH19* (At4g30290) and *ATEXT4* (At1g76930) mRNAs were also more present in mutant samples. The corresponding proteins are two extensins and one hydroxyproline-rich glycoprotein (HRGPs), which

are abundant in the cell wall and contribute to its elasticity by acting on sugar bounds. *XTH18* and *XTH19* are preferentially expressed during root development (Yokoyama and Nishitani, 2001; Vissenberg et al., 2005; Osato et al., 2006); *XTH19* expression is regulated by auxin (Osato et al., 2006) and *XTH18* is normally involved in primary root elongation. A slight decrease in *XTH18* transcript in RNAi transgenic plants leads to a small diminution in epidermal cell length (Osato et al., 2006). *ATEXT4* transcript is preferentially expressed in root development but, to a lower level, also in inflorescences. The *ATEXT4* is similar to *ATEXT1* which is strongly upregulated in leaves upon wounding, exogenous application of salicylic acid, methyl jasmonate, auxins, brassinosteroids (BR) (Merkouropoulos et al., 1999), and by the pathogen *Xanthomonas campestris* pv. *campestris* (Merkouropoulos and Shirsat, 2003). *ATEXT4* is up-regulated neither by dehydration nor by application of ABA but by rehydration, application of auxin (AIA) and gibberellic acid (GA) (Yoshiba et al., 2001). The At3g15720 gene, coding for a glycoside hydrolase attached to the plasma membrane by a glycosylphosphatidylinositol (GPI) anchor (Eisenhaber et al., 2003) and putatively involved in cell wall remodelling and bacteria defence, was also found to be upregulated in *lcr*, *fdh* and *bdg*. At last, the *GASA1* (At1g75750) mRNA was also more present in the mutants, its expression is modulated by brassinosteroids and gibberellic acid; *GASA1* peptide of unknown function is localised in the cell wall and associated with cell expansion and plant development (Herzog et al., 1995).

Genes potentially associated with plant defences, were upregulated in these three cuticular mutants, among them, the At1g74000 gene coding for the STRICTOSIDINE SYNTHASE 3 (SS3) enzyme and the At2g43510 coding for the extracellular ARABIDOPSIS THALIANA TRYPSIN INHIBITOR PROTEIN 1 (ATTL1). SS3, present in the cell wall, is involved in the biosynthesis of alkaloids (Fabbri et al., 2000) which are known to have antibacterial effects (Kutchan, 1995). The At2g43510 gene codes for ATTL1, a protease inhibitor. Transgenic tobacco plants expressing protease inhibitors from *Nicotiana glauca* were resistant to the fungi *Botrytis cinerea* (Dunaevskii et al., 2005). This protein is a member of the defensin-like (DEFL) family and was found to be upregulated in CUTE plants (Chassot et al., 2007). The production of another defensin (At5g33355) and a chitinase (At2g43620) was increased, so were that of MLO12 (At2g39200) and ELI3 (At4g37990). The transmembrane MLO12, seven-transmembrane domain receptor homologue to the

barley *MILDEW RESISTANCE LOCUS0* (*MLO*), is expressed in root and inflorescences (Chen et al., 2006). *ELI3* is involved in the hypersensitive response to *Pseudomonas syringae* (Kiedrowski et al., 1992), and its expression is linked to that of the *WRKY6* (Robatzek and Somssich, 2002).

Many genes coding for enzymes involved in cellular homeostasis or up-regulated in consequence of oxidative stress or drought were up-regulated in our mutants. For instance, the production of two aldo/keto reductases (*At2g37760*; *At2g37770*) was probably enhanced. In general aldo/keto reductases are NADPH-dependent oxidoreductases and through their activity contribute to reduction of cellular damage done by ROS on cellular components, such as membrane lipids. In humans, it was shown that not only these enzymes contribute to the detoxication process by the reduction of oxidation products but also by the synthesis of sorbitol (Bagnasco et al., 1987), which may retain water or be a radical scavenger. In barley, the expression of an aldehyde dehydrogenase coincides with onset of desiccation during embryogenesis (Bartels et al., 1988). The *At1g05680* gene encodes a UDP-glucosyl transferase related to the Arabidopsis *UGT73C5/DOGT1* (*At1g01470*), which inactivates ABA (Poppenberger et al., 2005), or to the mammalian UDP-glucuronosyl transferases (UDPGT) essential in detoxification, by inactivating aldehydes and other toxic compounds (Tephly and Burchell, 1990). The transcript of *ATSIP-2*, a raffinose synthase (*At3g57520*), leading to the production of raffinose family oligosaccharides (RFOs), water soluble non reducing sugars, was also expressed at higher levels in the mutant tissues. RFOs are used as carbon sources and storage and as antioxidant against various abiotic stresses such as drought cold or salt (Taji et al., 2002). RFOs accumulate in leaves of resurrection plant *Xerophyta viscosa* challenged by drought (Peters et al., 2007). Two transcripts of *LATE EMBRYOGENESIS ABUNDANT* (*LEA*) proteins accumulate in the three mutants. These highly hydrophilic proteins were found to accumulate during seed desiccation (Blackman et al., 1995) and in vegetative and reproductive tissues in response to water deficit (Close, 1996; Bray, 1997).

Other genes maybe more specifically involved in the regulation of the intracellular oxydo-reduction potential, for instance, the glutaredoxin encoded by the *At4g15700* gene or the metalothionein *MT1C* (Zhou and Goldsbrough, 1995). *MT1C* is a cystein

rich protein essential in heavy metal tolerance which may function as an ion or radical scavenger, may also be involved in intracellular signalling by zinc channelling, thus activating transcription factors with a zinc finger.

In the group of intracellular signalling genes, we observed the induction of the *MSS1/SPT13* gene (At5g26340) coding for a high affinity hexose transporter (Brodersen et al., 2002; Norholm et al., 2006), which expression is associated with programmed cell death (Brodersen et al., 2002). *MSS1/SPT13* is localised on the plasma membrane and normally expressed in the vascular bundles at petals emergence (Norholm et al., 2006). Genes from different membrane transporters were found to be upregulated (see **Appendix H**), among them *MLO12*, a protein G coupled receptor (Chen et al., 2006), and a ABC transporter, normally expressed in roots and involved in response to nematodes. The ABC transporters family from Arabidopsis is subdivided into four subfamilies among which the WBC (white-brown complex homologues). Two WBC transporters, namely *WBC12* (*CER5*) and *WBC11* (*DSO*) were recently characterised. The *cer5* (eceriferum= waxless) mutant deposits less wax on its outer cell wall and its epidermal cell contain intracellular linear inclusions of wax, this revealed the essential role in wax exportation played by the ABC transporter *CER5* (*WBC12*) (Pighin et al., 2004). A mutation in the *DESPERADO* (*DSO*; *WBC11*) gene triggers the accumulation of lamellar inclusions of cuticle material in the cytoplasm of epidermal cells, and less wax (3-fold decrease) and less cutin are found on their surface (Bird et al., 2007; Panikashvili et al., 2007). In our mutants the expression of *CER5* and *DSO* genes was not modified (data not shown).

To ensure the junction between the receptors sitting in the plasma membrane and the transcription factors, intracellular messenger are required. Among the induced genes in our mutants we found genes coding for a kinase, a delta adaptin essential for vesicle trafficking (Lee et al., 2007), and for *PPT1* (At5g47330). This gene which was also found up-regulated in *salt overly sensitive mutants* (*sos*) (Gong et al., 2001) codes for a palmitoyl-protein thioesterase which may detach proteins attached to the membrane from their palmitoyl anchor.

Apart from these categories, the transcript level of three WRKY and three ERF/AP2 transcription factors, was also higher in mutants. The *WRKY6* (At1g62300) seems to

be a positive regulator of plant senescence and involved in pathogen defence by activation of *PRI* (Robatzek and Somssich, 2002) and *ELI3* genes, whereas the WRKY48 (At5g49520) may be a negative regulator of plant defence: its overexpression leads to the repression pathogen-induced PR genes and to the increase of susceptibility to bacterial and fungal pathogens (Denghui et al., 2005). Nothing precise is known about the WRK47 (At4g01720). The AP2 domain transcription factors belong to the ethylene response factors (ERF): the RAP2.6L (At5g13330) seems to be involved in the regulation of many other genes in shoot regeneration (Che et al., 2006). Like RAP2.6L, the RAP2.6 (At1g43160) and the At5g61890 genes are members of the ERF-B4 sub-family. A high level of mRNA of the RESPONSE TO DESICCATION ELEMENT RD26 (At4g27410) accumulated in the three cuticular mutants. This transcription factor belongs to the NAC plant specific transcription factor family (Yamaguchi-Shinozaki et al., 1992) and is induced in response to dehydration, osmotic stress and abscisic acid (Fujita et al., 2004). The transcript from *BT4* (BTB AND TAZ DOMAIN PROTEIN 4) was also found in higher amounts in the mutants. This protein possesses a cAMP-binding domain which allows protein-protein interactions (BTB) and a zinc finger domain to contact DNA (Du and Poovaiah, 2004). As shown in yeast and confirmed by GST pull down, BT4 interacts with the proteins from the same family (Du and Poovaiah, 2004). H₂O₂ and salicylic acid trigger a quick up-regulation of the BTs genes (Du and Poovaiah, 2004).

The upregulation of similar genes in response to the *bdg*, *lcr* and *fdh* mutations is in accord with the phenotypic similarities between these mutants.

Commonly down-regulated genes

According to our sorting criteria, only one gene is commonly downregulated by the three mutants. It encodes the FSD1 (FE SUPEROXIDE DISMUTASE 1) involved in the regulation of the redox potential in the cell and is required for copper delivery in the chloroplasts (Kliebenstein et al., 1998; Abdel-Ghany et al., 2005).

Mis-regulated genes in one or the other mutants

Although the mutants are similar with regard to the presence of organ fusion, cuticle deficiency, cell wall bound lipid and wax overaccumulation, they are not identical and their responses may differ. The majority of genes included in these categories may also be epidermis specific (Suh et al., 2005) and are related by their nature or by their functions to genes from the commonly mis-regulated group (data not shown). More elements implicated in dehydration or oxidative stresses, defence, such as chitinases, intracellular signalling, such as calcium binding EF hand family protein, and receptor kinases, transcription factors, such as ERF/AP2 transcription factors, can, for instance, be found in these subcategories.

Thus we found that mutations in the *BDG*, *LCR* and *FDH* genes are responsible for important modifications of the transcriptome. This may explain that the mutants have a pleiotropic phenotypes.

3.1.9. Complementation of the *Arabidopsis fdh* mutant by the barley *FDH* allele

In collaboration with Klaus Oldach's lab (University of Adelaide; Australia), we checked whether the barley (*Hordeum vulgare*; hv) allele of the *FDH* gene is able to complement the *fdh* mutation in *Arabidopsis thaliana*. Although both plant species are only distant relatives, *Arabidopsis* and barley proteins share 70 % of identity (BLAST), and cluster together in the fatty acid elongase phylogenetic tree (Figure. 26).

to phenotype data, at the *FDH* locus using a multiplex PCR (Ye et al., 2001) (optimized by Jafar Jabbari; University of Adelaide). 25 of the transgenic plants, derived from 11 independent transformations, were found to be *fdh/fdh* and, among them, 23 had a WT appearance at the rosette stage and 11 had a WT appearance at the young inflorescence/ silique stage. Unlike *fdh*, the *AtFDH::HvFDH fdh/fdh* plants produced seeds showing that the barley *FDH* gene is able to complement the *fdh* mutation in the transgenic *Arabidopsis* plants.

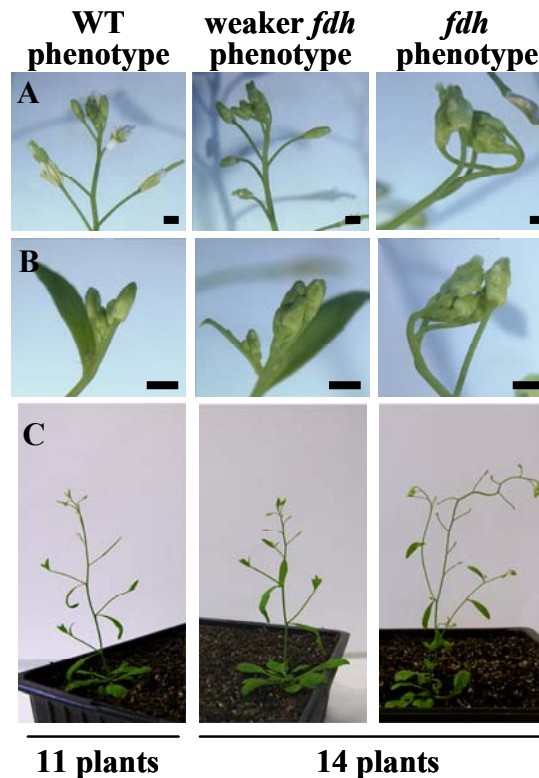


Figure 27. Phenotype of the *Arabidopsis fdh* plants carrying the barley *FDH* gene. By ARMS-PCR (see Methods), 25 *fdh/fdh* mutants were identified, out of them, 11 had a WT appearance and set seeds, 14 had a *fdh*-like appearance or a milder phenotype. (A) Main inflorescence. (B) Side inflorescence. (C) Whole plant. Bar: (A)(B)(C): 2 mm.

3-2. *HTM* (Atxgxxxxx), a putative acyl-transferase

This part of my PhD was done in collaboration with Dr. Hirokazu Tanaka and Prof. Yasunori Machida (from University of Nagoya, Japan) who described the *htm* mutant phenotype and cloned the *HTM* gene (Tanaka et al., 2004) and unpublished data). Because the identity of the mutant and the gene cannot be disclosed, we hitherto call it *HTM* (Hirokazu Tanaka's mutant). The observations and biochemical analyses were done on the *htm-1* mutant.

3-2.1. The *htm* mutant

Most of the time *htm* mutants are difficult to distinguish from WT plants at the rosette stage but with a low frequency (<10%), *htm* plants display postgenital organ fusion between rosette leaves. Yet, as previously reported in other fusion mutants such as *lcr* (Wellesen et al., 2001) or *fdh* (Lolle et al., 1992; Yephremov et al., 1999), the phenotype of *htm* is variable and can also lead to organ tearing or, later, premature plant death when no shoot can emerge (Figure. 28).

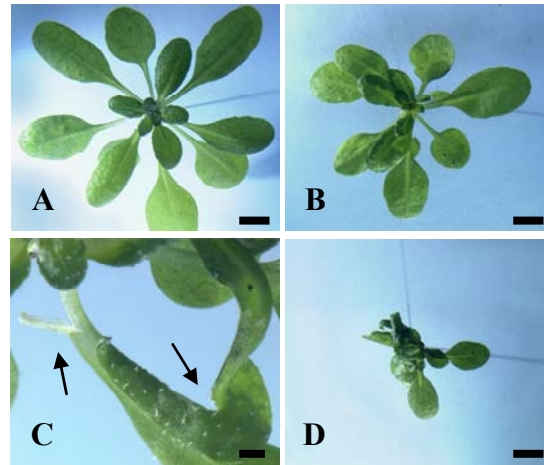


Figure 28. Effect of the *htm* mutation on rosette leaves. (A) WT; (B) to (D) *htm* mutant with a weak to strong leaf fusion phenotypes. In some cases, organ tearing is also observed in this mutant (C). Plants were seven weeks old (short day conditions). Bar: (A)(B)(D) 5 mm; (C) 1 mm.

In this new *Arabidopsis* mutant, ectopic organ fusion mainly takes place between floral organs within single floral buds; consequently flowers cannot open properly (Figure. 29). Hand dissection of individual *htm* buds reveals that petals and sepals account for most of the fusion phenotype, trapping the stamens, leading to their folding and that of the petals (Figure. 30_C). Because of the fusion, the emergence of the gynoecium is slowed down but self-pollination is not prevented. The organs appear to be of normal length and number. Suture zones are present between sepal periphery (Figure. 30_A_B) and, when involved, petal limb.

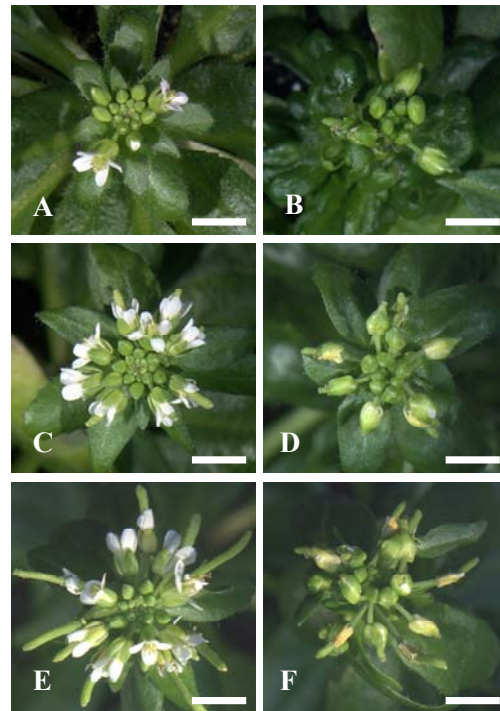


Figure 29. Effect of the *htm* mutation on flower buds. (A) (C) (E) WT Landsberg *erecta* inflorescences; (B) (D) (F) *htm* inflorescences. Fusion and bud deformations are visible from early stage until advanced stages of flowering, when petals and sepals dehisce. Notice that petals are not visible. Bar: 5 mm.

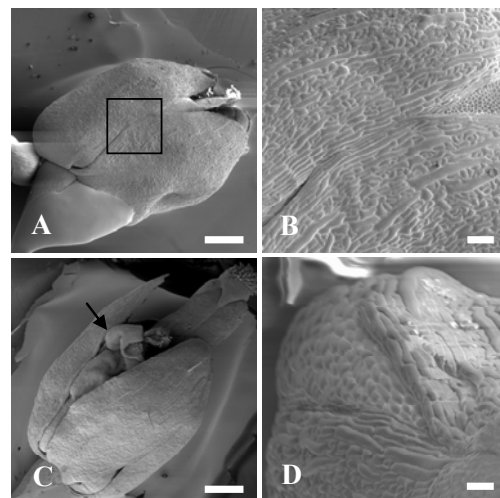


Figure 30. Electron micrographs of *htm* floral buds and open flowers. (A) (B) Ectopic fusion between adjacent sepals in *htm* buds. A detail from (A) is shown at higher magnification in (B). (C) Due to the physical constraint imposed by the sepal fusion, anthers and petals are folded. (D) Even after flower opening, some sepals remain joint. Bar: (A) (C) 500 μm ; (B) 100 μm ; (D) 50 μm .

As shown by toluidine blue staining, the petal limb and the sepal edges of this mutant are characterised by an increase in cuticle permeability (Figure. 31_E). Although the *HTM* gene is expressed beneath the papillae cells (see *HTM* expression in aerial organs), the mutant stigma have a wild-type appearance. However they are stained with toluidine blue at early stages (Figure. 31_D_F).

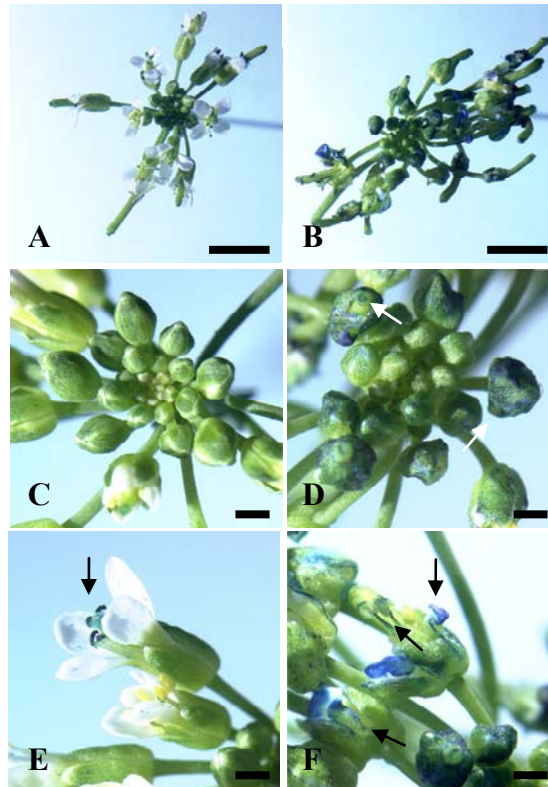


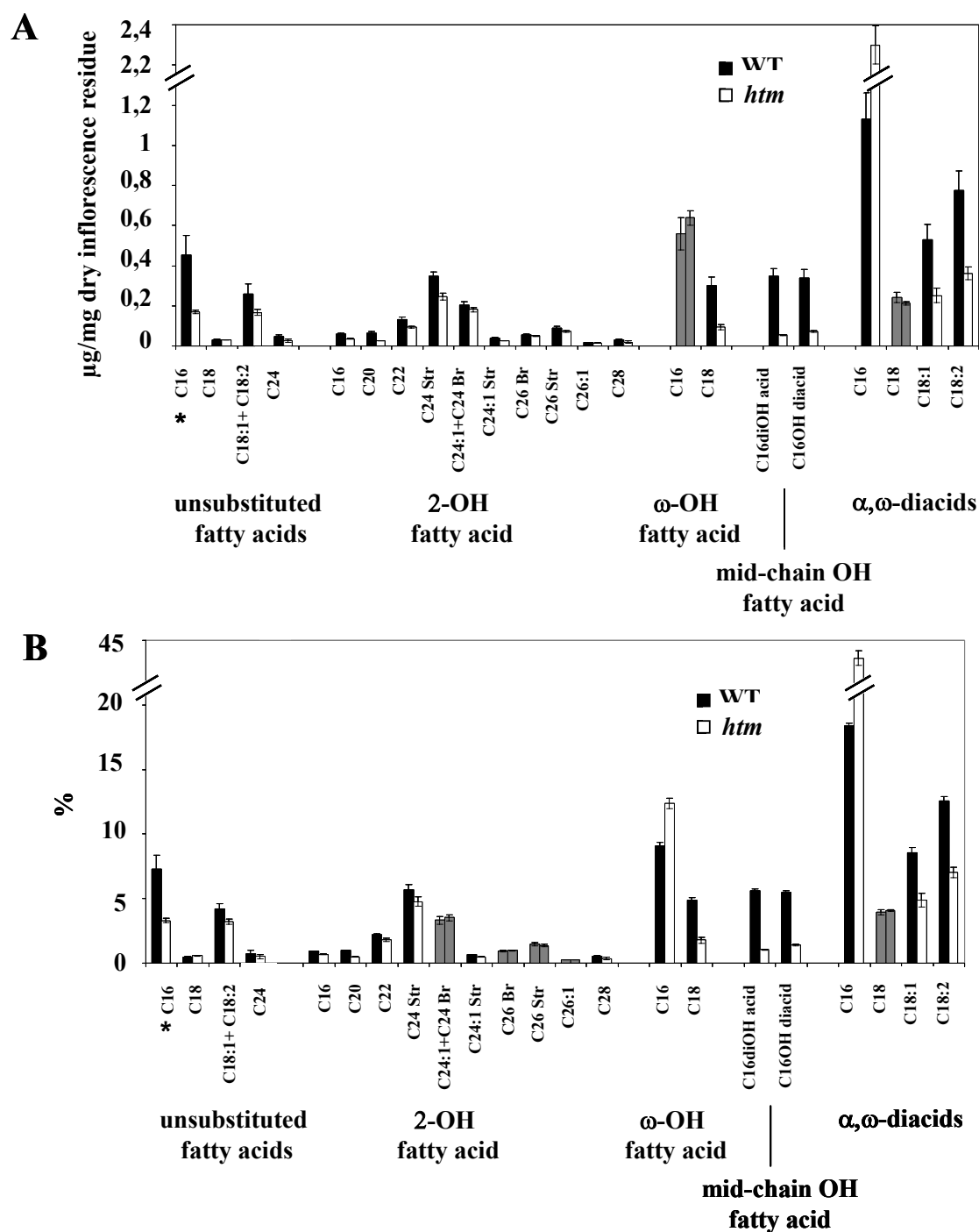
Figure 31. Toluidine blue staining assays. (A) (C) (E) WT inflorescences; (B) (D) (F) *htm* mutant. At the bud stage, the outer sepal surface and the top of the stigma from the mutant can get stained with a toluidine blue solution (D). Later on, the sepal margin, petal limb from open flowers and filament of mature anthers also retain the staining (F). Bar: (A) (B) 5 mm; (C) to (F) 1 mm.

Floral buds and upper cauline leaves from the *htm* mutants have a shiny appearance, reminiscent of other wax mutants such as *wax2* (Chen et al., 2003) and *cer10* (Zheng et al., 2005), although weaker, and display ectopic organ fusion probably linked to a modification of their cutin and/or of their wax composition. These lines of evidences prompted us to analyse waxes and cell wall bound lipids in *htm* inflorescences. Inflorescences at a developmental stage similar to that of the samples shown in the figure 31 (C_D) were used to perform this analysis. When we started, no particular method had been described to analyse cutin from inflorescences, and we introduced minor modifications (see Methods) into the general bound lipid analysis (Franke et al., 2005) and the wax analysis (Kurdyukov et al., 2006b) methods to determine the differences between WT control and *htm* inflorescences.

We analysed by GC and GC-MS the cell wall bound lipid composition of inflorescences, established the composition of WT Landsberg *erecta* lipid polyester and compared it to that of our *htm* mutant (see Methods). We identified monomers

falling into six categories: unsubstituted fatty acids, 2-hydroxy fatty acids, ω -hydroxy fatty acids, mid-chain-hydroxy fatty acids and mid-chain hydroxy- α,ω -diacids and α,ω -diacids (Figure. 32).

The WT and mutant cell wall bound lipid compositions were not found different, but slightly less monomers (in average $5 \pm 0,2 \mu\text{g}/\text{mg}$ for *htm* and $6 \pm 0,8 \mu\text{g}/\text{mg}$ for WT) seem to be deposited on the surface of the mutant inflorescences. As the shorter long chain unsubstituted fatty acids and the 2-hydroxy fatty acids may not only come from the cutin but also sphingolipids trapped in plant cell wall, we decided to consider them separately. The *Arabidopsis* typical cutin compounds (ω -hydroxy fatty acids, mid-chain-hydroxy-fatty acid and mid-chain hydroxy- α,ω -diacids and α,ω -diacids), represent 70% in WT and 77% in *htm* of the identified compounds. No difference between the absolute amount of typical cutin monomers in the WT and *htm* samples could be found. The decrease observed in the mutant in most of the compounds is compensated in weight by an increase in hexadecanoic diacid (C16 α,ω -diacid).(Figure. 32) According to our results this is the most abundant compound in bound lipids from inflorescences. The absolute and relative amounts of mid-chain hydroxy components and unsaturated diacids are two times lower in the *htm* mutant (Figure. 32).The strongest decrease was observed in the mid-chain-hydroxy fatty acids (4,5 times). There is a two times increase in C16 α,ω -diacids which is not reflected by an increase in C16 ω -acid, its precursor. We observed a decrease in C18 ω -hydroxy acid and in C18:1 and C18:2 α,ω -diacids but no modification of the quantity of C18 α,ω -diacid.



The wax composition of WT *Landsberg erecta* inflorescences was established by GC and GC-MS and compared to that of the *htm* mutant (see Methods). The wax extracts

used in this experiment come from the samples used for cell wall bound lipid analysis. Monomers from the following categories were identified: unsubstituted fatty acids, primary alcohols, esters, aldehydes, alkanes, secondary alcohols, ketones and sterols (Figure. 33). Mutant waxes were with regard to composition very similar to the WT. In total and in average, about $7,4 \pm 0,5 \mu\text{g}/\text{mg}$ dry weigh and $9 \pm 0,8 \mu\text{g}/\text{mg}$ dry weigh of wax were retrieved for *htm* and for the WT control, respectively. This corresponds to a global decrease of approximately 20% per mg dry weight in the mutant. No major shift between the classes of wax compounds could be observed (Figure. 33).

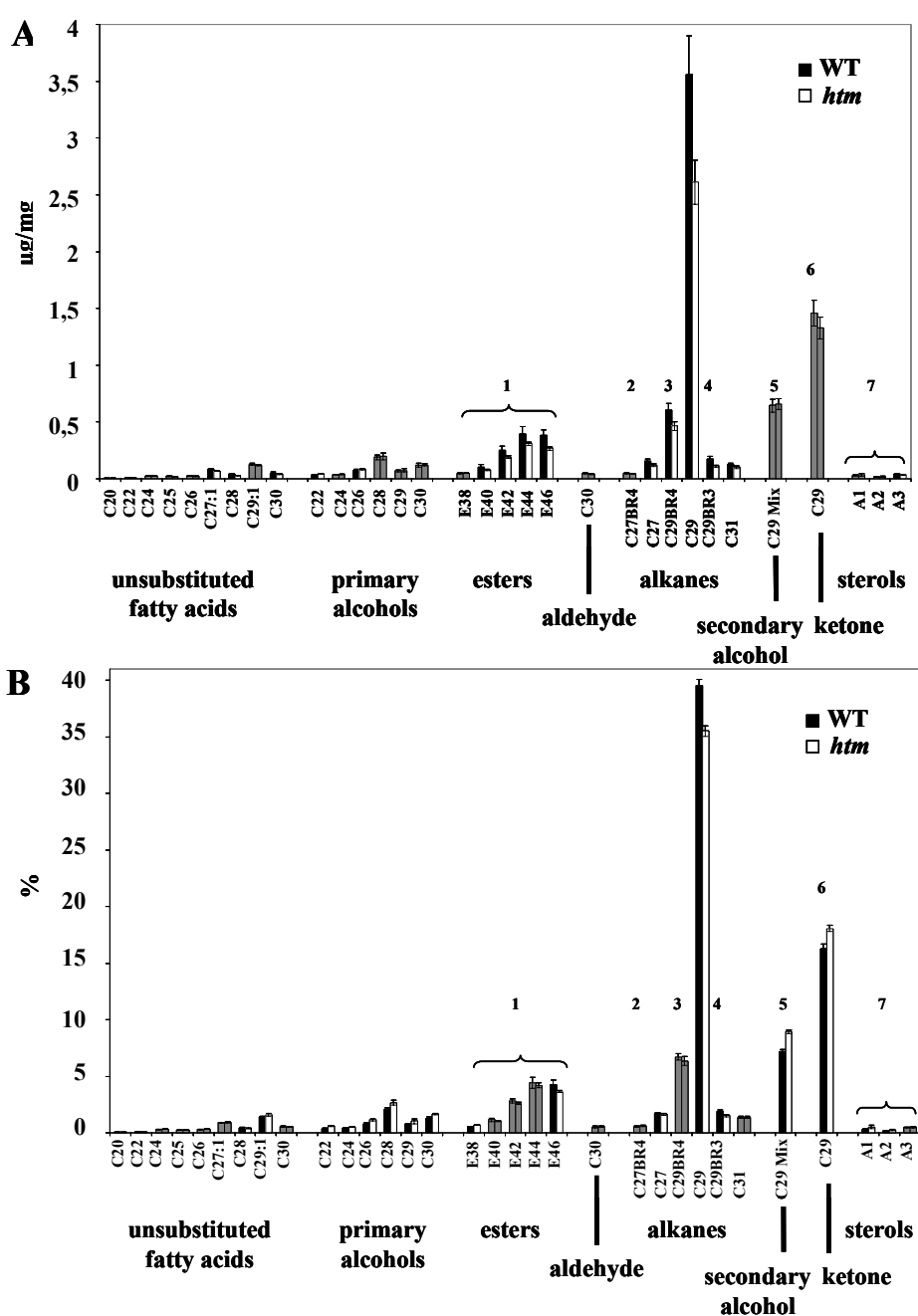


Figure 33. Wax analysis from wild type Landsberg *erecta* and *htm* inflorescences. Absolute changes (A) and relative changes (B) in wax composition. ¹Esters: hexadecanoic acid alkyl esters, with chain lengths ranging from C38 to C46 were identified. ² C27 BR4: C27 alkane branched at the position 4 (3-Methylhexacosane). ³ C29 BR4: C29 alkane branched at the position 4 (4-Methyloctacosane). ⁴ C29 BR3: C29 alkane branched at the position 3 (3-Methyloctacosane). ⁵ C29 keton: 15-nonacosanone. ⁶ C29 OH mix: mixture of three secondary alcohols, with an alcohol group at the position 14, 15 or 16 (14-nonacosanol, 15-nonacosanol and 16-nonacosanol). ⁷ Sterols: three distinct sterol compounds could be detected but not further identified by comparison with the available libraries. Mean values of five replicates \pm (SD) are shown. When WT and mutant amounts were not found different (Mann-Whitney U test; $p < 0,05$), bars are filled with grey.

Even though no precise enzymatic function was pointed out by these analyses, the *htm* mutation seems to lead to wax deposition insufficiency. The disequilibrium in cutin monomers and the general decrease observed in wax amount concur to the phenotype of the *htm* mutant. The modification in cutin composition is very likely to influence its structure and the inadequate deposition of the wax layer could result in the shiny appearance of the mutant inflorescences.

3-2.2. HTM expression in aerial organs

To study the *HTM* gene expression pattern, we fused 2,1 kb of its promoter region to the GFP and DsRED reporter genes. The fusion constructs were used to perform a stable transformation of wild-type Columbia and Landsberg *erecta* plants. The images of transgenic plants presented here are the overlay of the bright field image, auto-fluorescence (chlorophyll channel) and appropriated fluorescence channel (see Methods).

Absent from the vegetative meristem, *HTM::GFP* is expressed in the epidermis of leaf primordia (Figure. 34_A). In older leaves, its expression is only maintained in trichomes (Figure. 34_B_C_D_E). *HTM::DsRED* is expressed in most of the floral organs from early stage on: in the epidermis of sepals, petals, anther filaments and style (Figure. 34_F_G_H). The gene was also found to be expressed on the surface of the receptacle supporting floral buds and open flowers (Figure 34_I). The observations made with transgenic plants expressing either *HTM::GFP* or *HTM::DsRED* promoter constructs are coherent; showing that the *HTM* promoter is epidermis specific.

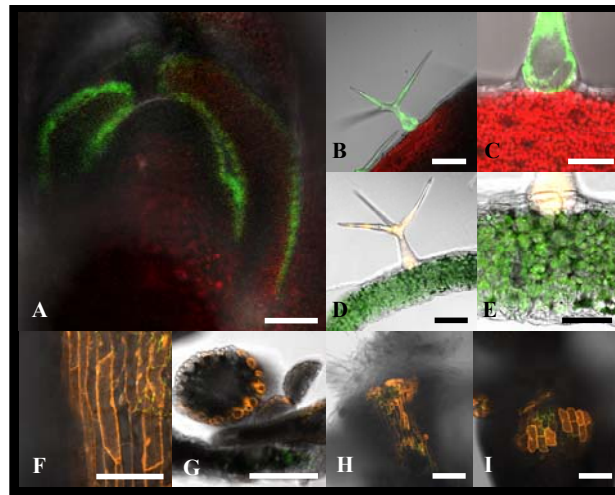


Figure 34. Expression of GFP and DsRED reporter genes under the control of the *HTM* promoter. (A) to (C): GFP was used as reporter gene; the green colour corresponds to the GFP signal and the red colour to the auto-fluorescence from chlorophyll. (D) to (I) DsRED was used as reporter gene; the orange colour corresponds to the DsRED signal and the green colour to the auto-fluorescence from the chlorophyll (A) Transversal cut through a vegetative bud; a strong GFP signal can be observed in leaf primordial. (B-E) Transversal cuts through young cauline leaves (8 mm and 5 mm long) expressing either the GFP (B)(C) or the DsRED reporter gene (D)(E); (F) view on a sepal expressing DsRED; (G)(I) transversal cut through organs from floral buds: (G) anther filament. (H) stigma and (I) area below the abscission zone from an open flower, just before anthesis, display the expression of DsRED. Bar: 100 μ m except for (C), (E), (G) and (H) 50 μ m.

To confirm the expression pattern of *HTM*, we produced protein constructs. In this case, 2,1 kb of the *HTM* promoter region and the *HTM* gene (from ATG to stop codon -1) were fused to the GFP, DsRED, GFP-StrepTagII or StrepTagII reporter sequences (see Methods). For some reason the GFP protein construct did not give rise to any signal. The following observations are based on the *HTM*-DsRED construct only.

We could detect the presence of the chimeric protein in trichomes and non specialised epidermal cells from developing rosette and cauline leaves (Figure. 35_A_B). The older the leaves, the less expressing cells.

On the surface of the stems, *HTM*-DsRED is present in trichomes and often seen in stomata, towards the stomatal opening but also in isolated pavement cells, (Figure. 35_C_D_E).

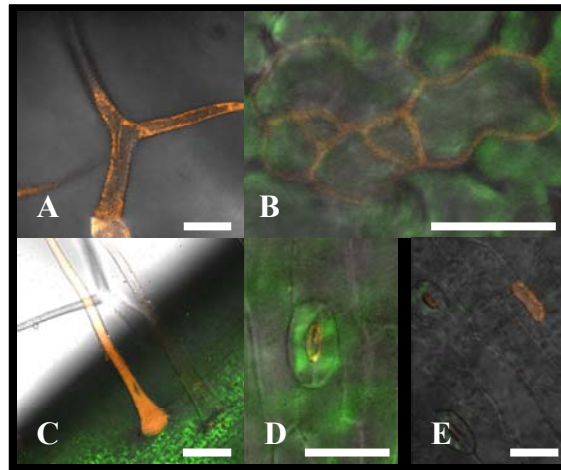


Figure 35. HTM-DsRED fusion construct in transgenic plants: observation in leaves and stems. The orange colour corresponds to the DsRED signal and the green colour to the auto-fluorescence from the chlorophyll. (A) and (B) cauline leaf (3-4 mm long). Not only do trichomes from developing leaves display fluorescence but also islets of other epidermal cells do. (C)(D)(E) On the stem surface, fluorescence was observed in trichomes (C), the inner face of the guard cells (D), and some pavement cells (E). Bar: 50 μ m in (A) and (B), 100 μ m in (C), and 20 μ m in (D) and (E).

The presence of the HTM-DsRED was detected in the epidermis of sepals, petals and anther filaments from floral buds and open flowers (Figure. 36_D_E_F_G). At the bud stage the signal from the sepal edges was particularly strong and the production of the protein appears uniform along the gynoecium (Figure. 36_D). At later stage of development, the fluorescent signal is more restricted to the epidermis from the top area of the gynoecium (Figure. 36_D). The HTM-DsRED protein can also be strongly detected in the epidermis of pedicels from young floral buds (Figure. 36_J_K), and also during seed development (white and green stage) in funiculus and placenta (Figure. 36_H_I). The chimeric protein was also found in the protoderm from embryos (Figure. 36_L_M).

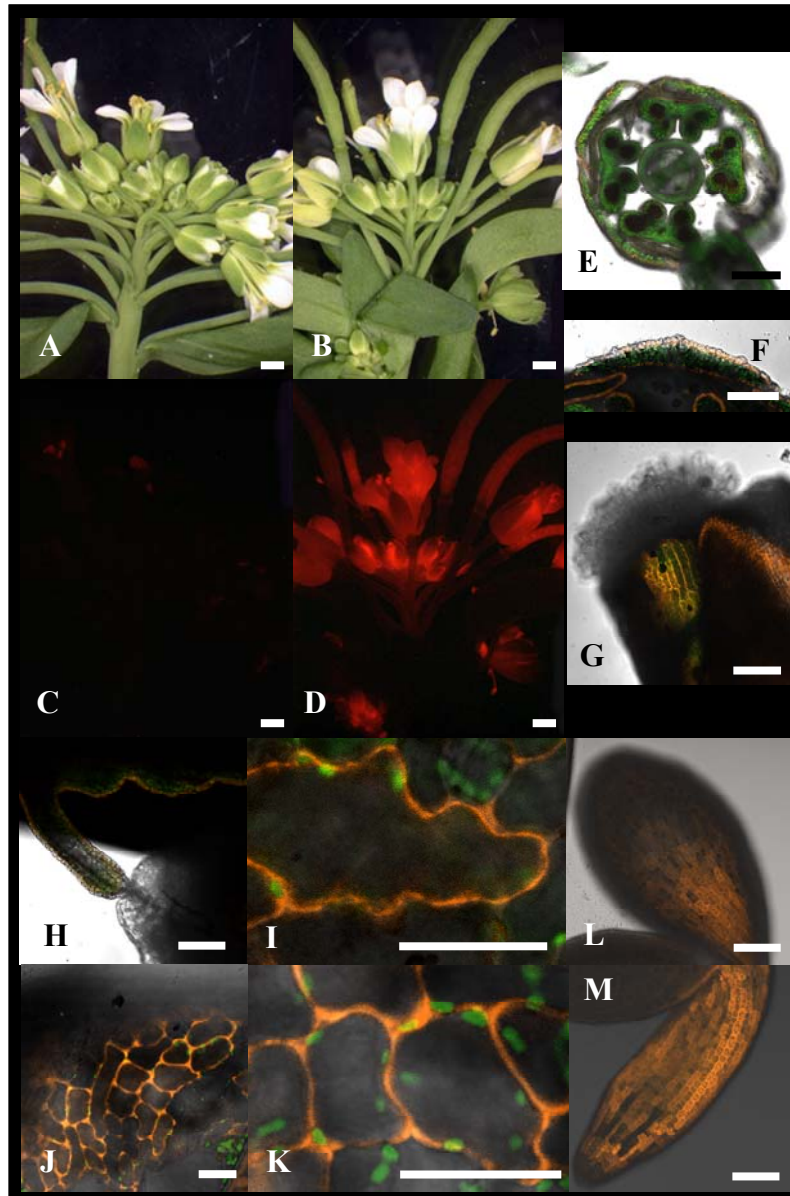


Figure 36. HTM-DsRED fusion construct in floral organs. (A)(B)(C)(D) were taken with a Leica MZ-FL-III stereomicroscope. (A)(B) bright field illumination; (C)(D) epifluorescence illumination. In absence of the construct (C), auto-fluorescence, probably coming from mature pollen, is observed in mature anthers. In presence of the construct (D), fluorescent signal is observed on the surface of ovary and style, sepals of young buds. In open flowers, fluorescence could also be observed on petals and on stamen filaments. In developing siliques (right hand side), fluorescence can be seen at the level of the funiculi. (E) and (F) transversal cut through floral buds; the epidermis of sepals, petals and anther filaments display DsRED signal (G) style and petals from open flowers displaying the fluorescent signal. (H) funiculus and placenta epidermal cells also express the transgene. (J)(K) Most of the epidermal cells from short pedicels (2-3 mm) supporting floral buds, and sepals from floral buds strongly expressed the HTM-DsRED chimeric protein, however in the later case, some cells much more than others (I). (L) and (M) An embryo at the torpedo stage. Epidermal cells of axis and cotyledons also displayed a bright fluorescent signal. Bar: (A) to (D) 1 mm, (E) 200 μ m, (F) to (H) 100 μ m, (I) to (K) 20 μ m, (L) and (M) 100 μ m.

According to the focal plane, the protein is detected on the periphery or like a uniform film in the epidermal cells; it maybe cytoplasmic, membrane bound or associated with the cell wall (Figure. 36_I and Figure. 37_A_B_C_D). To know more about the

localisation of the HTM-DsRED protein in the cell, we examined the surface of style from young floral buds after immersion in water or a saturated NaCl solution. The salt solution (>5M) constitutes a hypertonic medium, and as expected, cells from immersed organs expulse water to tend to bring the osmotic equilibrium back; their cytoplasm retracts. As the fluorescent signal also appears gathered in the centre of the cells, we concluded that the HTM-DsRED chimeric protein is either cytoplasmic or associated to the plasma membrane (Figure. 37_E_F_G_H).

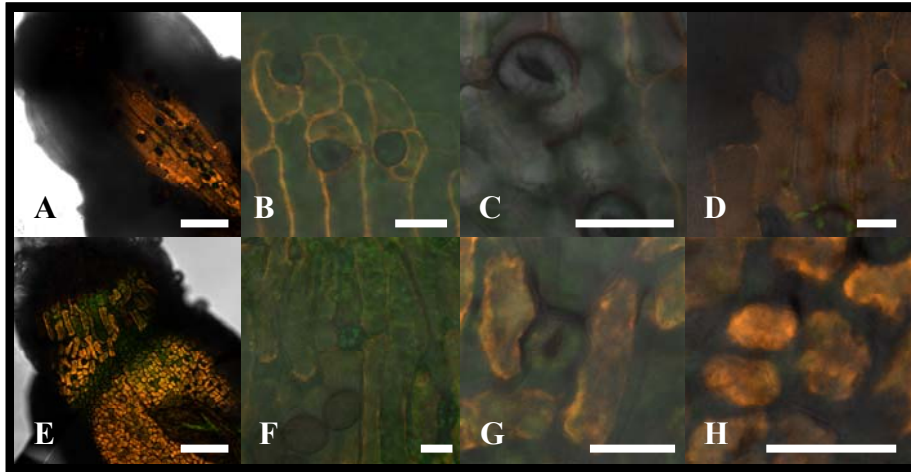


Figure 37. Hyperosmotic protein localisation assay. HTM-DsRED transgenic plants were used in this experiment. (A) to (D) styles were observed after immersion in water; the fluorescent signal is evenly distributed in the cell or seems to delimitate it according to the focal plane. (E) to (H) the addition of salt triggers the retraction of the fluorescent signal toward the centre of the cell. Bar: 20 µm except (A) and (E) 100 µm.

This simple experiment does not allow us to precise further the sublocalisation of the HTM-DsRED protein. To do so one could for instance cross transgenic plants expressing the HTM-DsRED chimeric protein and plants expressing membrane markers linked to GFP. It would also be possible to gain precision using our HTM-StrepTagII line for immunolocalisation or to detect the protein in cell fractions.

3-2.3. Heterologous expression in *E.coli*

We created three StrepTagII-tagged versions of the HTM protein using of the pASK-IBA vectors (see Methods). The pASK-IBA2C vector, designed for periplasmic expression of heterologous proteins, did not lead to the expression of our protein. The protein produced using the pASK-IBA5C, tagged in N-terminus, was not detectable using the Strep-Tactin conjugate (see Methods). Even though the protein extracts were denaturated and run in denaturing conditions, one may still suppose that the tag was not accessible when added at the N-terminal of the protein, or else that it had

been removed by the host. Sufficient amount of protein tagged in its C-terminus was obtained in the soluble fraction using the pASK-IBA3C vector and purified. The nature of the overexpressed protein was confirmed by liquid chromatography- mass spectrometry (LC-MS-MS/MS) (performed by Thomas Colby; Mass Spectrometry Unit; MPIZ Cologne).

3-2.4. Heterologous complementation assay in *E.coli*

The *E.coli* JC201 mutant is deficient in the 1-acyl-sn-glycerol-3-phosphate acyltransferase (LPAAT) (Coleman, 1990), enzyme catalysing the conversion of lysophosphatidic acid (LPA) into phosphatidic acid (PA) (see Discussion, Figure. 45). The latter is an essential membrane component which absence causes major changes in membrane fluidity. As a consequence of this mutation, JC201 can not grow at the natural temperature (37-42°C), but only at much lower ones (Coleman, 1990). The ATS2/LPAT1 lysophosphatidyl acyltransferase enzyme (Bin et al., 2004; Kim and Huang, 2004) from *Arabidopsis thaliana*, has been shown to complement this *E.coli* deficient strain. HTM and ATS2/LPAT1 have a low level of identity, still as the comparison of amino acid sequences does not account for all of enzyme specificities, we decided to try complementing the JC201 *E.coli* strain with HTM.

We have introduced the *HTM* gene in this JC201 mutant and its WT counterpart JC200 (See Methods). Both strains were grown at permissive and restrictive temperatures, 30°C and 42°C respectively. Preliminary results obtained on plates and in liquid culture seem to point out that HTM does not complement the bacteria mutation. We observed strong growth inhibition in our experimental conditions. It seems essential, to validate this result by repeating this experiment in presence of a positive control such as ATS2/LPAAT1, which has been shown to complement this mutation.

3.3 Investigation on putative cuticular genes

3.3.1. Characterisation of insertion lines in the *LEAKO* gene encoding a putative leukotrien-A4-hydrolase-like protein

In order to check whether the absence of a functional leukotrien-A4-hydrolase-like gene has any influence on cuticle formation in Arabidopsis, we studied the *LEAKO* gene (At5g13520). As they became available from the different stocks centres, two T-DNA insertions in this gene were genotyped, and the T-DNA causing the gene disruptions was localised (Figure. 38).

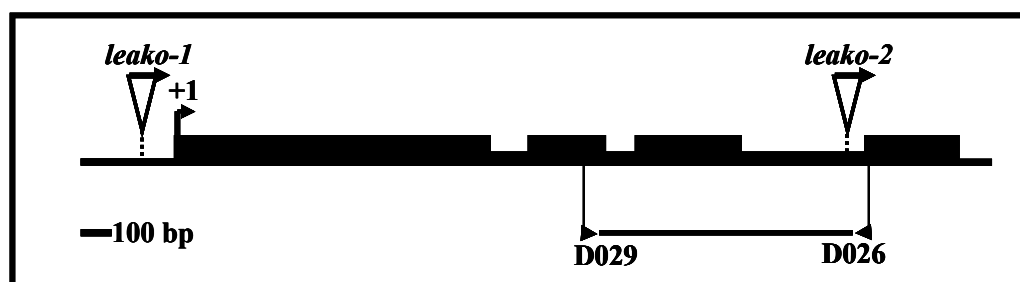


Figure 38. Position of the T-DNA insertions in the *leako* lines (*leako-1* = SALK_117791; *leako-2* = SAIL_636_D12) and of the primers used for RT-PCR. +1 indicates the putative start codon; exons are shown in thick black boxes and introns in thicker lines. Arrows indicate the orientation of the inserted T-DNA elements.

The presence of the T-DNA in the *leako-1* (SALK_117791) line did not impair the expression of the gene (Figure. 39) and the *leako-2* (SAIL_636_D12) line, lacking the expression of the *LEAKO* gene, did not have any striking phenotype, leaves from this mutant were not stained by toluidine blue (data not shown).

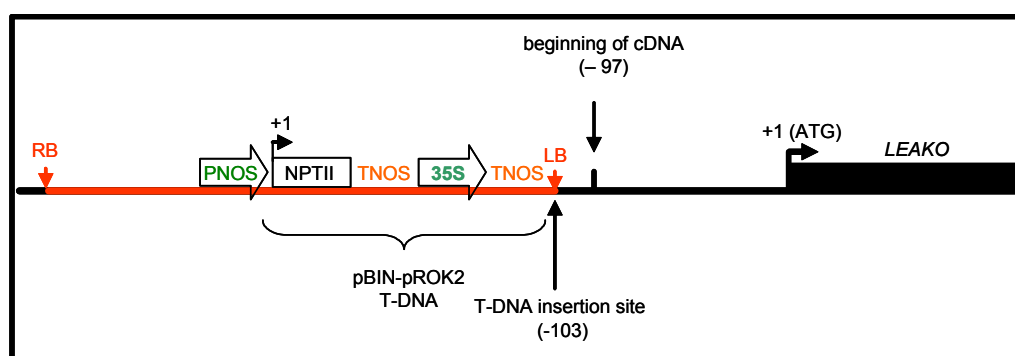


Figure 39. Insertion point of the T-DNA pBIN-pROK2 in the *leako-1* line. The *NPTII* gene gives kanamycin resistance to the plants carrying the insertion. On the left border of the T-DNA, a CaMV 35S promoter (35S) and a terminator T-NOS are present. As the T-NOS terminator may be leaky, the 35S promoter present upstream may be able to drive the expression of the *LEAKO* gene. A T-DNA map is available at: http://signal.salk.edu/tdna_protocols.html. The beginning of the cDNA was positioned according to the information available in the RIKEN database (<http://www.brc.riken.jp/lab/epd/Eng/>).

3.3.2. Aldehyde-dehydrogenases putatively involved in cuticle synthesis

Insertions lines of genes encoding three aldehyde-dehydrogenases were received from the SALK Institute (ALDH4; At1g44170 and ALDH5-1; At4g36250) or kindly supplied by Prof. Hans-Hubert Kirch and Prof. Dorothea Bartels (from University of Bonn) (ALDH3; At4g34240). The new Arabidopsis lines were checked for T-DNA insertions and inspected for any classical phenotype from cuticular mutant, such as organ fusion, trichome death or a weakened cuticle. As no obvious phenotype could be found, the different lines were crossed.

Regarding the *ALDH5* gene in the homozygous mutant plants, we confirmed the presence of the insert, and of the disruption of the gene expression by RT-PCR (Figure. 40).

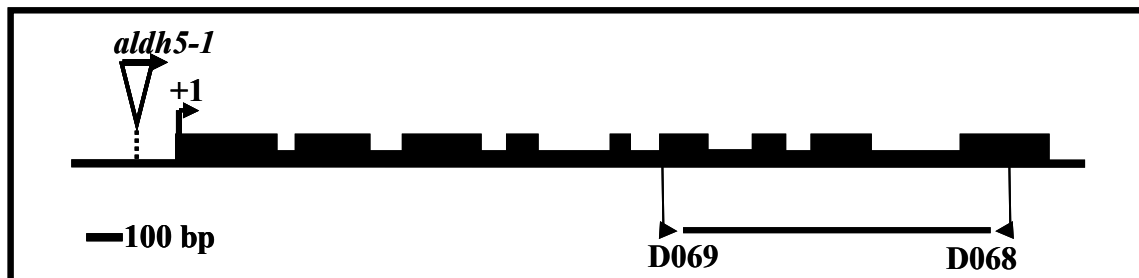


Figure 40. Position of the insertion in the *ald5-1* line and of the primers used for RT-PCR. +1 indicates the start codon; exons are shown in thick black boxes and introns in thicker lines.

However no macroscopic phenotype could be observed during vegetative growth but the formation of embryos seems to be partially impaired. We decided to investigate further the observation of embryo lethality using a binocular. Indeed, abortion could be observed at different stages of embryo development in the siliques of homozygous plants (Figure. 41). But not all homozygous plants did actually show this phenotype: three plants out of ten did not show any phenotype whereas the siliques from the seven other plants contained about 20% of aborted seeds (evaluated on a population of 800 ripening seeds). Neither the leaves nor the seeds from homozygous plants were stained using a 0,05% toluidine blue solution; the cuticle covering of those plants appeared normal (Figure. 41).

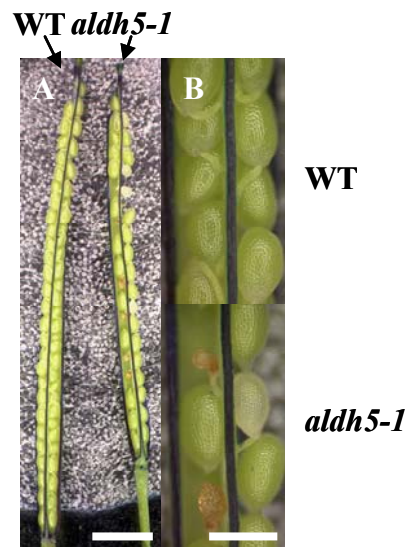


Figure 41. Aborted seeds were observed in some of the siliques produced by *aldh5-1* plants. After 2 min of immersion in a 0,05% toluidine blue solution, staining was neither observed on the WT (negative control) nor on *aldh5-1* ripening seeds. (A) Overview on siliques; (B) Close-up on ripening seeds. Bar: (A) 2 mm; (B) 0,5 mm.

3.3.3. HYD4, a putative α/β hydrolase-fold enzyme closely related to BDG

Progeny of the *En* transposon plants which had shown germination deficiency was sawn and examined. Some of the plants tended to have short, dwarfish siliques (poor elongation and enlargement; data not shown). Unfortunately, we failed to confirm the presence of an insertion in the *HYD4* gene from these plants (data not shown). This phenotype is therefore most likely due to an insertion elsewhere. We then turned to insertion mutants available in the different collections (Material and Methods; Table. 1).

Insertion lines in the *HYD4* gene, as they became available from the different stock centres, were genotyped. The different alleles were named *hyd4-1* to *hyd4-6*; the correspondence between these names and the stock centres' IDs are given in Figure. 42. All the insertion positions were found where indicated in the respective databases except for the *hyd4-2* insert which appears to be located about 200 bp downstream the indicated position (Figure. 42). All insertion lines are homozygous mutant except the *hyd4-2* population which is segregating. We genotyped 42 plants from the *hyd4-2* accession, 16 of them were found homozygous and had a dwarf appearance (see below), 13 were found WT and, of 13 heterozygote. We concluded that the *hyd4-2* mutation is recessive.

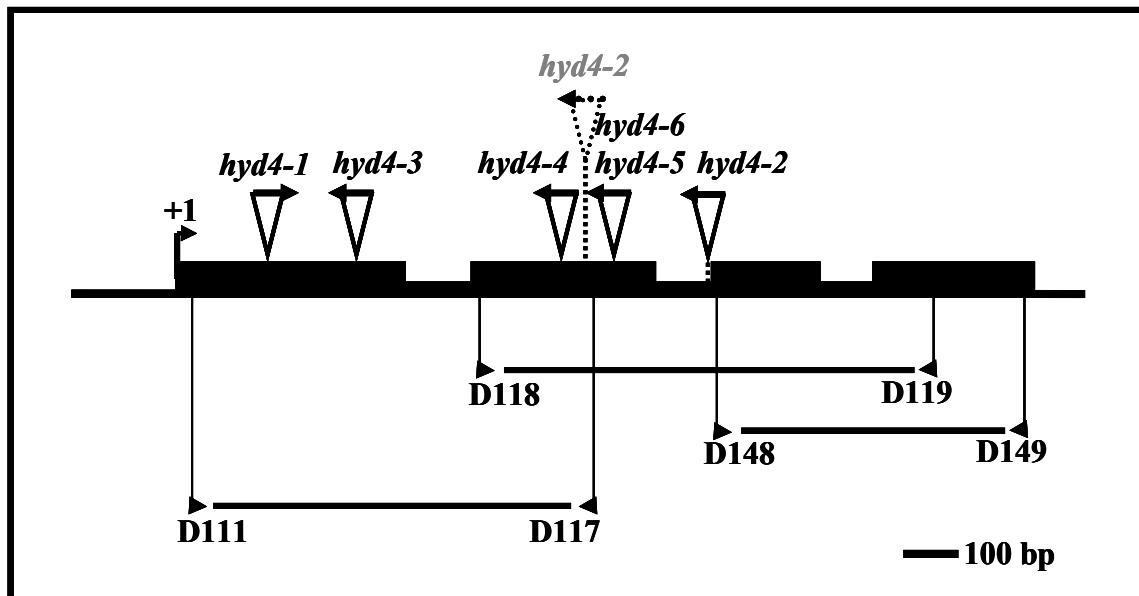


Figure 42. Position of the insertion in the different *hyd4* alleles and of the primers used for RT-PCR. +1 indicates the predicted start codon; exons are shown in thick black boxes and introns shown in thicker line. The arrows show the orientation of the T-DNA present in the respective *hyd4* lines. The *hyd4-1*, *hyd4-2*, *hyd4-3*, *hyd4-4*, *hyd4-5*, *hyd4-6* lines mentioned here respectively correspond to the following accessions SALK_069038, 711C08, 52-0951, 12-3258, SM_319056, SM_319060. The insertion in the *hyd4-2* line is depicted twice: once in grey, which corresponds to the insertion position indicated in the GABI database, once in black, indicating the position of this insertion according to our sequencing results.

Finally plants were grown side by side and two samples per plant type were tested by RT-PCR. All the inserts, present within the first, second exons or second intron of the *HYD4* gene, abolish the production of a WT transcript (Figure. 43) in their respective lines. However the production of chimeric transcripts is still taking place to a near WT level in mutants obtained in the Columbia background. The expression level of the *HYD4* gene appears to be lower in the Nossen ecotype than in the Columbia ecotype.

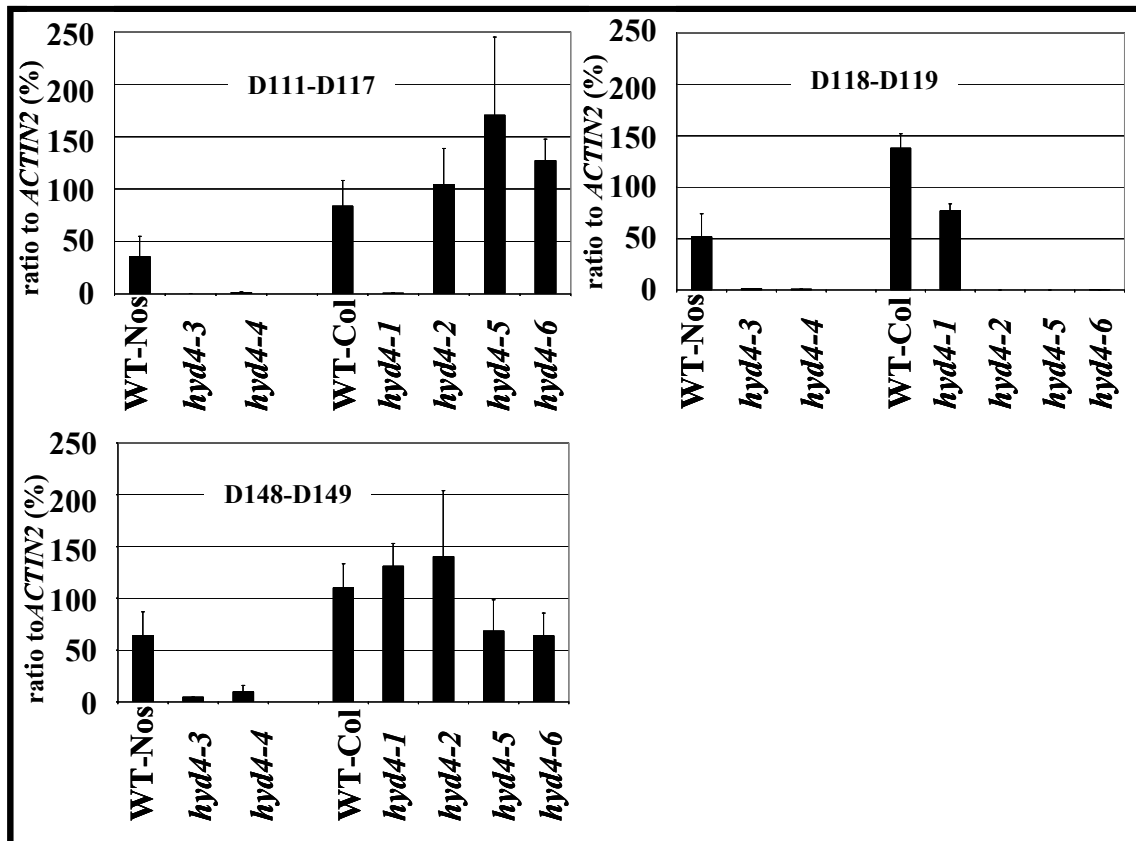


Figure 43. Expression level of the *hyd4* gene in the different *hyd4* insertion mutants and respective WT controls. The quantity of transcript present in each plant type was checked by semi-quantitative RT-PCR (optimised with regard to cycle numbers; see Methods). The graph shows the relative amount of *HYD4* transcript to the amount of *ACTIN2* (At3g18780) transcript. WT-Nos = WT Nossen and WT-Col = WT Columbia.

Most of the homozygous mutants show no macroscopical phenotype, except the *hyd4-2* homozygous mutant. The application of toluidine blue to leaves from this mutant and from WT plants led to no staining (data not shown). This suggests that this mutant does not have any cuticular deficiency, however we could observe other disorders: plants show a dark green pigmentation, are extremely dwarf (Figure. 44_A_B_C), late flowering and sterile. Moreover, the shoot architecture of this mutant is abnormal: the main inflorescence often does not tower above the secondary inflorescences, and dies (Figure. 44_D_E).



Figure 44. Illustration of the macroscopic phenotype of the *hyd4-2* mutant. (A) (B) (C) size difference between *hyd4-2* mutants and WT plants. (A)(B) On the left, WT Columbia control, on the right *hyd4-2* mutant. The rosettes from this mutant are two third smaller (*hyd4-2*: 3,3 cm \pm 0,5 cm; WT: 9,7 cm \pm 1 cm; the rosette diameter from 15 homozygous mutant and wild-type plants was measured) than that of the WT control. Plants were 11 weeks old (seven weeks short day and four weeks long day). (D) *hyd4-2* plants have a peculiar architecture: their secondary shoots tend to extend more than the main inflorescence which often dies. (E) While most of the *hyd4-2* plants had flowered, some of them were still at the rosette stage and had not bolted. Plants were 18 weeks old (seven weeks short day and eleven weeks long day). Bar: (C) 1 cm.

4. **Discussion**

4.1 **The *fdh*, *lcr* and *bdg* mutants**

4.1.1. A role of the cell wall matrix in the permeability to small hydrophilic molecules

Fiddlehead (*fdh*), *lacerata* (*lcr*), and *bodyguard* (*bdg*) mutants have pleiotropic phenotypes (Lolle et al., 1992; Yephremov et al., 1999; Wellesen et al., 2001; Kurdyukov et al., 2006b) but their obvious feature is the presence of ectopic organ fusions between rosette leaves and, in the case of *fdh*, between floral organs and flowers. Leaves from the *fdh* mutant have been shown to release their chlorophyll content faster than WT by Pruitt and co-workers (Lolle et al., 1997). On the other hand, the use of toluidine blue was described as a screening tool to identify new cuticular mutants (Tanaka et al., 2004). This prompted us to apply both techniques on our mutants to illustrate the permeability modification of their cuticle covering (In the chlorophyll leaching assay, *fdh* was used as control). As shown in Figure. 9, *lcr*, *bdg* and *fdh* leaf surface appears uneven after toluidine blue staining and the chlorophyll leaching assay showed that tissue of all mutants are more permeable than that of WT too. However all mutants did not behave the same way since the extraction curves from *lcr* and *bdg* are nearly superimposed whereas that of *fdh* is really distinct, and shows a steep increase. From TEM observations, we know that both *lcr* and *bdg* have a disrupted cuticle, that some portions of the cell wall seem devoid of cuticle and that cuticle material appear to be included in the cell wall (C. Nawrath personal communication; (Kurdyukov et al., 2006b), but that *fdh*, on the other hand, shows a regular cuticle layer on the surface of its leaves ((Lolle et al., 1992); C. Nawrath personal communication). Based on the appearance of the cutin layer of the different mutants we would have expected the opposite results: slower chlorophyll extraction in the case of *fdh* and quicker for *bdg* and *lcr*. It looks that *fdh* covering, even if regular, offers as little protection as *bdg* and *lcr*'s (toluidine blue staining) or even less (chlorophyll leaching). The cuticle may not be the only element that delays the release of pigment from WT leaves. The outer cell wall and the cell wall surrounding mesophyll cells may also influence this process.

The *fdh* and *lcr* mutations triggers similar changes in the cell wall bound lipid composition (Figure. 16), this is, however, not reflected at the cellular level: the

cuticle layer in *lcr* is discontinuous and partially intermixed with the outer cell wall but still covers large cell wall areas (C.Nawrath unpublished data) whereas that of *fdh* has a WT appearance (Lolle et al., 1992). This implies that *lcr* has an intermediate phenotype with regard to cuticle deposition as the cuticle covering of *bdg* looks more discontinuous: short polymers stacks are embedded in the outer cell wall which is only partially covered by cuticle (Kurdyukov et al., 2006b). The *bdg* mutant is however characterised by an overall increase in cutin monomer. Thus, the connection between alteration in cutin composition, cuticle structure and barrier properties of the cuticle is not straightforward.

4.1.2. *Lcr* and *bdg* mutations have an impact on epidermis maintenance

When grown under greenhouse conditions, the *bdg* mutant shows a progressive trichome death (Kurdyukov et al., 2006b). We suspected that this may be due to dehydration and grew the plants under *in vitro* culture conditions. However the progressive degeneration of the trichomes was also observed under these conditions. This ruled out a simple and localised death caused by dehydration and indicates an active process. When WT leaves are stained with toluidine blue for a longer period of time than two minutes, their trichomes are the first cells to retain the dye (data not shown). That trichomes from *bdg* leaves do not get preferentially or faster stained than WT trichomes (Figure. 9) goes well in hand with the fact that in this mutant, trichome death is not due to the environmental stress.

We also took the opportunity to further observe *bdg* and *lcr* under high humidity conditions. The mutants still showed leaf deformations, fusions and the early appearance of axillary apical meristems as they usually do under greenhouse conditions. The early formation of axillary apical meristems, before any shoot has developed, must lead to the bushy phenotype of these mutants (Wellesen et al., 2001; Kurdyukov et al., 2006b).

On top of the morphological and developmental defects observed in the greenhouse, we saw that under *in vitro* growth conditions both mutants tend to develop succulent-like leaves bearing out-growths on their surfaces (Figure. 12). The production of succulent-like leaves by the *bdg* mutant under *in vitro* culture conditions as also been reported in the Phenome database (<http://rarge.gsc.riken.jp/phenome/>; T. Kuromori).

The authors also mentioned the fasciation as a feature from the *bdg* mutant under greenhouse conditions. In our hands, this remained extremely rare, as seldom as in wild-type plants.

Young *bdg* leaves displayed epidermal ruptures, and petioles from older and succulent *bdg* leaves were found to lack the epidermis. This is reminiscent of the phenotype from the *atml1 pdf2* double mutant (Abe et al., 2003). *ARABIDOPSIS THALIANA* MERISTEM LAYER1 (ATML1) and PROTODERMAL FACTOR2 (PDF2) are epidermis specific homeobox-leucine zipper transcription factors (Lu et al., 1996; Abe et al., 2003). Their functions appear partially redundant (Abe et al., 2003) since single mutants do not show phenotype but double mutants are only able to develop until the rosette stage under *in vitro* culture conditions; their leaves have no epidermis. Both genes seem to be implicated in the epidermis differentiation and maintenance. In the case of *lcr*, tears were observed on the surface of petioles from succulent leaves, also suggesting a defect in the epidermal layer. *Bdg* and *lcr* mutants may not be able to maintain their epidermal layer thus showing the apparition of callus and lack of epidermal covering. This may be explained by a cell to cell adhesion deficiency: cells may loose contact resulting in ruptures, unmasking of the mesophyll layers and in the formation of cell bulges on the organ surface. The formation of callus at the surface of *bdg* and *lcr* petioles and leaves under *in vitro* culture conditions is reminiscent of the phenotype of cutinase expressing plants (CUTE plants). CUTE plants ubiquitously express a fungal cutinase which is secreted in the extracellular space. They develop bulges of mesophyll cells at rupture points (Sieber et al., 2000). We observed the formation of mini plants on these callus-like cell bulges (Figure. 13). The mutations in the epidermis specific *LCR* and *BDG* genes only lead to the formation of callus under *in vitro* culture conditions. Thus compared to our mutants, the CUTE plants seems to have an enhance capacity of forming callus-like tissues. This may be due to the ubiquitous expression of the cutinase gene. We observed that under greenhouse conditions the callus-like structures formed on CUTE plants tend to dry quickly and do not develop mini plants if the trays are not partially covered to maintain some humidity. Therefore the absence of callus-like structures on our mutants under greenhouse condition may also be due to the lower humidity level.

Bdg and *lcr* develop more secondary roots (Figure. 14) and produce more biomass when grown on ½ MS media or on media supplemented with PEG, this may explain

the better growth of both mutants under these conditions. However what actually triggers the early appearance of secondary roots is not clear. The mutations may mimic what usually takes place in WT plants when grown under dry and hot conditions. In WT plants, water evaporation may lead to localised cuticle rupture and to the emission of a signal from leaf epidermis to extend the plants root net. In the *bdg* and *lcr* mutants, where the cuticle is discontinuous, this signal may be sent permanently, leading by default, to the formation of more secondary roots.

4.1.3. A defective cuticle triggers a compensatory response at the cuticular level

Analysis of cell wall bound lipids in rosette leaves was performed after the removal of soluble lipids. The residues were hydrolysed and prepared for gas-chromatography and mass-spectrometry (GC-MS) analysis (Franke et al., 2005; Kurdyukov et al., 2006b); see methods).

Chemical changes do not match proposed enzymatic functions of *FDH* and *LCR*

LCR, also known as CYP86A8, belongs to the CYP86 enzymes and has been shown to catalyse the ω -hydroxylation of fatty acids, amongst others, of the C16 and C18:1 acids (Wellesen et al., 2001). As the *lcr* mutant has a defective cuticle, we were expecting a decrease of the C16 and C18:1 ω -hydroxy fatty acids and of their respective α,ω -diacids (Figure. 2). A decrease in C16 acid derivatives was indeed observed: slightly less in the case of the C16 ω -hydroxy fatty acid and significantly less in the case of the C16 α,ω -diacid; but no change or a significant increase could be detected in C18 acid derivatives (Figure. 16).

FDH is a homologue of the seed specific FATTY ACID ELONGASE 1 (FAE1) (Yephremov et al., 1999; Efremova et al., 2004), which belongs to the β -ketoacyl-CoA synthase family and is a part of the elongase complex (Kunst et al., 1992). This complex catalyses the elongation of C16 and C18 fatty acids by the addition of two carbons per elongation cycle. In *Arabidopsis*, the very long chain fatty acids (VLCFA) present in cutin reach a length of 26 carbons (Franke et al., 2005). In the case of the *fdh* mutant, we were therefore expecting a decrease in monomers with 18 carbons and VLC 2-hydroxy fatty acids, which was not observed. Although cutin contains some very long chain fatty acids, it may not be the best ground to attest the

elongase function of *FDH* as most compounds have a chain length of C16 and C18. Thus, a significant share of C18 compounds probably comes from the *de novo* lipid biosynthesis.

One cannot rule that other fatty acid elongases or ω -hydroxylases compensate for the absence of the original proteins in the respective mutants (see Microarray). The regulation of either these homologue enzymes or of their genes may not be as good as the one from *lcr* or *fdh*, leading to the observed accumulations.

In *att1* and *ace/hth* cuticular mutants the absence of the enzyme is reflected directly by a change in cutin composition: in *att1*, there is a reduction in ω -hydroxy fatty acids and α,ω -diacids that was expected as this gene codes for an ω -hydroxylase of the CYP86 family (Xiao et al., 2004). As the *ace/hth* mutant accumulates less α,ω -diacids but more ω -hydroxy-fatty acids, it was proposed that *ACE/HTH* encodes an ω -hydroxy-dehydrogenase catalysing the production of diacids from ω -hydroxy fatty acids (Kurdyukov et al., 2006a).

The enzymatic function of LCR is supported by *in vitro* assays and sequence homology to the confirmed CYP86A1 ω -hydroxylase (Welleesen et al., 2001) and *FDH*'s by sequence homology to FAE, mutation in which prevents the formation of C20 and C22 monomers in seed storage lipids (Lolle et al., 1992) and to *CUT1*, absence of which mainly leads to the accumulation of C24 wax monomers and a decrease in longer chain compounds (Millar et al., 1999). The enzymatic function of *FDH* is also supported by the fact that other FAE members, such as *FAE1*, *KCS1*, *KCS2*, are inhibited by herbicides (Lechelt-Kunze et al., 2003) known to affect the biosynthesis of VLCFAs (Kolattukudy and Brown, 1974; Boerger and Matthes, 2002) and to phenocopy the *fdh* phenotype when applied on WT plants (Lechelt-Kunze et al., 2003). However the analysis of cell wall bound lipids did not provide new evidence that LCR and *FDH* are respectively, as ω -hydroxylase and β -ketoacyl-CoA synthase, directly involved in cutin biosynthesis.

The changes observed in cell wall bound lipids in these two mutants (and in *bdg*; (Kurdyukov et al., 2006b) can not be explained by the absence of the respective enzymes only. The changes are too similar and do not seem to be correlated with the

putative function of the proteins. Other factors, such as the oxidative stress (see Microarray), the perception of cuticle rupture as a signal of drought or infection, may concur to these modifications. In other words, the absence of both enzymes, and of *BDG*, may trigger a compensatory response in the respective mutants leading to the accumulation of cutin monomers, constituents of their protective layer, the cutin.

The mutations in three cuticular genes, *bdg* (Kurdyukov et al., 2006b), *lcr* and *fdh*, paradoxically lead to an accumulation of cutin monomers. It seems that the *fdh* and *lcr* mutations trigger a weaker compensatory response than *bdg*, as no massive global overaccumulation is observed in these two mutants. Cuticle does not only contain wax and cutin but also cutan (Villena et al., 1999), which in WT *Arabidopsis* plants represents only few percentages of the cutin. It remains unknown whether the ratio cutan/cutin may not be affected in these three mutants. The absence of *BDG* may also trigger a more efficient boosting of cutin polymerases than that of the two other enzymes, probably implicated in the biosynthesis of the cutin monomers.

The correlation between cutin appearance and wax overaccumulation is not obvious

The wax loads from leaves of *lcr* and *fdh* were analysed by GC and GC-MS (Kurdyukov et al., 2006b); see methods) and proved to be, as in *bdg* (Kurdyukov et al., 2006b), higher in both mutants.

As reported in WIN1 transgenic over-expressors (Broun et al., 2004), the increase in wax load led to the formation of visible crystals on the surface of *fdh* and *lcr*.

As a continuous cuticle layer is present on the surface of *fdh* aerial tissue (Lolle et al., 1992; Lolle et al., 1997), we were expecting a milder wax increase than the one observed in *lcr* and *bdg*; a priori, a regular cuticle layer should be a better protection than the patchy cuticle layers present in the two other mutants. Our results suggest that defective cutin layer triggers in *fdh* a compensatory response in wax production in the same proportion as the defective cuticle from the other mutants does; the scaffolding properties of *fdh* cuticle being far from being WT, as shown by chlorophyll leaching ((Lolle et al., 1997); Figure. 9) and toluidine blue staining.

The compensatory response may be because of a higher turnover of the biosynthesis or due to the extension of the production period of cuticle monomers, but this remains unknown. This compensatory response and the secondary effect of the mutations seem to involve a complete reorganisation of metabolic and signalling pathways as shown by the analysis of the transcriptome from the *lcr*, *fdh* and *bdg* mutants.

4.1.4. *Bdg* and *lcr* mutations do not have a strong influence on seed coat composition

Developing seeds are sheltered from environmental stresses such as air dryness, UV and oxidation. As we suspected a strong impact of the growth environment on the composition of cell wall bound lipid from leaves, we turned to seed coat which may display the direct consequences of the mutations only. The staining of *bdg* and *lcr* developing seeds with toluidine blue illustrated the increased permeability of their covering. We therefore analysed the seed coat composition of *bdg* and *lcr* mutants. Seeds were cracked and soluble lipids from the samples were removed. The seed residues were then analysed by GC/GC-MS similarly to leaf residues. On the contrary to what was observed at the cutin level, no significant changes in seed coat monomers was formed in the respective mutants.

During this PhD work, another group working on lipid bio-polymers published a method to perform seed coat analysis (Molina et al., 2006). Compare to their method, we started from less seed material, 10 mg instead 500 mg, which can represent an advantage with mutants producing low seed set. Instead of pre-cracking the seeds in boiling isopropanol, then starting the delipidation with chloroform: methanol, and then after regrinding, passing the seed residue through a series of solvents for further extraction and finally filtering the samples and drying them under vacuum, we simply cracked the seeds to fine powder into a chilled mortar and extracted the seed residues for seven days changing the solvent (chloroform: methanol) daily, collecting the pellet by centrifugation, before letting the seed residue air dry for two days. This proved efficient and should limit the loss of seed material. The monomer composition reported for *Arabidopsis* seeds by M. Pollard and co-workers is similar to ours, although they did not mention the 2-hydroxy components (Molina et al., 2006). The latter may in this case as well be associated with the cell wall material.

It is worth mentioning that, to the difference to what was previously reported (Molina et al., 2006), we did not calculate the monomer quantity per mg of residue after delipidation but we rooted the monomer quantity on the initial seed weight. The proportion between seed coat and the rest of the seed may differ between WT and mutant seeds. Mutant seeds may form a heterogeneous population, have smaller seeds and more seeds may then be present in 10 mg, thus more seed coat material finally. Although the level of precision was sufficient in the case of *lcr* and *bdg* mutants, it appears more precise to weigh seed residues after delipidation as well.

4.1.5. A poor cuticular insulation triggers a compensatory response at the transcriptional level

Using ATH1 Affymetrix arrays comprising probes for about 22500 Arabidopsis genes, we analysed the transcriptome of *lcr*, *bdg* and *fdh* mutants. This gave us the opportunity to have an overall view on the transcriptional changes occurring in these three mutants.

We found out that about one fifth of the commonly mis-regulated genes in *lcr*, *fdh* and *bdg* mutants are genes involved in lipid biosynthesis or trafficking. Genes related to cell wall maintenance or biosynthesis of cell wall component, represent another major subgroup among the commonly upregulated genes and also account for a fifth of them.

Cuticle homeostasis

Data presented in this manuscript show that a good number (14/56) of commonly induced genes in the three cuticular mutants are involved in cuticle homeostasis. They encode enzymes involved in fatty acid elongation such as CER4 (Rowland et al., 2006) or DAISY (Trenkamp et al., 2004), fatty acid ω -oxydation CYP94C1 (Kandel et al., 2007), HTL7 (Krolikowski et al., 2003) or putative lipid trafficking protein, such as LTP2 (Dunkley et al., 2006) or LTP3 (Arondel et al., 2000). Some of the induced genes are known cuticular genes (WAX2 (Chen et al., 2003), CER4 (Rowland et al., 2006)) or their homologues (CYP94C1 (Kandel et al., 2007), HTL7 (Krolikowski et al., 2003), WBC1 (Sanchez-Fernandez et al., 2001). The overexpression of these genes may represent an attempt of the mutants to repair their cuticles by accelerating the biosynthesis, the intracellular lipid flow and the secretion

of monomers. A direct correlation between drought, wax accumulation and the up-regulation of three LTP genes was recently shown in tree tobacco (*Nicotiana glauca* L. Graham) (Cameron et al., 2006). Although not very closely related to CER5 (WBC12) and DSO (WBC11) (see **Appendix H**), WBC1 may also contribute to the overaccumulation of cuticle material on the epidermal surface of *lcr*, *bdg* and *fdh* mutants. The *wbc 11* (*dso*) and *wbc 12* (*cer5*) mutants deposit less cuticle and less wax on their outer cell wall (Pighin et al., 2004; Bird et al., 2007; Panikashvili et al., 2007). It was also shown that the overexpression of some cuticular genes leads to the overaccumulation of cutin (Li et al., 2007a) or wax monomers (Aharoni et al., 2004; Broun et al., 2004).

In the *fdh* and *lcr* mutants, we observed the upregulation of the gene coding for the CYP94C1 which was recently shown to produce α,ω -diacids from C16 and C18 acids *in vitro* (Kandel et al., 2007). This P450 is very likely to catalyse the same reaction *in vivo* and thus, may contribute to adjust the amount of α,ω -diacids in these mutants.

This suggests that plants are capable of perceiving the quality of their cuticle and to specifically activate a set of genes, which are very likely implicated in its repair. We named them “cuticle repair genes”.

Upregulation of cell wall genes may account for elements of the mutant phenotype

Cell wall and cuticle are tightly linked as the former supports the latter. The structure and the composition of the cell wall are also very likely to influence the build up of cuticle material. However, virtually nothing is known about the junctions between cell wall and cuticle. In *bdg*, the cell wall has a stretchy appearance (Kurdyukov et al., 2006b).

Nine genes coding for structural proteins (hydroxyproline and glycin rich proteins) of the cell wall or for enzymes (extensins and hydroxyproline-rich glycoproteins (HRGPs)) associated with its maintenance were found upregulated in the three mutants, suggesting that the mutants may try to reinforce their cell wall by incorporating more structural protein. The modification in cell wall plasticity in the mutants probably accounts for the loss of contact between epidermal cells and the presence of out-growth on the surface of *bdg* and *lcr* mutants grown under *in vitro*

culture conditions. *Gnom/emb30* mutants are among others characterised by a weaker cell adhesion (Shevell et al., 1994), which may be due to an altered exportation of pectin in the extracellular space (Shevell et al., 2000). Pectin network is essential for cell wall structure as it supports the deposition of cellulose and as it is the major component of the middle lamella that is shared by adjacent cells. The probable changes in cell wall composition and structure may also explain the irregularity of the leaf surface from the *lcr* mutant (Yephremov and Schreiber, 2005). The up-regulation of the GPR5 gene associated with shoot initiation and also with somatic embryo formation (Herzog et al., 1995; Magioli et al., 2001) may especially contribute to the formation of callus-like tissues in the epidermis of the mutants, and to the increased number of lateral shoots observed in the mutants.

Intracellular signalling in response to stress in cuticular mutants

Bdg, *lcr* and *fdh* mutants tend to repair their defective cuticle but do not manage to restore a WT protective layer and undergo stress.

Gene coding for different elements of intracellular signalling, such as membrane receptors, kinases and transcription factors were found up regulated in these mutants. The accumulation of signal molecules related to stress, such as H₂O₂, aldehydes and other ROS were implicitly stated by the upregulation of genes implicated in detoxification for instance, glutaredoxins and aldo/keto reductases. The putative overaccumulation of ROS, detoxication enzymes and ion scavengers went with an increase in ROS responsive elements such as the transcription factor BT4 and the metallothionein MTIC.

The upregulation of the *RD26*, *BT4*, *LTP3* and *LTP4* genes which are among others ABA responsive, the induction of an ethylene-forming enzyme and of three ERF/AP2 transcription factors may indicate that the ethylene and ABA signalling pathways are activated in these three cuticular mutants.

The accumulation of LEA proteins and ROFs normally found in tissue undergoing dehydration (Delseny et al., 2001; Peters et al., 2007) and the wax accumulation observed in the *lcr*, *bdg* and *fdh* mutants strongly support the hypothesis that these

mutants suffer from dehydration. It was for instance shown in tobacco tree (*Nicotiana glauca* L. Graham) that the exposure to dry condition enhance wax deposition (Cameron et al., 2006).

The RD26 transcription factor from the NAC family was found up regulated in response to drought and in transgenic plants overexpressing RD26 ABA and stress induced genes were also found induced (Fujita et al., 2004). We found that ERF/AP2 transcription factors namely RAP2.6 and RAP2.6L are induced in our plants. The latter are distantly related to WIN/SHN1 and RAP2.4 (the closest homologue to WXP1; (Alonso et al., 2003; Zhang et al., 2005); see **Appendix I**). The overexpression of WIN1/SHN1 (Aharoni, Dixit et al. 2004) and WXP1 (Zhang et al., 2005) promote wax accumulation and enhance drought tolerance, it could be of the same for RAP2.6 and RAP2.6L.

All these line of evidences concur to tell that as a consequence of the *lcr*, *bdg* and *fdh* mutations intracellular signalling takes place, and that these three cuticular mutants very probably suffer from desiccation and, this shows through at the transcription level.

Activation of defence responses

Cuticular damage has been recently shown to give resistance against *Botrytis cinerea* (*B. cinerea*) to Arabidopsis transgenic plants expressing a fungal cutinase (CUTE plants; (Sieber et al., 2000; Bessire et al., 2007; Chassot et al., 2007). *Bdg* has been shown to have a resistance level comparable to that of the CUTE plants (Chassot et al., 2007), and *lcr* appeared to be more resistant than Columbia WT plants but not as resistant as *bdg* and CUTE plants (Bessire et al., 2007). To explain this, it was proposed that fungitoxic compounds permeate cuticle more easily in the CUTE, *bdg* and *lcr* plants leading to their resistance to *B. cinerea* (Bessire et al., 2007; Chassot et al., 2007). However it appears that other mechanisms may be involved. For instance, the perception of free (unbound) cutin monomers could differ in mutants and WT and may also enhance the production of fungitoxic compounds. It was shown that the exogenous application of C18 fatty acid derivatives on barley leaves confer some

resistance against the powdery mildew fungus *Erysiphe graminis* (Schweizer et al., 1996b).

Also, overexpression of cutinase triggers significant transcriptome changes (Chassot et al., 2007). Using Affymetrix microarrays, candidate genes were defined and overexpressed in WT *Arabidopsis thaliana* plants. The overexpression of respectively three LTPs and three peroxidases protected the WT transgenic plants against *B. cinerea*. The overexpression of two protease inhibitors respectively did not seem a very efficient protection. The three overexpressed LTPs are homologues to the LTP genes found to be induced in our mutants. Two genes from their short RT-PCR candidate list were also found up-regulated in our mutants, namely LTP2 (At2g38530) and GRP5 (At3g20470).

In the list of commonly upregulated genes by *lcr*, *bdg* and *fdh*, genes putatively implicated in plant defence such as SS3, ELI-3, ATT1 were found up-regulated. They may contribute to synthesis of alkaloids, aromatic aldehydes or trypsin inhibitor and thus contribute to the resistant phenotype observed in *lcr* and *bdg* against *B. cinerea* (Bessire et al., 2007; Chassot et al., 2007). Five LTPs were found to be upregulated in the three mutants. They are homologues of the LTPs, which overexpression gave resistance to the transgenic plants against *B. cinerea* (Chassot et al., 2007). Thus, they may also provide resistance to the mutants.

To have a better overview, it would be advantageous to be able to compare our datasets to the growing number of microarray data released by other groups. This meta-analysis would, for instance, allow the direct comparison of the effect of a mutation to the effects of other mutations or different treatments (application of elicitors, hormones, etc...). and may help further to establish a link between cuticular formation and signalling or regulatory pathways. Such a statistical package for meta-analysis of microarray data is currently developed in our lab by A.Yephremov (personal communication).

4.1.6. FDH function may be conserved throughout plant evolution

We could show that the barley (*Hordeum vulgare*) allele of the *FDH* gene is able to complement the *fdh* mutation in *Arabidopsis*. On one hand this was rather expected as the *Hordeum vulgare* gene clusters quite close of *Arabidopsis thaliana* and *Antirrhinum majus* *FDH* (Figure. 26). This later has been shown to complement the *Arabidopsis* mutant (Efremova et al., 2004). This was, on the other hand, quite unexpected as *Hordeum vulgare* and *Arabidopsis thaliana* are distantly related species; monocotyledons and dycotyledons split more than 200 million years ago (Wolfe et al., 1989). It follows that *FDH* function appears to be conserved throughout the evolution. This result is also supported by the fact that application of herbicides leading to the *fdh* phenotype in *Arabidopsis* and *Antirrhinum* also lead to the apparission of organ fusion in millet and corn (Lechelt-Kunze et al., 2003). We observed more WT-like homozygous mutants bearing the *hvFDH* construct at the rosette stage than at the flowering stage. More *FDH* protein may be required during flower development than during leaf onset, this may explain the absence of complementation in the flowers even though it was achieved at the leaf stage. It may also be that floral expression of the *FDH* gene is fine tuned, tuning which could not be fully carried out in our case.

That barley *FDH* is able to complement the *Arabidopsis* *fdh* mutant also implies that if *FDH* is involved in cutin biosynthesis, they should perform the same reaction i.e., the products of the *FDH* enzyme should be present in both species. The cutin of barley leaves contains secondary alcohols with a chain length ranging from C16 to C22, free fatty acids with a chain length of 16 to 22 carbons, ω -hydroxy-acids, and diol and epoxide derivatives with 18 carbons (Espelie et al., 1979). So barley and *Arabidopsis* cutins do not have that much in common. However as both species contain C20 and C22 fatty acids and C18 ω -hydroxy-acids, one could suggest that *FDH* is involved in the elongation steps leading to their production.

4.2 The *htm* mutant

4.2.1. Expression pattern of *HTM*

Making use of transgenic plants expressing promoter or protein reporter constructs enabled us to determine that both, the *HTM* promoter and the HTM protein, are epidermis specific and preferentially expressed in young organs, particularly, during floral development. This was quite expected because *htm* shows a cuticular phenotype and that until now all cuticular genes have been found epidermis specific. The promoter activity was detected in leaf primordia, trichomes of mature leaves, in petals, sepals and just below the papillae cells of floral buds and flowers. The HTM protein was detected in epidermal cells of developing leaves, stems and floral organs. The HTM protein is still present in trichomes, in some pavement cells from leaves and stems epidermis long after the *HTM* transcript has disappeared, thus it seems to be quite stable. DsRED fusion may, however, be responsible for the stabilisation of the HTM protein.

Our expression results are in a good agreement with the data presented by Genevestigator (Zimmermann et al., 2004), which suggests that *HTM* is expressed in aerial organs, strongly in flowers. Our results also do not contradict the microarray data obtained on epidermal peels from Arabidopsis stem (Suh et al., 2005). The authors reported a ratio close to two and a ratio below two, which might indicate that the gene is epidermis specific. That the ratio epidermal signal/ general signal is only about two in this experiment is probably due to the low amount of *HTM* transcript present in stem epidermis.

HTM is expressed in each of the floral whorls, from early developmental stage on and also during seed development. This gene seems to be particularly important for separation of sepals and petals as its absence leads to organ fusion between these two whorls and to an increased permeability of their cuticle. We found that *HTM* expression is stronger at the edges of sepals, where, in the *htm* mutant, toluidine blue dye stains tissue preferentially. Mature organs of the perianth of *htm* mutant were easily stained with toluidine blue, whereas mature stigma, style and developing siliques remain unstained. The *htm* mutation may not have the same effect on all organs, as the native HTM enzyme may not have the same importance everywhere.

Due to the presence of HTM putative homologues, it may as well not have been the right stage to illustrate their permeability defect, notice that at earlier stages of development the apex of *htm* styles gets stained. Leaf fusion are less frequent than sepal-petal fusion in the *htm* mutant, this may be because petals and sepals grow in closer proximity than rosette leaves and also because HTM protein may not have a preponderant role throughout the development of all aerial organs. The expression of the *HTM* gene is not maintained in developing leaves, whereas it is detected in mature petals and sepals.

The application of a hypertonic salt solution on stigma from transgenic plants expressing the HTM-DsRED construct triggers the retraction of the plasma membrane and at the same time of the chimeric HTM-DsRED protein. The application of the salt solution may also affect the localisation of the protein, as more intense spots of fluorescence were observed in the cytoplasm after the application of the salt solution.

4.2.3. Is HTM directly implicated in the cuticle biosynthesis?

Our cell wall bound lipid and wax analyses revealed that the cuticle covering of the *htm* mutant is generally composed of less fatty acid derivatives. This may account for the increase of epidermal permeability, finally leading to an increase in adherability of the floral organs from the *htm* mutant. As a consequence of their reduction in cuticle and wax covering, the *bloomless-22* (*bm-22*) and *glossyl* (*gl1*) mutants have increased cuticle permeability (Jenks et al., 1994; Sturaro et al., 2005) and the *wxp1* mutant, which deposits more wax, a reduced cuticle permeability (Zhang et al., 2005). As illustrated by the *bdg* and the *gpat4/gpat8* mutants, amounts of monomers is not all, deposition and reticulation of the cuticle layer are essential to the establishment of cuticle impermeability (Li et al., 2007b). *Bdg* accumulates more cutin and wax but shows greater cuticle permeability due to a discontinuous cuticle (Kurdyukov et al., 2006b). The *gpat4/gpat8* double mutant which has a normal wax load but a reduced amounts of cutin monomers leading to a drastic reduction of its cuticle permeability.

In the *htm* mutant, no major shift between the classes of wax compounds can be observed, however our cell wall bound lipid analysis revealed that in the *htm* mutant, there is a deficit in mid-chain hydroxy fatty acids, a two-fold increase in C16 α,ω -

diacids and that, the quantity of C18:1 and C18:2 are divided by two. This difference in monomer composition may be directly linked to the enzymatic function of *HTM*, which shows homology to acyl-transferases.

Almost nothing is known about the assembly of the cutin polymer, which for instance may result of the incorporation of individual monomers or of short polymers in the on-growing polyester. However C16 and C18 acids, products of the *de novo* lipid biosynthesis, have to be elongated, oxidised, exported and linked to the on-growing cutin polymer. *HTM* could be involved in the delivery of fatty acids to the extracellular space by linking acyl chains to acyl carriers. To be exported or processed fatty acids need a carrier, this may be CoA, glycerol or something else for instance phenolic compounds. *HTM* may precisely transfer free or acyl-CoA derivatives of C18 ω -hydroxy acid, C16 di-hydroxy acid, C16 hydroxy α,ω -diacid, C18:1 and C18:2 α,ω -diacids to acyl carriers, such as glycerol derivatives. In absence of *HTM*, less of these compounds are incorporated, so maybe less is delivered to the cutin polymerisation site. Formely it could also be that, in the absence of *HTM*, more acyl carrier may be free to export C16 α,ω -diacid which is then more available to extracellular synthases, which take care of cutin polymerisation. Cutin monomers may not be exported one by one but already as short polyesters, therefore *HTM* could also be involved in the attachment of these monomers to short polymers prior to their exportation.

As the *HTM* protein may be localised in the plasma membrane (PM) it may have an extracellular role consisting of activating these compounds to facilitate their transport across the PM and incorporation in the on-growing cutin. As a direct consequence of the absence of *HTM*, one would then expect the incorporation of other compound such as C16 diacids and less of its substrate.

The results of our wax and cell wall bound lipid analyses also suggest that *HTM* is involved in fatty acid elongation. Less C18 acid derivatives are present among the cutin monomers and more C16 acid derivatives can be found. The general decrease in wax monomers (20%) may be due to lower amount of C18 acid which has to be elongated further to yield wax compounds.

Htm mutation does not trigger a global increase in wax or cutin constituents. There may be no compensatory response or else one that bring the cuticle composition nearly back to normal takes place, and manages to counterbalance pretty well the effect of the *htm* mutation with regards to the global quantity of monomers.

4.2.4. Is HTM an acyltransferase?

As *HTM* putatively belongs to the acyltransferases, we have expressed *HTM* in *E.coli* and isolated the protein for *in vitro* assays. One could for instance, incubate HTM with various substrates (Luo et al., 2007), or check whether the HTM protein binds to different kinds of lipids immobilized on membranes. Another approach to learn more about the HTM function would be to examine the *E.coli* cells by TLC coupled with GC-MS to see whether any modifications in the lipid composition are triggered by the introduction of the HTM protein in *E. coli* (Coleman, 1990).

HTM is expressed in flowers and although *Arabidopsis thaliana* flowers are odourless to us and white, the presence of acyltransferases able to use aromatic compounds as substrate in flowers is not original (Dudareva et al., 2000). HTM may take part in the biosynthesis of phenolic derivatives especially abundant in flowers.

Cutin and suberin are polymers of aliphatic monomers cross-linked by glycerol molecules (Moire et al., 1999; Graca et al., 2002). Thus cutin and suberin biosynthesis imply the formation of glycerolipids which may be first synthesised within the cell, or else glycerol and fatty acids derivatives may be sequentially incorporated in the on-growing polyester. Glycerol-phosphate and CoA esters of fatty acids are precursors of the biosynthetic pathway of glycerophospholipids (Kennedy pathway) which produces, among others, triacylglycerol (TAG), essential form of energy storage, and phospholipids acting as intracellular messengers, such as phosphatidylinositol (PI) or phosphatidylserine (PS). The two first steps of this pathway respectively involve the transfer of a fatty acid CoA ester first to glycerol-3-phosphate (G3P) and then to lysophosphatidic acid (LPA) to form phosphatidic acid (PA) (Figure. 45). PA is then used by the branches of the pathway to yield storage lipids or membrane phospholipids such as PI, PS. The first step leading to the formation of LPA from G3P is catalysed by a glycerol-3-phosphate acyl transferase (GPAT) and the second step,

turning LPA into PA is catalysed by a lysophosphatidic acid acyltransferase (LPAAT).

Recently, Arabidopsis enzymes able to catalyse both reactions have been identified. GPAT5 belongs to a small multigenic family of acyltransferases and has an acyl-CoA: glycerol-3-phosphate acyltransferase activity (Beisson et al., 2007). Knock-out mutants in this enzyme accumulate less aliphatic monomers in their suberin and seed coat, which is consistent with the expression pattern of the *GPAT5* gene, preponderantly expressed in root and seed coat of developing seeds. Two more members of the GPAT family, namely GPAT4 and GPAT8, were recently shown to be essential in cutin biosynthesis and epidermis specific (Li et al., 2007b). The *gp4/gpat8* double mutant has a reduced cutin amount. The *ATS2/LPAT1* enzyme could complement the *E.coli* mutant JC201 deficient in lysophosphatidic acid acyltransferase (LPAT) (Coleman, 1990; Bin et al., 2004; Kim and Huang, 2004). *ATS2/LPAT1* localised in the plastids (Bin et al., 2004) and expressed in most organs (Kim and Huang, 2004). The loss of the *ATS2* function is embryo lethal.

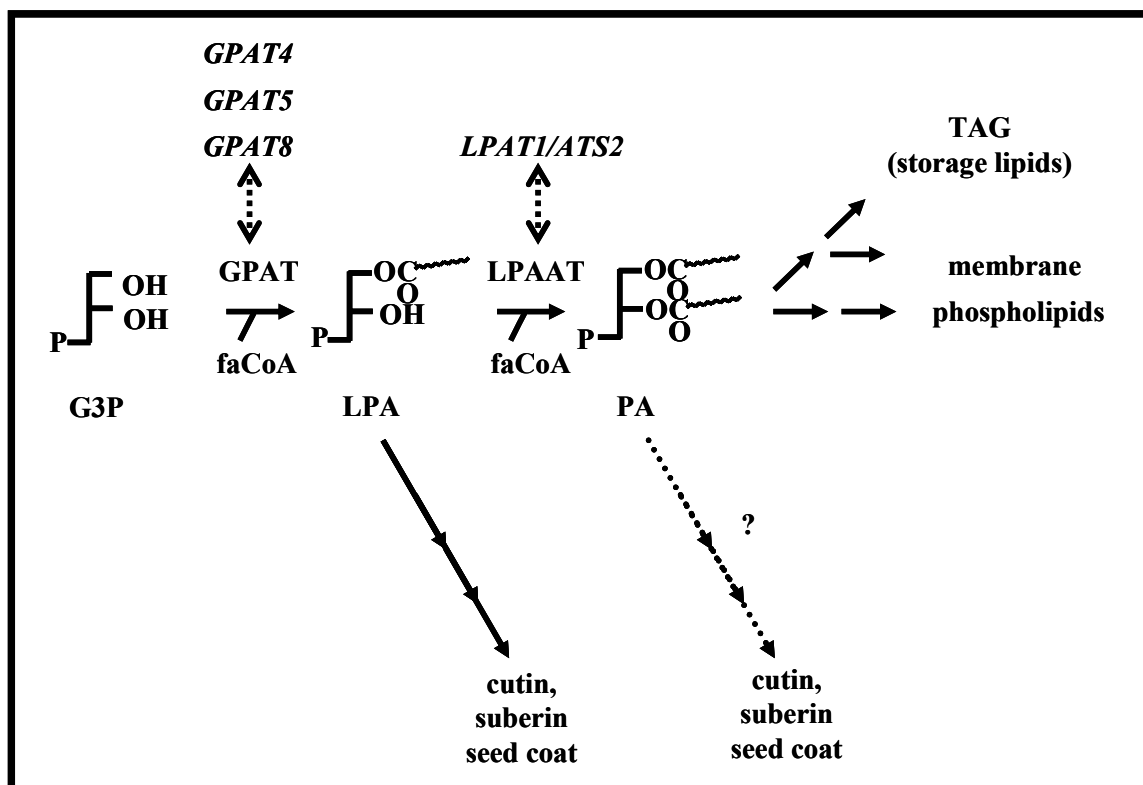


Figure 45. Putative pathway showing biosynthesis of glycerolipid precursors cutin, suberin and seed coat. Acyltransfer reactions are catalysed by GPAT and LPAAT however the function of *HTM* remains unknown. G3P: glycerol-3-phosphate; LPA: lysophosphatidic acid; PA: phosphatidic acid; faCoA: fatty acyl-CoA; GPAT: glycerol-3-phosphate acyl transferase; LPAAT: lysophosphatidic acid acyltransferase.

The fact that the *gpat4/gpat8* double mutant has a cutin phenotype like *htm*, and that HTM is an homologue of ATS2/LPAT1, let us suppose that the HTM enzyme may function as a lysophosphatidic acid acyltransferase (LPAAT). Among the LPAT1 homologues there is LPAT2 which is essential during ovule development; its absence is female gametophytic lethal (Kim et al., 2005). According to the results on *gpat* mutants, LPA is used as precursor to synthesised cutin, suberin and seed coat, PA may also be used. However, as the amounts of storage lipids and membrane phospholipids are not modified in *gpat5* mutant (Beisson et al., 2007) and *gpat4/gpat8* double mutant (Li et al., 2007b) there may be distinct pools of G3P and CoA esters of fatty acid within the cell. Alternatively, only a pool of G3P and CoA esters only may be available but the channelling of precursors for cutin biosynthesis has no influence on branches of Kennedy biosynthesis pathway leading to the production of storage and membrane phospholipids.

Thus HTM could be an acyltransferase but its exact biochemical function remains to be elucidated and it is not likely to be equivalent to that of LPAT or GPAT.

4.3 Investigation on candidate genes

4.3.1. The function of the *LEAKO* gene remains unknown

The leukotrien A₄-hydrolase is bifunctional in both human and yeast (Kull et al., 1999; Kull et al., 2001) and belongs to the metalloenzymes (Medina et al., 1988). One of its functions, of unknown physiological importance, is a peptidase activity; its second function is the ability to catalyse the formation of LTB₄ in human (Soberman et al., 1988) or DHETE in yeast (Kull et al., 1999) starting from LTA₄. In mammals, various epoxide hydrolases are involved in detoxication processes (Wixtrom, 1985) turning oxylipins, epoxides of C20 (arachidonic) and C18 double unsaturated (linoleic) fatty-acids into their corresponding di-hydroxy compounds. In some plant species, the opening of epoxide rings leads to the production of cutin precursors (Croteau and Kolattukudy, 1975; Pinot et al., 1992; Blee and Schuber, 1993) or antifungal substances (Hamberg, 1999).

Recent work on maize has shown that epoxides present in plant cuticles are important for cuticle integrity and that the prevention of their formation was accompanied by

drastic changes in the cuticle structure and properties (Lequeu et al., 2003): the altered cuticle is thinner and offers a poor protection against fungi and pesticides. Thus, Blée and co-workers showed that global inhibition of C18 fatty acids epoxidation greatly affects the cuticle formation, for instance, in maize (the percentage of C18 compounds is approximately equal to the percentage of C16 compounds) and in barley (the percentage of C18 compounds is approximately six times higher than the percentage of C16 compounds) (Lequeu et al., 2003). They showed that the structure of the cuticle of soybean or pea, species rich in C16 fatty acids, is not affected by the inhibition of the peroxygenase activity.

As the *Arabidopsis* cuticle contains both C16/C18 fatty acid (the percentage of C18 compounds is approximately three times higher than the percentage of C16 compounds; (Franke et al., 2005)), we originally hypothesised that the absence of epoxide hydrolase activity perhaps executed by the homologous enzyme of the leukotrien-A₄-hydrolase in *Arabidopsis* may affect the properties of *Arabidopsis* cuticle in a similar way. During this PhD work, Schreiber and co-workers, and Pollard and co-workers described the composition of *Arabidopsis* cutin as a mixture of mostly, α,ω -diacids, mid-chain hydroxylated fatty acids and ω -hydroxy acids (Bonaventure et al., 2004; Franke et al., 2005). In addition Schreiber and co-workers, reported the presence of 2-hydroxy fatty acids (Franke et al., 2005).

As we found out that mid-chain di-oxygenated fatty acids are only present as traces in the *Arabidopsis* cuticle, that LEAKO may be involved in the biosynthesis of cutin precursors is unlikely. As shown in *Lycopersicon esculentum* or *Hedera helix*, another player seem actually to allow most of the fatty acids cross-linking using their carboxy groups: glycerol (Graca et al., 2002).

The function of the *LEAKO* gene remains for now unknown. Genevestigator suggests that this gene is mainly expressed in roots, and the microarray data obtained on epidermis peels from stems indicate that this gene may not be epidermis specific (Zimmermann et al., 2004; Suh et al., 2005). However as, according to Genevestigator, the level of expression of the *LEAKO* gene in the stem is quite low, no reliable conclusion about its epidermis specificity can thus be drawn. If this gene is indeed involved in the biosynthesis of cutin-like polyester, it has therefore a higher

probability to be involved in suberin production. One should observe the roots of the *leako-2* mutant to see whether any visible phenotype occurs as a consequence of *LEAKO*'s absence.

The *LEAKO* enzyme may have evolved on the peptidase side and only retain a function linked to this activity. We could challenge *leako* mutants with different stresses or pathogens to gain insight in the function of this unique gene.

4.3.2. The putative impact of *ALDH5* needs further confirmation.

We suspected that mutants impaired in one or the other aldehyde dehydrogenases may have a modified cuticle composition and show a cuticle phenotype. A decrease in α,ω -diacids could for instance lead to a lower reticulation of the cutin polymer, and finally to a weakened cuticle layer. The *ALDH5* gene is, according to the microarray data obtained on *Arabidopsis* stem, most likely to be epidermis specific (Suh et al., 2005). Genevestigator (<https://www.genevestigator.ethz.ch/at/>) suggests that *ALDH5* is expressed ubiquitously, particularly strongly in aerial organs. Thus this gene may be a good cuticular candidate. In our hands, however the *aldh5-1* homozygous mutant only showed a defect in fertility but none in seed coat or cutin permeability. We observed that embryo death takes place at different stages of development, therefore the *ALDH5* gene maybe sporophytic lethal. *ALDH5* is member of a multigenic family (Kirch et al., 2004) and may functionally be replaced in the *aldh5-1* plants which thus do not show any phenotype during most developmental phases. Thus to investigate the potential impact of the absence of some aldehyde dehydrogenase on the cuticle biosynthesis of *Arabidopsis*, one should indeed investigate multiple *aldh* mutants.

Classically the production of α,ω -diacids is presented as a two-step process, starting from a fatty acid which is first oxidised on its ω -carbon by a ω -hydroxylase and, which then is taken in charge by an ω -aldehyde dehydrogenase, leading from the aldehyde to the α,ω -diacid (Kurdyukov et al., 2006a). An alternative could reside in ω -hydroxylase from the CYP94 group; F. Pinot and co-workers (Le Bouquin et al., 2001; Kandel et al., 2007) showed that the CYP94A5 enzyme is able to catalyse efficiently the two oxidation steps turning 18-hydroxy-9,10-epoxystearic acid into its corresponding α,ω -diacid.

Drought, high salinity, temperature alterations, wounding, pathogen attack or a high level of UV radiations are known to trigger the formation of reactive oxygen species (ROS) in plant tissues. During the degradation of these highly toxic compounds, other reactive compounds, such as aldehydes, are formed (Dhindsa et al., 1981; Chia et al., 1984). It has been highlighted that in various species such as rice (Nakazono et al., 2000) *Tortula vulgaris* (Chen et al., 2002) or *Arabidopsis thaliana* (Kirch et al., 2001) genes encoding ALDHs were upregulated in stressed plants. On the other hand, it was shown that *Arabidopsis* plants over-expressing the *ALDH3* gene were more resistant to stress (Sunkar et al., 2003). As already mentioned, a way to dispose of the aldehydes is to turn them into carboxylic acids. We observed embryo lethality in some *aldh5-1* homozygous mutants; it may be due to the absence of an efficient recycling circuit for the naturally occurring ROS. After showing by transgenic complementation, that the *aldh5-1* mutation is the cause of the observed embryo lethality, one could for instance try to quantify the presence of ROS in WT and mutant.

4.3.3. Is the *hyd4-2* insertion responsible for the phenotype of the *hyd4-2* mutant?

We recently started the investigation on the *HYD4* gene, which is closely related to *BDG* and might have a similar role in plant development. Apart from the *hyd4-2* homozygous mutants none of the other homozygous mutants showed a macroscopic phenotype. The phenotype of the *hyd4-2* mutant is reminiscent of gibberellin mutants such as *gai* (Wilson et al., 1992), *shi* (Fridborg et al., 1999) and of brassinosteroid mutants such as *dwarf4* (Azpiroz et al., 1998), which are dark green and dwarf. Yet since only one accession, *hyd4-2*, out of six insertion lines shows this phenotype, this may imply that the mutation in the *HYD4* gene is actually not responsible for the phenotype of the *hyd4-2* homozygous mutants. However the dark green and dwarf phenotype and the mutant genotype seem to be closely linked: all plants showing a dark green and dwarf phenotype were found to be homozygous mutants (16/16) and none of the other plants were. No other ORF is present at this position, but an insertion in a neighbouring gene may be responsible for the phenotype. It may also be that this gene does not have the same importance in the Columbia and Nossen ecotypes, which could already justify the WT appearance of the *hyd4-5* and *hyd4-6* mutants.

To finally prove that the insertion in the *hyd4-2* population is responsible for the phenotype of the *hyd4-2* mutants, one could genotype more plants to gain information on the physical distance between the *HYD4* gene and the *hyd4-2* mutation. However our result, based on 42 plants, indicates a tight link between the mutation and the *HYD4* gene. Thus one should try to rescue the phenotype of these plants by transgenic complementation, introducing a WT copy of the gene.

Our working hypothesis was that *HYD4* may also be involved in cuticle biosynthesis; we however did not observe any change in cuticle permeability using toluidine blue. According to the microarray data from epidermis peels of *Arabidopsis* (Suh et al., 2005), this gene has a weak level of expression in the stem and could be epidermis specific, the function of this gene may therefore be linked to the cuticle. According to Genvestigator, this gene is expressed in most plant organs but stronger in pollen and stamens which may contribute to the sterility from the *hyd4-2* plants (Zimmermann et al., 2004).

If the mutant phenotype is confirmed, this would possibly mean that the *HYD4* enzyme could either be involved in the biosynthesis of a hormone or in the signalling pathway involving this hormone. *BDG*, to which *HYD4* is closely related, seems to be involved in cuticle biosynthesis but shows similarities to fungal cutinase and is localized in the outer-most epidermal cell-wall (Kurdyukov et al., 2006b). Therefore if *HYD4* shares its extracellular localization, one could suppose that *HYD4* possibly releases signalling molecules from the cell wall and doing so, would be likely to trigger the intracellular signalling cascade leading to cell elongation and plant growth.

5. Summary

Biochemical and genetic responses in cuticular mutants

The cuticle layer is essential for maintaining organ integrity and protecting plants against biotic and abiotic stresses present in their natural environment. *Arabidopsis thaliana* mutants with a defective cuticle layer may help to precisely determine which genes are actually taking part in the formation of the cuticle. The functions of some cuticular genes seem to be conserved between monocots and dicots as we could complement the *Arabidopsis fiddlehead (fdh)* mutant with the barley allele of the *FDH* gene. In addition to a defective cuticle, *fdh*, *bodyguard (bdg)*, *lacerata (lcr)* and the novel *htm Arabidopsis* mutant show ectopic organ fusions and other developmental phenotypes.

As the isolation of pure cutin from cuticular mutants is not doable, we analysed the cell wall bound lipid composition from leaves of the *fdh* and *lcr* mutants. As a consequence of *fdh* and *lcr* mutations, a significant increase in cutin monomer amount takes place. Even though *FDH* and *LCR* enzymes have very different functions, similar alterations in cell wall bound lipid composition were observed in their mutants. As it was observed in *bdg* earlier, we could also show that both *fdh* and *lcr* accumulated more wax. Even though each of these three mutants has its own particularities that, mutations in three genes coding for so different enzymes trigger similar phenotypical alterations was quite unexpected. This brought us to study the compensatory response to cuticular damage and to compare the transcriptome of mutants using microarrays. This analysis supports the idea that plants are able to compensate for cuticle defects specifically altering gene expression.

We characterised the expression pattern of the recently cloned *HTM* gene using promoter and protein fusion reporter constructs. We found that the *HTM* gene is epidermis specific, and is particularly strongly expressed in petals and sepals. This goes well in hand with the phenotype of the *htm* mutant which is characterised by postgenital organ fusion within floral buds. The bound lipid analysis revealed that whereas *htm* deposits similar quantity of monomers on its outer cell wall, there is a shift in monomer proportions. The wax composition of this mutant was not found different from that of the wild type but a global decrease of 20% was observed. Thus it is more likely that *HTM* is indirectly involved in wax and cutin biosynthesis.

We also characterised insertion lines in genes putatively involved in cutin biosynthesis, respectively encoding an aldehyde dehydrogenase, an epoxide hydrolase-like enzyme, and a member of the α/β hydrolase-fold super family.

6. Zusammenfassung

Biochemische und genetische Folgen von kutikulären Defekten in *Arabidopsis thaliana*

Die Kutikula ist essentiell, um Organintegrität zu bewahren, und sie schützt Pflanzen vor biotischem und abiotischem Streß von außen. *Arabidopsis thaliana* Mutanten mit einer defekten Kutikula könnten genutzt werden, um Gene zu identifizieren, die an der Biosynthese der Kutikula beteiligt sind. Die Funktionen einiger Kutikulagene scheinen in monokotyledonen und dikotyledonen Pflanzen konserviert zu sein, da die *Arabidopsis fiddlehead (fdh)* Mutante mit dem *FDH* Gen von Gerste komplementiert werden konnte. Außer einer defekten Kutikula, zeigen *fdh*, *bodyguard (bdg)*, *lacerata (lcr)* und die hier neue *htm Arabidopsis* Mutante ektopische Organfusionen und weitere Entwicklungsphänotypen.

Da eine Isolierung des reinen Kutins aus *Arabidopsis* nicht möglich ist, wurden zellwandgebundene Lipide von Blättern von *fdh* und *lcr* analysiert. Mutationen in *LCR* und *FDH* führen zu signifikanten Erhöhungen des Anteils an Kutinmonomeren. Obwohl *FDH* und *LCR* sehr unterschiedliche Funktionen besitzen, wurden ähnliche Änderungen der zellwandgebundene Lipide nachgewiesen. Ähnlich wie es in *bdg* vorher beschrieben war, wurde auch eine Wachsakkumulation in *fdh* und *lcr* festgestellt. Unerwartet war die gleichartige Änderung der Kutinmonomere in den drei Mutanten, da die drei Enzyme sehr unterschiedlich sind. Um Kompensierungsmechanismen von Pflanzen mit defektem Kutin genauer zu verstehen, wurde das Transkriptom der Mutanten und des Wildtyps mit Hilfe von Microarrays verglichen. Die Analyse bestätigte die Vermutung, daß diese drei Mutanten eine spezifische Modifizierung der Gen-Expression aufweisen.

Das kürzlich klonierte *HTM* wurde durch das Expressionsmuster mit Hilfe von Promoter- und Protein-Reporterkonstrukten charakterisiert. Es wurde rausgefunden, daß *HTM* epidermisspezifisch ist, und daß es besonders stark in Blütenblättern und in Kelchblättern exprimiert wird. Das Expressionsmuster paßt gut zu dem beobachteten Phänotyp von *htm*, da die Mutante postgenitale Organfusionen in der Blüte aufweist. Die Analyse der zellwandgebundenen Lipide zeigte, daß die *htm* Mutante ähnliche Mengen an Kutin-Monomeren auf ihrer Zellwand ablagert wie der Wildtyp, aber daß es eine Verschiebung im Anteil der unterschiedlichen Monomere gibt. Die Ergebnisse der Wachsanalyse von *htm* war dervom Wildtyp sehr ähnlich, abgesehen von einer allgemeinen Abnahme von 20%. Deshalb ist es wahrscheinlich, daß *HTM* auf indirektem Wege in der Kutin- und Wachs- Biosynthese involviert ist.

Wir haben auch insertione Linien in Genen, die wahrscheinlich in der Kutinbiosynthese involviert sind, charakterisiert. Die kodieren jeweils für eine Aldehyd-Dehydrogenase, ein Epoxid-Hydrolase ähnliches Enzym und für einen Angehörigen der α/β -Hydrolase-Familie.

7.1 Appendix A. List of primers used in this study

Line genotyping

insertion line	gene name	allele	primer name	primer sequence (5'-->3')
shyd4	<i>HYD4</i>	WT	D111	CCG AGA AAA TTC GGG ACA GCG ATT CA
			D117	AAA GAA TCT AAT TGG TAT GGC TT
			D117	AAA GAA TCT AAT TGG TAT GGC TT
ghyd4	<i>HYD4</i>	WT	D032 (SALK_b1)	GCG TGG ACC GCT TGC TGC AAC T
			D118	ACT CTG TTC AAG AGC CGT CCG AGA A
			D119	ATT GTG CAT ACT ATG CCA TGC AGA GTG
	<i>HYD4</i>	mutant	D118	ACT CTG TTC AAG AGC CGT CCG AGA A
			Y076 (GABI_left)	GGG AAT GGC GAA ATC AAG GCA TCG
			D111	CCG AGA AAA TTC GGG ACA GCG ATT CA
nos1/nos2	<i>HYD4</i>	WT	D117	AAA GAA TCT AAT TGG TAT GGC TT
			D117	AAA GAA TCT AAT TGG TAT GGC TT
			D147	CCG GAT CGT ATC GGT TTT CG
jic2/jic3	<i>HYD4</i>	WT	D111	CCG AGA AAA TTC GGG ACA GCG ATT CA
			D119	ATT GTG CAT ACT ATG CCA TGC AGA GTG
			D111	CCG AGA AAA TTC GGG ACA GCG ATT CA
			D164 (JIC Spm32)	TAC GAA TAA GAG CGT CCA TTT TAG AGT GA
			LTA-2	ACG GTT TCA ACT TTA TGCACT AAA TG
			5_13520	AGT AAG TCA AAT CTC TCC CAC TCG
leakosalk	<i>LEAKO</i>	WT	D032-	GCG TGG ACC GCT TGC TGC AAC T
			5_13520	AGT AAG TCA AAT CTC TCC CAC TCG
			D096	TGT ACT TGG AGC TGT ACT TGC TGA
			D099	TAC AAG CAC CAG CAA GAG AGG TTA TAA TG
			D098	TTC ATA ACC AAT CTC GAA TAC AC
			D099	TAC AAG CAC CAG CAA GAG AGG TTA TAA TG
aldh5	<i>ALDH5</i>	WT	ALDH5_3	AAT TGT CTT GGC AAG GAA GGC AG TGT CAC CGA TAC ATA TAC TTC ATA T
			N021496	TGT CAC CGA TAC ATA TAC TTC ATA T
			D032	GCG TGG ACC GCT TGC TGC AAC T
			N021496	TGT CAC CGA TAC ATA TAC TTC ATA T

:

Appendix A (continued)

RT-PCR

gene	locus ID	primer name	primer sequence (5'-->3')	number of cycles
<i>HYD4</i>	At5g17780	D148	CCT TCA TCG GTA GAA GGA TCG GTC T	34
		D149	ATC AGC ACC AGT AAT GAT ATC AAC T	
		D118	ACT CTG TTC AAG AGC CGT CCG AGA A	34
		D119	ATT GTG CAT ACT ATG CCA TGC AGA GTG	
		D111	CCG AGA AAA TTC GGG ACA GCG ATT CA	34
		D117	AAA GAA TCT AAT TGG TAT GGC TT	
<i>LEAKO</i>	At5g13520	D026	ATT CTG CCA GTC TGT ACC GCT TGT CCA AG	36
		D029	CAG ATG ATG TAT ATT CTC AGG TCC CAT AT	
<i>ALDH5</i>	At4g36250	D068	GTT CCA TGG AGG GTA TCG AGC TTC A	26
		D069	ATT GAT ATG TTG AAG CCT ACG ATA	
<i>LTP</i>	At5g01870	D169	GTG TTA CCA CTA TGC CTG CTT CTT GCT	30
		D170	CAC TAA ACT CCG GTT ACA TTA GAC GA	
<i>LTP2</i>	At2g38530	D171	GGA GTG ATG AAG TTG GCA TGC ATG	26
		D172	ATT GAA AAG AGT ACA GCC ATT CG	
<i>LTP3</i>	At5g59320	D173	GCA GGT AGC TTG GCT CCA TGT GCA AC	24
		D174	TAT TTT ATT CTA GTA CTT CTG GTA A	
<i>LTP4</i>	At5g59310	D175	GTG GCA CAG TGG CAA GTA GCT TGA G	24
		D176	GAT AGC CGT CTT ATT TTA CGT ATA CG	
<i>CER1</i>	At1g02205	D027	CAG GAA CGG AGA GGT GTA TAT CCA CAA CCA T	22
		D028	CTA TCA ATG CTG GTG TGG TAT GAT AGA TAC	
<i>CER4</i>	At4g33790	D179	ACT CAC GTG CTT CCT CTG TGA TCT TG	24
		D180	GTC GTC CCA ATC GAG AAC CTT TGG AT	

Appendix A (continued)

gene	locus ID	primer name	primer sequence (5'-->3')	number of cycles
<i>WAX2</i>	At5g57800	D021	AAG CAT CCT GAC CTT AGA GTT CGT GTG GTT CAT	24
		D022	TAA GAC CAT ACT TCA TGG CTG CTT CCC ACA	
<i>WIN1/SHN1*</i>	At1g15360	D017	GTC GCT GAG ATT CGT CAT CCT CTC TTG A	36
		D018	TGC AAA GCA ACC TTT TCT TCC TCA TCC A	
<i>DAISY*</i>	At1g04220	D177	TCT CTT CGC CGC TCT TCT TAT CTT	26
		D178	AGC GGT CGG AGG AGC GGT TAG	
<i>palmitoyl</i>	At5g47330	D185	AAG GTT TGA AGC GGT CTG GTG TTG C	28
		D186	TCC CTT GAT TAG CTC ATC TGC TAA C	
<i>carbo</i>	At4g30280	D187	AAC AAT ACA TTT GAG ATA TCA ATA CA	36
		D195	TAC ACA AAC ACC GCA TAC ATA TGA G	
<i>aldo/keto-reductase</i>	At2g37770	D183	CAC GGA TAA AGA AAG GTT CTG TTG GAA	28
		D184	TAG TGT CTC ATG AAC AAG GAA GGA A	
<i>ERF/AP2 member</i>	At1g43160	D189	TGA TTA CCG GTT CAG CTG TGA CTA A	38
		D190	CAA AGC GTT GAC AAT ATG TTA GTT A	
<i>ERF/AP2 calli*</i>	At5g13330	D191	ACC AGA CCA AGA TCA ACC AAG A	38
		D192	TTA TTC TCT TGG GTA GTT ATA A	
<i>ACE7</i>	At5g51950	D193	ATG CAG ACA AGC CGT ACT ACT AGT	30
		D194	ATA CTC TTT AAG TTA ATC ATA CAT T	
<i>Actine2*</i>	At3g18780	D019	AGA GAT TCA GAT GCC CAG AAG TCT TGT TCC	22*
		D020	AAC GAT TCC TGG ACC TGC CTC ATC ATA CTC	

The sequences of *WIN1/SHN1* and *ACTIN2* primers are from (Broun et al., 2004).
The sequences of *ERF/AP2* primers are from (Che et al., 2006).
Sequences of *DAISY* primers, R. Franke personal communication.

Appendix A (continued)

Primers for ARMS PCR:

Primer name	Primer sequence 5'-3'
D155-At <i>FDHF3</i>	GAGCAAGATCTGCTCTCTACCGAGATC
D157-At <i>FDHR2</i>	TCTGCTTAAACTCCCAACCTCAGGACT
D156-At <i>FDHR3</i>	CAATAAGATAAACAGAGCGAGGACGAGAC
D166-At <i>FDHFm3</i>	CGGTTCTTGTGCTGGTTTTTAGTGAG

Designed by Jaffar Jabbari Sheick.

7.2 Appendix B. PRC mixes and programmes

Amplification mixes corresponding to the different types of PCR.

Standard PCR mix (gDNA)

component	Volume (µl)
DNA	3
Buffer 10X	2,5
dNTPs 10mM	0,5
Primer A 10mM	1
Primer B 10mM	1
Dist. Water	16,5
Isa Taq	0,5

Standard PCR mix (colony PCR)

component	Volume (µl)
DNA	2*
Buffer 10X	2,5
dNTPs 10mM	0,5
Primer A 10mM	1,5
Primer B 10mM	1,5
Dist. Water	16,5
Isa Taq	0,5

*Template for colony PCR was prepared as follows: a bit of the colony was resuspended in 100µl of distilled water. Then, the suspension was boiled for 3 min at 100°C and centrifuged at 10000 rpm or higher for 3 min (RT). The crude DNA extracts were kept on ice until further use.

Standard PCR mix (high fidelity PCR)
mix

component	Volume (µl)
DNA	2
Buffer 10X	2,5
dNTPs 10mM	2,5
Primer A 10mM	1,875
Primer B 10mM	1,875
Dist. Water	15,25
High fidelity enz	0,375

Standard semi-quantitative RT-PCR
mix

component	Volume (µl)
RNA	(500 ng) 1-6
5X QIAGEN One-Step buffer	5
dNTPs 10mM	1
Primer A 10mM	1,5
Primer B 10mM	1,5
RNase free water	Variable (14-9)
Enzyme mix	1

ARMS PCR mix

component	Volume (µl)
DNA	3
Buffer 10X	2,5
dNTPs 10mM	0,5
Primer D155 and D156 10mM	1
Primer D157 and D166 10mM	3
Dist. Water	8,5
High fidelity enz	0,5

Appendix B (continued)

Amplification programmes corresponding to the different types of PCR.

gDNA

	94 °C	2 min
Step 2	94°C	1 min
	58°C	45 s
	72°C	variable
	Go to 2 nd step	variable
	72°C	15 min
	15°C	For ever

colony PCR

	94 °C	2 min
Step 2	94 °C	1 min
	58°C	45 s
	72°C	variable
	Go to 2 nd step	variable
	72°C	15 min
	15°C	For ever

High fidelity PCR

	94°C	2 min
Step2	94°C	30s
	56-58°C	1min
	68°C	variable
	Go to the 2 nd step	variable
Step5	94°C	30s
	60-64°C	1min
	68°C	variable
	Go to the 5 th step	variable
	68°C	5 min
	15°C	For ever

semi-quantitative RT-PCR

	50°C	30 min
	95 °C	15 min
Step 3	94°C	1 min
	58°C	45 s
	72°C	variable
	Go to 3 rd step	variable
	72°C	15 min
	15°C	For ever

7.3 Appendix C. Bound lipid analysis: weight-area conversion

To estimate the area of the mutant leaves we used a linear regression between the measured WT weights and areas of their WT counterpart.

experiment	samples	total leaf area (cm ²)	total dry weigh (mg)
bound lipid analysis	WT total	138,36	142,8
<i>fdh</i> 2004	WT total	130,79	150,2
	WT total	167,02	185,9
	WT total	135,07	160,8
	WT total	122,62	140,9
bound lipid analysis	WT total	127,96	146
<i>lcr</i> 2004	WT total	204,42	148,5
	WT total	160,43	106,9
	WT total	162,02	105,8
	WT total	183,63	127,7
	WT total	168,24	111,8
bound lipid analysis	WT total	170,96	107,2
<i>Lcr_fdh</i> 2007	WT total	133,41	72,8
	WT total	152,42	82,5
	WT total	146,24	79,4
	WT total	180,94	91
	WT total	169,97	89,5
	WT total	168,75	87,8
	WT total	184,28	97,2
wax analysis	WT total	34,73	13,7
<i>lcr_fdh</i> 2007	WT total	32,26	13,5
	WT total	38,66	15,6
	WT total	34,78	14,4
	WT total	32,47	12,3
	WT total	35,45	12,7
	WT total	41,35	15,5

Table 3. Measured weight and scanned areas for the WT controls used in the different biochemical analyses.

Appendix C (continued)

As the weigh of tissue used for the experiments is usually not the total amount but far lower, we decided to divide the total cm² and mg WT values, both measured, by a fixed number bringing their values into the domain of weight from used tissue.

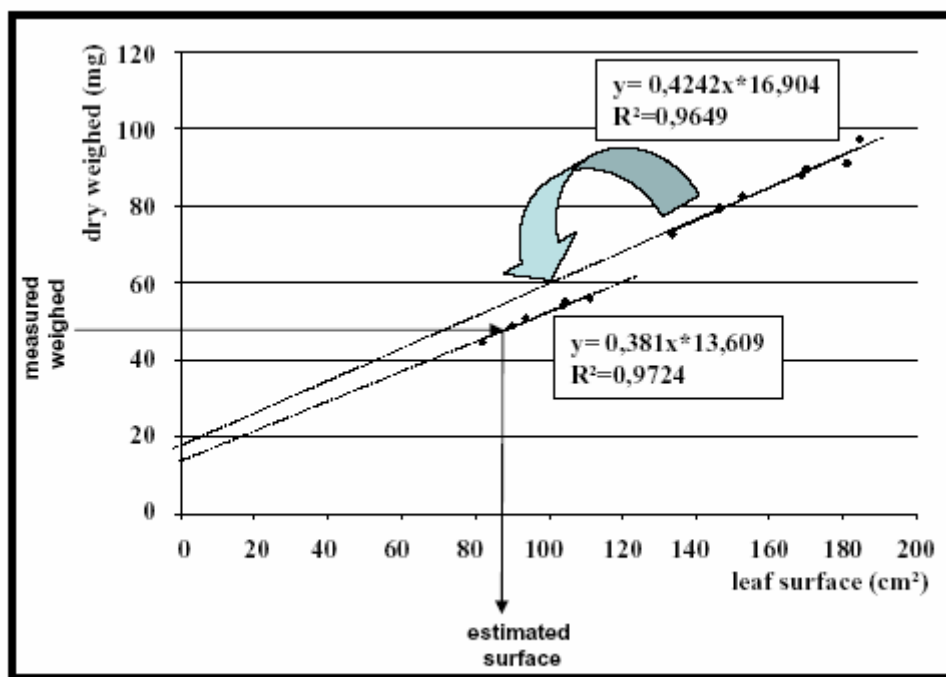


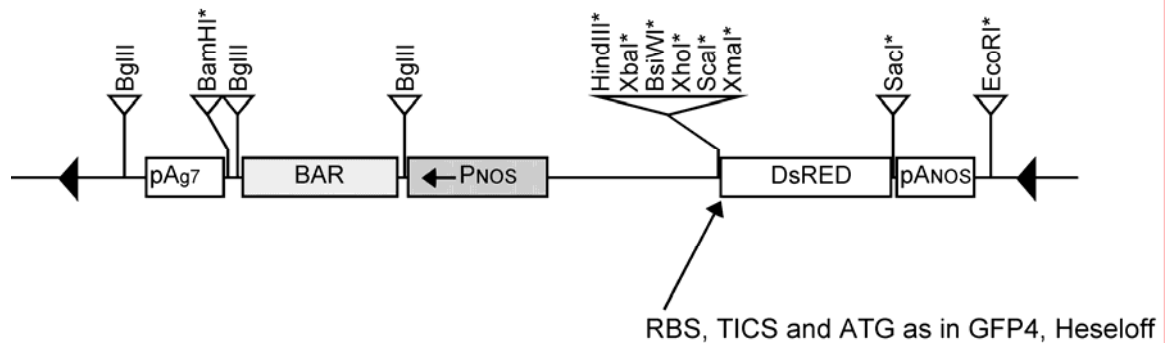
Figure 46. Estimating the area of mutant leaves. Using both, the scanned area and the weight values from the WT samples a linear regression was drawn. This equation was then shifted into a lower “mass/area region” corresponding to that of the amount of used tissue.

experiment	equation	data used to build the equation
<i>fdh_2004</i> (bound lipid analysis)	$y = 0,9837x + 7,1628$	WT total/2,75
<i>lcr_2004</i> (bound lipid analysis)	$y = 1,0028x - 28,73$	WT total/2
<i>lcrfdh_2007</i> (bound lipid analysis)	$y = 0,3891x + 13,609$	WT total/1,625
<i>lcr_fdh_2007</i> (wax analysis)	$y = 0,3188x + 2,5834$	////////////////////

Table 4. Linear regression and ratio for each analysis. The equations are linear regressions, calculated in Microsoft Excel (2003). Equations are based on weigh expressed in mg. y= mg; x=cm².

7.4 Appendix D. Map of the vectors used to build promoter fusion constructs.

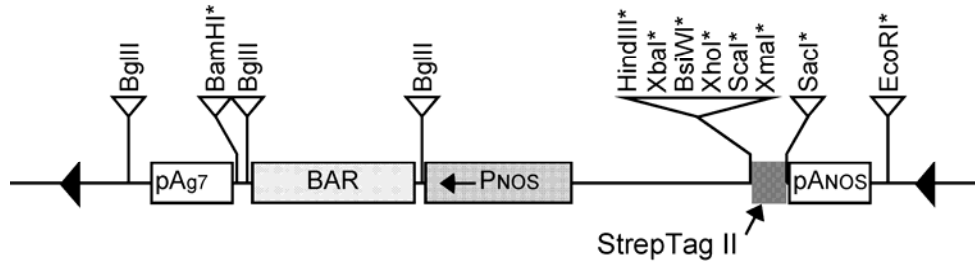
pBDsRED



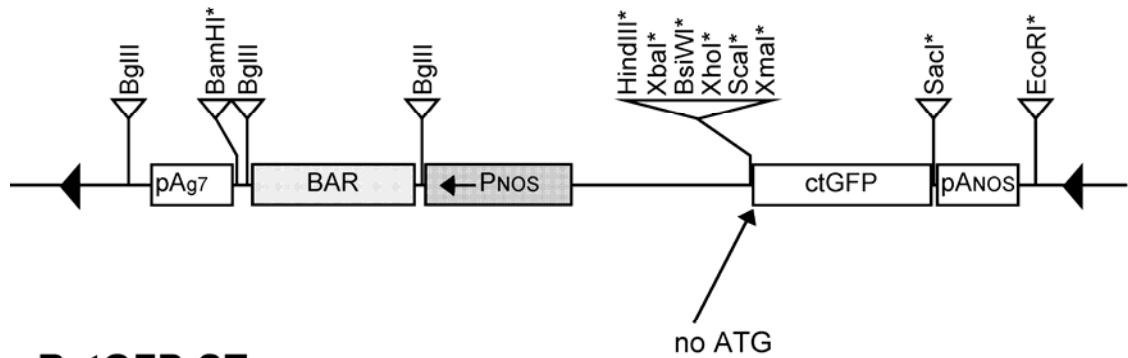
The *HTM* promoter was cloned using the *HindIII*-*XbaI* restriction enzymes in the place of the FAE promoter in front of GUS and GFP genes carried by similar vectors.

7.5 Appendix E. Map of the vectors used to build protein fusion constructs.

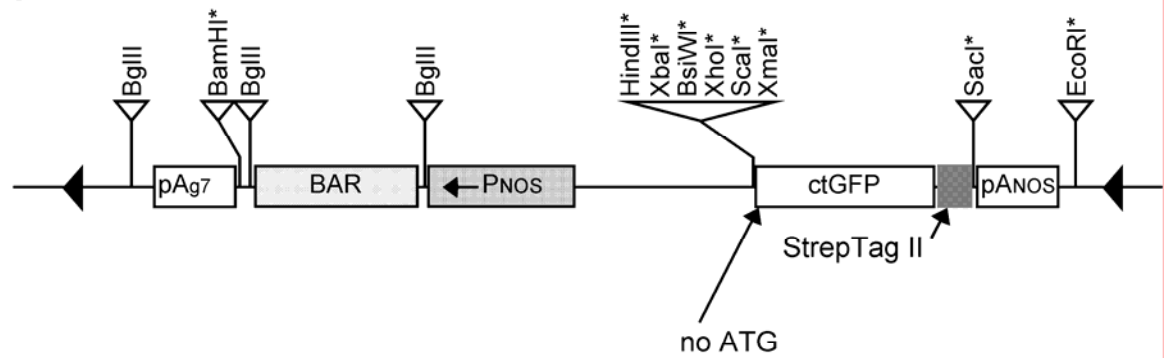
pBct-ST



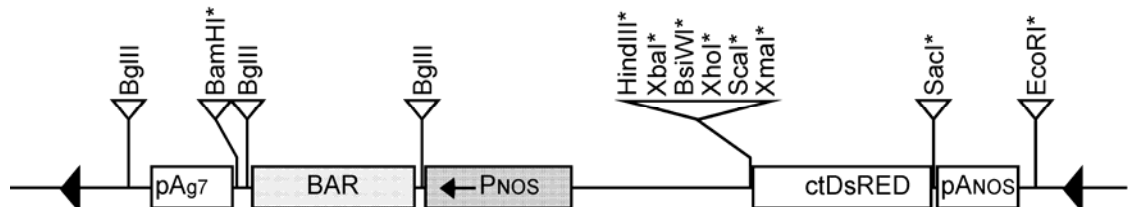
pBctGFP (pBHSGFP62)



pBctGFP-ST



pBctDsRED



7.6 Appendix F. Cell Wall Bound Lipid Analyses of lcr and fdh mutants

Summary table

	Experiment A				Experiment B			
	fdh	WT for fdh	lcr	WT for lcr	fdh	WT	lcr	WT
total amount of bound lipid	2.37	1.88	2.70	2.14	2.22	1.70	1.51	1.10
average	0.22	0.18	0.26	0.20	0.13	0.06	0.08	0.03
std dev	0.10	0.07	0.12	0.08	0.06	0.03	0.03	0.01
std error								
typical cutin monomers								
average	1.33	1.15	1.52	1.31	1.22	0.76	0.79	0.49
std dev total	0.16	0.08	0.18	0.09	0.09	0.03	0.05	0.02
std error	0.07	0.03	0.08	0.04	0.04	0.01	0.02	0.01
concomitant cutin monomers								
average	1.04	0.73	1.18	0.83	1.10	0.94	0.71	0.61
std dev	0.10	0.10	0.11	0.12	0.05	0.07	0.03	0.04
std error	0.04	0.04	0.05	0.05	0.02	0.03	0.01	0.02
total cutine compounds								
statistically different ? (Utest<0.05)	0.011		0.011		0.006		0.006	0.007
typical cutine compounds								
statistically different ? (Utest<0.05)	0.045		0.045		0.006		0.006	0.003
concomitant cutine compounds								
statistically different ? (Utest<0.05)	0.011		0.011		0.006		0.006	0.003
ratio mutant / WT								
ratio for total bound lipids amounts	1.26		1.26		1.37		1.37	0.92
ratio for typical cutin compounds	1.16		1.16		1.61		1.61	1.34
ratio for concomitant cutin compounds	1.43		1.43		1.17		1.18	0.72
total bound lipid: change of app.	25%		25%		40%		40%	-10%
typical cutin compound: change of app.	15%		15%		60%		60%	35%
concomitant cutin compounds: change of app.	45%		45%		20%		20%	-30%
plant age	11 weeks	11 weeks	11 weeks	11 weeks	11 weeks	11 weeks	11 weeks	10 weeks
growth conditions	S.D.	S.D.	S.D.	S.D.	S.D.	S.D.	S.D.	S.D.
issue / sample composition								

S.D.= short day; typical cutin monomers = very long chain unsubstituted fatty acids (chain lengths of C22, C24), very long chain alcohols, ω-hydroxy fatty acids, α,ω-diacids; cutin concomitant monomers = shorter long chain unsubstituted fatty acids and 2-hydroxy fatty acids.

7.7 Appendix G. List of commonly mis-regulated genes in the three cuticular mutants

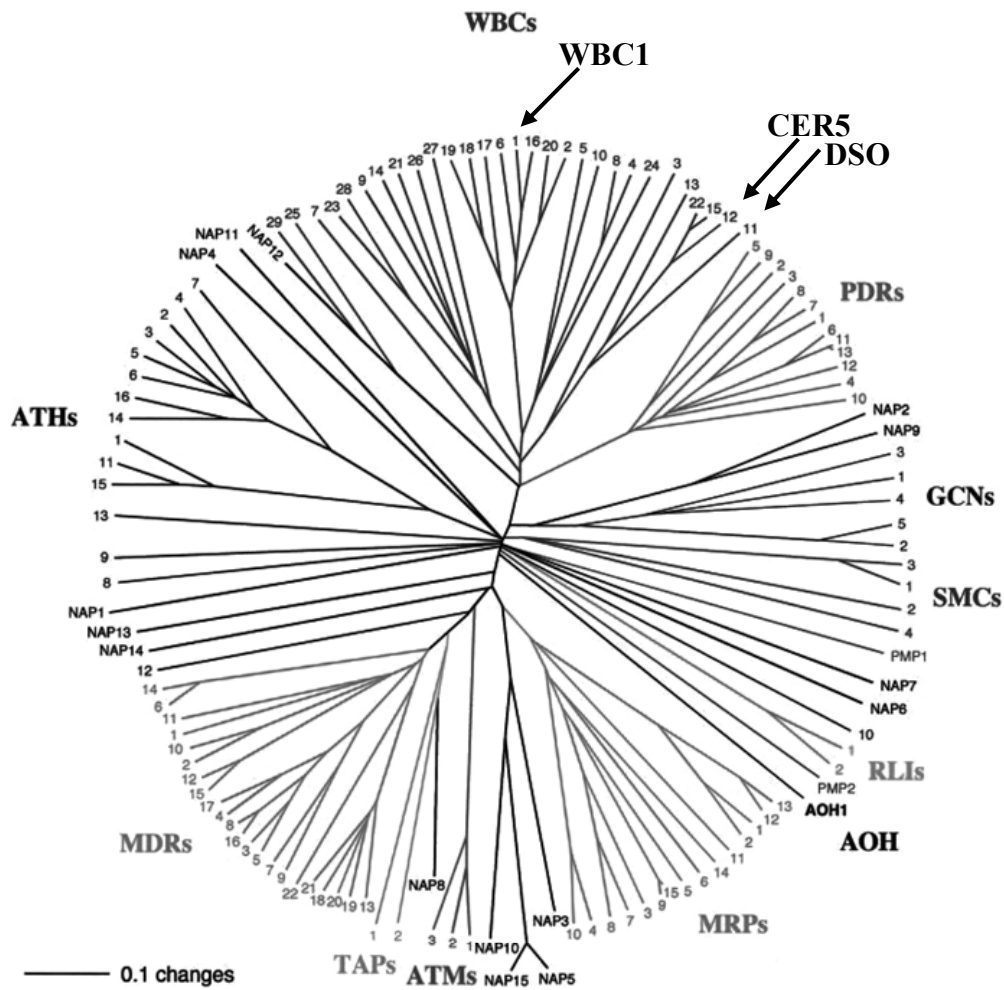
The average fold change displayed in this table is equal to the average of nine mutant/WT ratios per mutant. If the mis regulated gene is likely to be epidermis specific according to the data obtained on stem epidermis peals by Beisson and co-workers, the line is filled in blue (Suh et al., 2005). The RT-PCR candidate genes are in bold.

Locus code	short description	average fold change		
		lcr	bdg	fdh
At5g53710	UNKNOWN	3,7	4,6	5,0
At1g05340	UNKNOWN	17,1	11,6	15,0
At3g14060	UNKNOWN	9,5	10,0	10,8
At5g33355	defensin	6,4	4,9	3,8
At3g16430	jacalin/lectin	6,6	4,2	14,5
At4g37990	ELI3-2	11,3	10,5	10,5
At2g39200	MLO12	8,2	4,5	10,1
At2g43620	chitinase	12,3	6,1	14,7
At2g43510	ATTI1	2,6	3,2	5,4
At1g74000	SS3	6,1	5,2	6,3
At5g59310	LTP4	44,4	42,5	53,5
At5g59320	LTP3	39,4	34,9	49,9
At2g38530	LTP2	23,6	21,3	28,1
At5g01870	LTP put. similar to LTP6	15,8	20,5	15,4
At3g22600	LTP put. plasma membrane	13,4	17,1	20,5
At2g16630	proline rich	4,3	4,4	4,9
At5g47330	PPT1	20,8	18,1	20,1
At2g04570	GDSL lipase	1,9	1,7	3,2
At1g04220	DAISY	12,6	16,2	14,7
At5g57800	WAX2	2,6	2,7	2,8
At4g33790	CER4	2,6	3,9	3,1
At5g51950	HTL7	10,2	8,2	10,6
At2g37760	aldo/keto reductase	4,0	6,0	5,9
At2g37770	aldo/keto reductase	11,0	12,5	12,3
At1g48760	DELTA-ADAPTIN	2,4	2,5	2,9
At5g09530	hydroxyproline-rich	28,1	43,6	44,7
At3g20470	GRP5- glycine-rich	7,6	11,2	14,3
At4g21620	glycine-rich	3,5	4,4	4,8
At4g30290	AtXTH19	15,4	16,5	16,8
At4g30280	XTH18	19,5	8,7	12,9
At1g76930	ATEXT4	16,3	18,9	26,4
At3g15720	glycosyl hydrolase family 28	19,6	18,7	16,9
At1g75750	GASA1	9,6	8,3	10,0
At1g02850	glycosyl hydrolase family 1	5,3	4,8	7,4
At5g26340	MSS1/ STP13	8,1	4,8	17,8
At3g57520	ATSIP2	4,9	2,0	9,1

Appendix G (continued)

Locus code	short description	average fold change		
		lcr	bdg	fdh
At1g05680	UDP-glucuronosyl/UDP-glucosyl transferase	11,3	12,3	6,9
At4g21680	POT; membranar peptid transporter	15,5	11,5	9,6
At4g34950	ABC; small molecules transporter	4,8	4,0	4,1
At2g39350	ABC transporter	9,2	7,2	11,4
At1g07610	MT1C	13,9	10,3	6,1
At2g25450	Ehtylen production	6,7	6,8	4,5
At4g15700	glutaredoxin	4,8	2,6	3,2
At1g30720	electron transporter	15,5	10,4	20,6
At1g52690	LEA	28,1	19,0	18,6
At3g02480	ABA_LEA	27,9	22,6	23,9
At1g01470	LEA 14	-2,7	-4,6	-2,3
At5g11410	kinase	13,4	13,0	9,9
At5g24080	kinase	3,9	4,7	3,7
At5g67480	BT4	6,9	6,5	5,2
At1g62300	WRKY6	5,2	4,1	8,3
At5g49520	WRKY48	4,8	3,4	5,0
At4g01720	WRKY47	1,6	1,7	4,9
At4g27410	RD26	6,5	3,3	4,0
At5g13330	RAP2.6L	5,2	5,6	4,4
At1g43160	RAP2.6	46,7	31,4	36,9
At5g61890	AP2_TF	3,4	4,3	4,8
At4g25100	FSD1	4,9	-12,3	20,2

7.8 Appendix H. The ABC transporter family in Arabidopsis.



The two cuticular genes cluster together whereas WBC1, which is upregulated in *lcr*, *bdg* and *fdh* mutants, belongs to another subgroup of the WBC family. WBC1 shares 30% identity with CER5 and 31% identity with DSO; CER5 and DSO share 52% identity (Panikashvili et al., 2007). Figure adapted from (Sanchez-Fernandez et al., 2001).

7. References

- Aarts, M.G.M., Keijzer, C.J., Stiekema, W.J., and Pereira, A.** (1995). Molecular characterization of the CER1 gene of Arabidopsis involved in epicuticular wax biosynthesis and pollen fertility. *Plant Cell* **7**, 2115-2127.
- Abdel-Ghany, S.E., Muller-Moule, P., Niyogi, K.K., Pilon, M., and Shikanai, T.** (2005). Two p-type ATPases are required for copper delivery in Arabidopsis thaliana chloroplasts. *Plant Cell* **17**, 1233-1251.
- Abe, M., Katsumata, H., Komeda, Y., and Takahashi, T.** (2003). Regulation of shoot epidermal cell differentiation by a pair of homeodomain proteins in Arabidopsis. *Development* **130**, 635-643.
- Aharoni, A., Dixit, S., Jetter, R., Thoenes, E., van Arkel, G., and Pereira, A.** (2004). The SHINE clade of AP2 domain transcription factors activates wax biosynthesis, alters cuticle properties, and confers drought tolerance when overexpressed in Arabidopsis. *Plant Cell* **16**, 2463-2480.
- Allison, D.B., Gadbury, G.L., Heo, M.S., Fernandez, J.R., Lee, C.K., Prolla, T.A., and Weindruch, R.** (2002). A mixture model approach for the analysis of microarray gene expression data. *Comput. Stat. Data Anal.* **39**, 1-20.
- Alonso, J.M., Stepanova, A.N., Leisse, T.J., Kim, C.J., Chen, H.M., Shinn, P., Stevenson, D.K., Zimmerman, J., Barajas, P., Cheuk, R., Gadrinab, C., Heller, C., Jeske, A., Koesema, E., Meyers, C.C., Parker, H., Prednis, L., Ansari, Y., Choy, N., Deen, H., Geralt, M., Hazari, N., Hom, E., Karnes, M., Mulholland, C., Ndubaku, R., Schmidt, I., Guzman, P., Aguilar-Henonin, L., Schmid, M., Weigel, D., Carter, D.E., Marchand, T., Risseuw, E., Brogden, D., Zeko, A., Crosby, W.L., Berry, C.C., and Ecker, J.R.** (2003). Genome-wide Insertional mutagenesis of Arabidopsis thaliana. *Science* **301**, 653-657.
- Aronel, V., Vergnolle, C., Cantrel, C., and Kader, J.C.** (2000). Lipid transfer proteins are encoded by a small multigene family in Arabidopsis thaliana. *Plant Sci.* **157**, 1-12.
- Azpiroz, R., Wu, Y.W., LoCasio, J.C., and Feldmann, K.A.** (1998). An Arabidopsis brassinosteroid-dependent mutant is blocked in cell elongation. *Plant Cell* **10**, 219-230.
- Bagnasco, S.M., Uchida, S., Balaban, R.S., Kador, P.F., and Burg, M.B.** (1987). Induction of Aldose Reductase and Sorbitol in Renal Inner Medullary Cells by Elevated Extracellular NaCl. *Proc. Natl. Acad. Sci. U. S. A.* **84**, 1718-1720.
- Bartels, D., Singh, M., and Salamini, F.** (1988). Onset of Desiccation Tolerance During Development of the Barley Embryo. *Planta* **175**, 485-492.
- Baumann, E., Lewald, J., Saedler, H., Schulz, B., and Wisman, E.** (1998). Successful PCR-based reverse genetic screens using an En-1-mutagenised Arabidopsis thaliana population generated via single-seed descent. *Theor. Appl. Genet.* **97**, 729-734.
- Becker, D., Kemper, E., Schell, J., and Masterson, R.** (1992). New Plant Binary Vectors with Selectable Markers Located Proximal to the Left T-DNA Border. *Plant Molecular Biology* **20**, 1195-1197.
- Becraft, P.W., Stinard, P.S., and McCarty, D.R.** (1996). CRINKLY4: A TNFR-like receptor kinase involved in maize epidermal differentiation. *Science* **273**, 1406-1409.

- Beisson, F., Li, Y.H., Bonaventure, G., Pollard, M., and Ohlrogge, J.B.** (2007). The acyltransferase GPAT5 is required for the synthesis of suberin in seed coat and root of *Arabidopsis*. *Plant Cell* **19**, 351-368.
- Bellec, Y., Harrar, Y., Butaeye, C., Darnet, S., Bellini, C., and Faure, J.D.** (2002). Pasticcino2 is a protein tyrosine phosphatase-like involved in cell proliferation and differentiation in *Arabidopsis*. *Plant J.* **32**, 713-722.
- Benitez, J.J., Matas, A.J., and Heredia, A.** (2004). Molecular characterization of the plant biopolyester cutin by AFM and spectroscopic techniques. *J. Struct. Biol.* **147**, 179-184.
- Benveniste, I., Saito, T., Wang, Y., Kandel, S., Huang, H.W., Pinot, F., Kahn, R.A., Salaun, J.P., and Shimoji, M.** (2006). Evolutionary relationship and substrate specificity of *Arabidopsis thaliana* fatty acid omega-hydroxylase. *Plant Sci.* **170**, 326-338.
- Bessire, M., Chassot, C., Jacquat, A.C., Humphry, M., Borel, S., Petetot, J.M.C., Metraux, J.P., and Nawrath, C.** (2007). A permeable cuticle in *Arabidopsis* leads to a strong resistance to *Botrytis cinerea*. *Embo J.* **26**, 2158-2168.
- Bin, Y., Wakao, S., Fan, J.L., and Benning, C.** (2004). Loss of plastidic lysophosphatidic acid acyltransferase causes embryo-lethality in *Arabidopsis*. *Plant Cell Physiol.* **45**, 503-510.
- Bird, D., Beisson, F., Brigham, A., Shin, J., Greer, S., Jetter, R., Kunst, L., Wu, X.W., Yephremov, A., and Samuels, L.** (2007). Characterization of *Arabidopsis* ABCG11/WBC11, an ATP binding cassette (ABC) transporter that is required for cuticular lipid secretion. *Plant J.* **52**, 485-498.
- Blackman, S.A., Obendorf, R.L., and Leopold, A.C.** (1995). Desiccation Tolerance in Developing Soybean Seeds - the Role of Stress Proteins. *Physiol. Plant.* **93**, 630-638.
- Blee, E., and Schuber, F.** (1993). Biosynthesis of Cutin Monomers - Involvement of a Lipoxygenase Peroxygenase Pathway. *Plant J.* **4**, 113-123.
- Boerger, P., and Matthes, B.** (2002). Inhibitors of biosynthesis of very-long-chain fatty acids. In *Herbicide classes in development* (Heidelberg: Springer Verlag, Berlin), pp. 115-137.
- Bonaventure, G., Beisson, F., Ohlrogge, J., and Pollard, M.** (2004). Analysis of the aliphatic monomer composition of polyesters associated with *Arabidopsis* epidermis: occurrence of octadeca-cis-6, cis-9-diene-1,18-dioate as the major component. *Plant J.* **40**, 920-930.
- Bray, E.A.** (1997). Plant responses to water deficit. *Trends Plant Sci.* **2**, 48-54.
- Brodersen, P., Petersen, M., Pike, H.M., Olszak, B., Skov, S., Odum, N., Jorgensen, L.B., Brown, R.E., and Mundy, J.** (2002). Knockout of *Arabidopsis* ACCELERATED-CELL-DEATH11 encoding a sphingosine transfer protein causes activation of programmed cell death and defense. *Genes Dev.* **16**, 490-502.
- Broun, P., Poindexter, P., Osborne, E., Jiang, C.Z., and Riechmann, J.L.** (2004). WIN1, a transcriptional activator of epidermal wax accumulation in *Arabidopsis*. *Proc. Natl. Acad. Sci. U. S. A.* **101**, 4706-4711.
- Cameron, K.D., Teece, M.A., and Smart, L.B.** (2006). Increased accumulation of cuticular wax and expression of lipid transfer protein in response to periodic drying events in leaves of tree tobacco. *Plant Physiol.* **140**, 176-183.
- Chassot, C., Nawrath, C., and Metraux, J.P.** (2007). Cuticular defects lead to full immunity to a major plant pathogen. *Plant J.* **49**, 972-980.

- Che, P., Lall, S., Nettleton, D., and Howell, S.H.** (2006). Gene expression programs during shoot, root, and callus development in Arabidopsis tissue culture. *Plant Physiol.* **141**, 620-637.
- Chen, X.B., Zeng, Q., and Wood, A.J.** (2002). The stress-responsive *Tortula ruralis* gene ALDH21A1 describes a novel eukaryotic aldehyde dehydrogenase protein family. *J. Plant Physiol.* **159**, 677-684.
- Chen, X.B., Goodwin, S.M., Boroff, V.L., Liu, X.L., and Jenks, M.A.** (2003). Cloning and characterization of the WAX2 gene of Arabidopsis involved in cuticle membrane and wax production. *Plant Cell* **15**, 1170-1185.
- Chen, Z.Y., Hartmann, H.A., Wu, M.J., Friedman, E.J., Chen, J.G., Pulley, M., Schulze-Lefert, P., Panstruga, R., and Jones, A.M.** (2006). Expression analysis of the AtMLO gene family encoding plant-specific seven-transmembrane domain proteins. *Plant Molecular Biology* **60**, 583-597.
- Chia, L.S., Mayfield, C.I., and Thompson, J.E.** (1984). Simulated Acid-Rain Induces Lipid-Peroxidation and Membrane Damage in Foliage. *Plant Cell Environ.* **7**, 333-338.
- Close, T.J.** (1996). Dehydrins: Emergence of a biochemical role of a family of plant dehydration proteins. *Physiol. Plant.* **97**, 795-803.
- Coleman, J.** (1990). Characterization of Escherichia-Coli-Cells Deficient in 1-Acyl-Sn-Glycerol-3-Phosphate Acyltransferase Activity. *J. Biol. Chem.* **265**, 17215-17221.
- Croteau, R., and Kolattukudy, P.E.** (1975). Biosynthesis of Hydroxyfatty Acid Polymers - Enzymatic Epoxidation of 18-Hydroxyoleic Acid to 18-Hydroxy-Cis-9,10-Epoxy stearic Acid by a Particulate Preparation from Spinach (*Spinacia-Oleracea*). *Arch. Biochem. Biophys.* **170**, 61-72.
- Delseny, M., Bies-Etheve, N., Carles, C., Hull, G., Vicient, C., Raynal, M., Grellet, F., and Aspart, L.** (2001). Late Embryogenesis Abundant (LEA) protein gene regulation during Arabidopsis seed maturation. *J. Plant Physiol.* **158**, 419-427.
- Denghui, X., Zuyu, Z., Kurumathurmadam, V., Baofang, F., and Zhixiang, C.** (2005). Pathogen induced AtWRKY48 functions as a negative regulator in plant defense. In *Molecular & General Genetics*, pp. 318-328.
- Dhindsa, R.S., Plumbdhindsa, P., and Thorpe, T.A.** (1981). Leaf Senescence - Correlated with Increased Levels of Membrane-Permeability and Lipid-Peroxidation, and Decreased Levels of Superoxide-Dismutase and Catalase. *J. Exp. Bot.* **32**, 93-101.
- Douliez, J.P., Michon, T., Elmorjani, K., and Marion, D.** (2000). Structure, biological and technological functions of lipid transfer proteins and indolines, the major lipid binding proteins from cereal kernels. *J. Cereal Sci.* **32**, 1-20.
- Du, L.Q., and Poovaiah, B.W.** (2004). A novel family of Ca²⁺/calmodulin-binding proteins involved in transcriptional regulation: interaction with fsh/Ring3 class transcription activators. *Plant Molecular Biology* **54**, 549-569.
- Dudareva, N., Murfitt, L.M., Mann, C.J., Gorenstein, N., Kolosova, N., Kish, C.M., Bonham, C., and Wood, K.** (2000). Developmental regulation of methyl benzoate biosynthesis and emission in snapdragon flowers. *Plant Cell* **12**, 949-961.
- Dunaeva, M., and Adamska, W.** (2001). Identification of genes expressed in response to light stress in leaves of Arabidopsis thaliana using RNA differential display. *Eur. J. Biochem.* **268**, 5521-5529.

- Dunaevskii, Y.E., Tsybina, T.A., Belyakova, G.A., Domash, V.I., Sharpio, T.P., Zabreiko, S.A., and Belozerskii, M.A.** (2005). Proteinase inhibitors as antistress proteins in higher plants. *Appl. Biochem. Microbiol.* **41**, 344-348.
- Dunkley, T.P.J., Hester, S., Shadforth, I.P., Runions, J., Weimar, T., Hanton, S.L., Griffin, J.L., Bessant, C., Brandizzi, F., Hawes, C., Watson, R.B., Dupree, P., and Lilley, K.S.** (2006). Mapping the Arabidopsis organelle proteome. *Proc. Natl. Acad. Sci. U. S. A.* **103**, 6518-6523.
- Eapen, D., Barroso, M.L., Campos, M.E., Ponce, G., Corkidi, G., Dubrovsky, J.G., and Cassab, G.I.** (2003). A no hydrotropic response root mutant that responds positively to gravitropism in Arabidopsis. *Plant Physiol.* **131**, 536-546.
- Efremova, N., Schreiber, L., Bar, S., Heidmann, I., Huijser, P., Wellesen, K., Schwarz-Sommer, Z., Saedler, H., and Yephremov, A.** (2004). Functional conservation and maintenance of expression pattern of FIDDLEHEAD-like genes in Arabidopsis and Antirrhinum. *Plant Molecular Biology* **56**, 821-837.
- Eisenhaber, B., Wildpaner, M., Schultz, C.J., Borner, G.H.H., Dupree, P., and Eisenhaber, F.** (2003). Glycosylphosphatidylinositol lipid anchoring of plant proteins. Sensitive prediction from sequence- and genome-wide studies for arabidopsis and rice. *Plant Physiol.* **133**, 1691-1701.
- Espelie, K.E., Dean, B.B., and Kolattukudy, P.E.** (1979). Composition of Lipid-Derived Polymers from Different Anatomical Regions of Several Plant-Species. *Plant Physiol.* **64**, 1089-1093.
- Fabbri, M., Delp, G., Schmidt, O., and Theopold, U.** (2000). Animal and plant members of a gene family with similarity to alkaloid-synthesizing enzymes. *Biochem. Biophys. Res. Commun.* **271**, 191-196.
- Faust, A.** (2006). Characterisation of cuticular mutants in *Arabidopsis thaliana*. In *Biochemistry* (Cologne: University of Cologne).
- Fehling, E., and Mukherjee, K.D.** (1991). Acyl-Coa Elongase from a Higher-Plant (*Lunaria-Annua*) - Metabolic Intermediates of Very-Long-Chain Acyl-Coa Products and Substrate-Specificity. *Biochimica Et Biophysica Acta* **1082**, 239-246.
- Franke, R., Briesen, I., Wojciechowski, T., Faust, A., Yephremov, A., Nawrath, C., and Schreiber, L.** (2005). Apoplastic polyesters in Arabidopsis surface tissues - A typical suberin and a particular cutin. *Phytochemistry* **66**, 2643-2658.
- Fridborg, I., Kuusk, S., Moritz, T., and Sundberg, E.** (1999). The Arabidopsis dwarf mutant shi exhibits reduced gibberellin responses conferred by overexpression of a new putative zinc finger protein. *Plant Cell* **11**, 1019-1031.
- Fujita, M., Fujita, Y., Maruyama, K., Seki, M., Hiratsu, K., Ohme-Takagi, M., Tran, L.S.P., Yamaguchi-Shinozaki, K., and Shinozaki, K.** (2004). A dehydration-induced NAC protein, RD26, is involved in a novel ABA-dependent stress-signaling pathway. *Plant J.* **39**, 863-876.
- Garcion, C., and Metraux, J.** (2006). FiRe and microarrays: a fast answer to burning questions. *Trends Plant Sci.* **11**, 320-322.
- Gong, Z.Z., Koiwa, H., Cushman, M.A., Ray, A., Bufford, D., Kore-eda, S., Matsumoto, T.K., Zhu, J.H., Cushman, J.C., Bressan, R.A., and Hasegawa, P.M.** (2001). Genes that are uniquely stress regulated in salt overly sensitive (sos) mutants. *Plant Physiol.* **126**, 363-375.

- Gormann, R., Schreiber, L., and Kolodziej, H.** (2004). Cuticular wax profiles of leaves of some traditionally used African Bignoniaceae. *Z.Naturforsch.(C)* **59**, 631-635.
- Graca, J., Schreiber, L., Rodrigues, J., and Pereira, H.** (2002). Glycerol and glyceryl esters of omega-hydroxyacids in cutins. *Phytochemistry* **61**, 205-215.
- Haberer, G., Erschadi, S., and Torres-Ruiz, R.A.** (2002). The Arabidopsis gene PEPINO/PASTICCINO2 is required for proliferation control of meristematic and non-meristematic cells and encodes a putative anti-phosphatase. *Dev. Genes Evol.* **212**, 542-550.
- Hamberg, M.** (1999). An epoxy alcohol synthase pathway in higher plants: Biosynthesis of antifungal trihydroxy oxylipins in leaves of potato. *Lipids* **34**, 1131-1142.
- Heredia, A.** (2003). Biophysical and biochemical characteristics of cutin, a plant barrier biopolymer. *Biochim. Biophys. Acta-Gen. Subj.* **1620**, 1-7.
- Heredia, A., Matas, A., and Dominguez, E.** (2000). Investigating plant lipid biopolymers. *Biochem. Educ.* **28**, 50-51.
- Herzog, M., Dorne, A.M., and Grellet, F.** (1995). Gasa, a Gibberellin-Regulated Gene Family from Arabidopsis-Thaliana Related to the Tomato Gast1 Gene. *Plant Molecular Biology* **27**, 743-752.
- Jakoby, M.J., Weini, C., Pusch, S., Kuijt, S.J.H., Merkle, T., Dissmeyer, N., and Schnittger, A.** (2006). Analysis of the subcellular localization, function, and proteolytic control of the Arabidopsis cyclin-dependent kinase inhibitor ICK1/KRP1. *Plant Physiol.* **141**, 1293-1305.
- James, D.W., Lim, E., Keller, J., Plooy, I., Ralston, E., and Dooner, H.K.** (1995). Directed Tagging of the Arabidopsis Fatty-Acid Elongation-1 (Fae1) Gene with the Maize Transposon Activator. *Plant Cell* **7**, 309-319.
- Jenks, M.A., Tuttle, H.A., Eigenbrode, S.D., and Feldmann, K.A.** (1995). Leaf Epicuticular Waxes of the Eceriferum Mutants in Arabidopsis. *Plant Physiol.* **108**, 369-377.
- Jenks, M.A., Joly, R.J., Peters, P.J., Rich, P.J., Axtell, J.D., and Ashworth, E.N.** (1994). Chemically-Induced Cuticle Mutation Affecting Epidermal Conductance to Water-Vapor and Disease Susceptibility in Sorghum-Bicolor (L) Moench. *Plant Physiol.* **105**, 1239-1245.
- Jetter, R., and Riederer, M.** (1994). Epicuticular Crystals of Nonacosan-10-Ol - in-Vitro Reconstitution and Factors Influencing Crystal Habits. *Planta* **195**, 257-270.
- Kader, J.C.** (1996). Lipid-transfer proteins in plants. *Annual Review of Plant Physiology and Plant Molecular Biology* **47**, 627-654.
- Kandel, S., Sauveplane, V., Compagnon, V., Franke, R., Millet, Y., Schreiber, L., Werck-Reichhart, D., and Pinot, F.** (2007). Characterization of a methyl jasmonate and wounding-responsive cytochrome P450 of Arabidopsis thaliana catalyzing dicarboxylic fatty acid formation in vitro. *Febs J.* **274**, 5116-5127.
- Kannangara, R., Branigan, C., Liu, Y., Penfield, T., Rao, V., Mouille, G., Hofte, H., Pauly, M., Riechmann, J.L., and Broun, P.** (2007). The transcription factor WIN1/SHN1 regulates cutin biosynthesis in Arabidopsis thaliana. *Plant Cell* **19**, 1278-1294.
- Kerstiens, G.** (1996). Cuticular water permeability and its physiological significance. *J. Exp. Bot.* **47**, 1813-1832.
- Kiedrowski, S., Kawalleck, P., Hahlbrock, K., Somssich, I.E., and Dangel, J.L.** (1992). Rapid Activation of a Novel Plant Defense Gene Is Strictly Dependent on the Arabidopsis-Rpm1 Disease Resistance Locus. *Embo J.* **11**, 4677-4684.

- Kim, H.U., and Huang, A.H.C.** (2004). Plastid lysophosphatidyl acyltransferase is essential for embryo development in Arabidopsis. *Plant Physiol.* **134**, 1206-1216.
- Kim, H.U., Li, Y.B., and Huang, A.H.C.** (2005). Ubiquitous and endoplasmic reticulum-located lysophosphatidyl acyltransferase, LPAT2, is essential for female but not male gametophyte development in Arabidopsis. *Plant Cell* **17**, 1073-1089.
- Kirch, H.H., Nair, A., and Bartels, D.** (2001). Novel ABA- and dehydration-inducible aldehyde dehydrogenase genes isolated from the resurrection plant *Craterostigma plantagineum* and *Arabidopsis thaliana*. *Plant J.* **28**, 555-567.
- Kirch, H.H., Bartels, D., Wei, Y.L., Schnable, P.S., and Wood, A.J.** (2004). The ALDH gene superfamily of Arabidopsis. *Trends Plant Sci.* **9**, 371-377.
- Kliebenstein, D.J., Monde, R.A., and Last, R.L.** (1998). Superoxide dismutase in Arabidopsis: An eclectic enzyme family with disparate regulation and protein localization. *Plant Physiol.* **118**, 637-650.
- Kolattukudy, P.E.** (1980). Bio-Polyester Membranes of Plants - Cutin and Suberin. *Science* **208**, 990-1000.
- Kolattukudy, P.E.** (1981). Structure, Biosynthesis, and Biodegradation of Cutin and Suberin. *Annual Review of Plant Physiology and Plant Molecular Biology* **32**, 539-567.
- Kolattukudy, P.E., and Brown, L.** (1974). Inhibition of Cuticular Lipid Biosynthesis in *Pisum-Sativum* by Thiocarbamates. *Plant Physiol.* **53**, 903-906.
- Koncz, C., and Schell, J.** (1986). The Promoter of TI-DNA Gene 5 Controls the Tissue-Specific Expression of Chimeric Genes Carried by a Novel Type of *Agrobacterium* Binary Vector. *Mol. Gen. Genet.* **204**, 383-396.
- Krolkowski, K.A., Victor, J.L., Wagler, T.N., Lolle, S.J., and Pruitt, R.E.** (2003). Isolation and characterization of the Arabidopsis organ fusion gene HOTHEAD. *Plant J.* **35**, 501-511.
- Kull, F., Ohlson, E., and Haeggstrom, J.Z.** (1999). Cloning and characterization of a bifunctional leukotriene A(4) hydrolase from *Saccharomyces cerevisiae*. *J. Biol. Chem.* **274**, 34683-34690.
- Kull, F., Ohlson, E., Lind, B., and Haeggstrom, J.Z.** (2001). *Saccharomyces cerevisiae* leukotriene A(4) hydrolase: Formation of leukotriene B-4 and identification of catalytic residues. *Biochemistry* **40**, 12695-12703.
- Kunst, L., and Samuels, A.L.** (2003). Biosynthesis and secretion of plant cuticular wax. *Prog. Lipid Res.* **42**, 51-80.
- Kunst, L., Taylor, D.C., and Underhill, E.W.** (1992). Fatty-Acid Elongation in Developing Seeds of *Arabidopsis-Thaliana*. *Plant Physiol. Biochem.* **30**, 425-434.
- Kurdyukov, S., Faust, A., Trenkamp, S., Bar, S., Franke, R., Efremova, N., Tietjen, K., Schreiber, L., Saedler, H., and Yephremov, A.** (2006a). Genetic and biochemical evidence for involvement of HOTHEAD in the biosynthesis of long-chain alpha-omega-dicarboxylic fatty acids and formation of extracellular matrix. *Planta* **224**, 315-329.
- Kurdyukov, S., Faust, A., Nawrath, C., Bar, S., Voisin, D., Efremova, N., Franke, R., Schreiber, L., Saedler, H., Metraux, J.-P., and Yephremov, A.** (2006b). The Epidermis-Specific Extracellular BODYGUARD Controls Cuticle Development and Morphogenesis in Arabidopsis
10.1105/tpc.105.036079. *Plant Cell* **18**, 321-339.
- Kutchan, T.M.** (1995). Alkaloid Biosynthesis - the Basis for Metabolic Engineering of Medicinal-Plants. *Plant Cell* **7**, 1059-1070.

- Le Bouquin, R., Skrabs, M., Kahn, R., Benveniste, I., Salaun, J.P., Schreiber, L., Durst, F., and Pinot, F.** (2001). CYP94A5, a new cytochrome P450 from *Nicotiana tabacum* is able to catalyze the oxidation of fatty acids to the omega-alcohol and to the corresponding diacid. *Eur. J. Biochem.* **268**, 3083-3090.
- Lechelt-Kunze, C., Meissner, R.C., Drewes, M., and Tietjen, K.** (2003). Flufenacet herbicide treatment phenocopies the fiddlehead mutant in *Arabidopsis thaliana*. *Pest Manag. Sci.* **59**, 847-856.
- Lee, G.J., Kim, H., Kang, H., Jang, M., Lee, D.W., Lee, S., and Hwang, I.** (2007). EpsinR2 interacts with clathrin, adaptor protein-3, AtVTI12, and phosphatidylinositol-3-phosphate. Implications for EpsinR2 function in protein trafficking in plant cells. *Plant Physiol.* **143**, 1561-1575.
- Lequeu, J., Fauconnier, M.L., Chammai, A., Bronner, R., and Blee, E.** (2003). Formation of plant cuticle: evidence for the occurrence of the peroxygenase pathway. *Plant J.* **36**, 155-164.
- Li, Y., Beisson, F., Koo, J.K.A., Molina, A., Pollard, M., and Ohlrogge, J.B.** (2007a). Identification of acyltransferases required for cutin biosynthesis and production of cutin with suberin-like monomers. *PNAS* **104**, 18339-18344.
- Li, Y.H., Beisson, F., Koo, J.K.A., Molina, A., Pollard, M., and Ohlrogge, J.B.** (2007b). Identification of acyltransferases required for cutin biosynthesis and production of cutin with suberin-like monomers. *Proc. Natl. Acad. Sci. U. S. A.* **104**, 18339-18344.
- Lolle, S.J., and Cheung, A.Y.** (1993). Promiscuous Germination and Growth of Wildtype Pollen from *Arabidopsis* and Related Species on the Shoot of the *Arabidopsis* Mutant, Fiddlehead. *Dev. Biol.* **155**, 250-258.
- Lolle, S.J., Cheung, A.Y., and Sussex, I.M.** (1992). Fiddlehead - an *Arabidopsis* Mutant Constitutively Expressing an Organ Fusion Program That Involves Interactions between Epidermal-Cells. *Dev. Biol.* **152**, 383-392.
- Lolle, S.J., Berlyn, G.P., Engstrom, E.M., Krolkowski, K.A., Reiter, W.D., and Pruitt, R.E.** (1997). Developmental regulation of cell interactions in the *Arabidopsis* fiddlehead-1 mutant: A role for the epidermal cell wall and cuticle. *Dev. Biol.* **189**, 311-321.
- Lu, P.Z., Porat, R., Nadeau, J.A., and Oneill, S.D.** (1996). Identification of a meristem L1 layer-specific gene in *Arabidopsis* that is expressed during embryonic pattern formation and defines a new class of homeobox genes. *Plant Cell* **8**, 2155-2168.
- Luo, J., Nishiyama, Y., Fuell, C., Taguchi, G., Elliott, K., Hill, L., Tanaka, Y., Kitayama, M., Yamazaki, M., Bailey, P., Parr, A., Michael, A.J., Saito, K., and Martin, C.** (2007). Convergent evolution in the BAHD family of acyl transferases: identification and characterization of anthocyanin acyl transferases from *Arabidopsis thaliana*. *Plant J.* **50**, 678-695.
- Magioli, C., Barroco, R.M., Rocha, C.A.B., de Santiago-Fernandes, L.D., Mansur, E., Engler, G., Margis-Pinheiro, M., and Sachetto-Martins, G.** (2001). Somatic embryo formation in *Arabidopsis* and eggplant is associated with expression of a glycine-rich protein gene (*Atgrp-5*). *Plant Sci.* **161**, 559-567.
- Marchant, A., Kargul, J., May, S.T., Muller, P., Delbarre, A., Perrot-Rechenmann, C., and Bennett, M.J.** (1999). AUX1 regulates root gravitropism in *Arabidopsis* by facilitating auxin uptake within root apical tissues. *Embo J.* **18**, 2066-2073.
- Mayfield, J.A., Fiebig, A., Johnstone, S.E., and Preuss, D.** (2001). Gene families from the *Arabidopsis thaliana* pollen coat proteome. *Science* **292**, 2482-2485.

- Medina, J.F., Haeggstrom, J., Kumlin, M., and Radmark, O.** (1988). Leukotriene-A4 - Metabolism in Different Rat-Tissues. *Biochimica Et Biophysica Acta* **961**, 203-212.
- Merkouropoulos, G., and Shirsat, A.H.** (2003). The unusual Arabidopsis extensin gene atExt1 is expressed throughout plant development and is induced by a variety of biotic and abiotic stresses. *Planta* **217**, 356-366.
- Merkouropoulos, G., Barnett, D.C., and Shirsat, A.H.** (1999). The Arabidopsis extensin gene is developmentally regulated, is induced by wounding, methyl jasmonate, abscisic and salicylic acid, and codes for a protein with unusual motifs. *Planta* **208**, 212-219.
- Michaels, S.D., and Amasino, R.M.** (2001). High throughput isolation of DNA and RNA in 96-well format using a paint shaker. *Plant Mol. Biol. Rep.* **19**, 227-233.
- Millar, A.A., and Kunst, L.** (1997). Very-long-chain fatty acid biosynthesis is controlled through the expression and specificity of the condensing enzyme. *Plant J.* **12**, 121-131.
- Millar, A.A., Clemens, S., Zachgo, S., Giblin, E.M., Taylor, D.C., and Kunst, L.** (1999). CUT1, an arabidopsis gene required for cuticular wax biosynthesis and pollen fertility, encodes a very-long-chain fatty acid condensing enzyme. *Plant Cell* **11**, 825-838.
- Moire, L., Schmutz, A., Buchala, A., Stark, R.E., and Ryser, U.** (1999). Glycerol is a suberin monomer. New experimental evidence for an old hypothesis. *Plant Physiol.* **119**, 1137-1146.
- Molina, A., and GarciaOlmedo, F.** (1997). Enhanced tolerance to bacterial pathogens caused by the transgenic expression of barley lipid transfer protein LTP2. *Plant J.* **12**, 669-675.
- Molina, I., Bonaventure, G., Ohlrogge, J., and Pollard, M.** (2006). The lipid polyester composition of Arabidopsis thaliana and Brassica napus seeds. *Phytochemistry* **67**, 2597-2610.
- Nakazono, M., Tsuji, H., Li, Y.H., Saisho, D., Arimura, S., Tsutsumi, N., and Hirai, A.** (2000). Expression of a gene encoding mitochondrial aldehyde dehydrogenase in rice increases under submerged conditions. *Plant Physiol.* **124**, 587-598.
- Nawrath, C.** (2002). The biopolymers Cutin and Suberin. (American Society of Plant Biologists).
- Norholm, M.H.H., Nour-Eldin, H.H., Brodersen, P., Mundy, J., and Halkier, B.A.** (2006). Expression of the Arabidopsis high-affinity hexose transporter STP13 correlates with programmed cell death. *FEBS Lett.* **580**, 2381-2387.
- O'Neill, C.M., Gill, S., Hobbs, D., Morgan, C., and Bancroft, I.** (2003). Natural variation for seed oil composition in Arabidopsis thaliana. *Phytochemistry* **64**, 1077-1090.
- Ohlrogge, J., and Browse, J.** (1995). Lipid Biosynthesis. *Plant Cell* **7**, 957-970.
- Okada, K., and Shimura, Y.** (1990). Reversible Root-Tip Rotation in Arabidopsis Seedlings Induced by Obstacle-Touching Stimulus. *Science* **250**, 274-276.
- Osato, Y., Yokoyama, R., and Nishitani, K.** (2006). A principal role for AtXTH18 in Arabidopsis thaliana root growth: a functional analysis using RNAi plants. *J. Plant Res.* **119**, 153-162.
- Panikashvili, D., Savaldi-Godstein, S., Mandel, T., Yifhar, T., Franke, R.B., Höfer, R., Schreiber, L., Chory, J., and Aharoni, A.** (2007). The Arabidopsis *DESPERADO/AtWBC11* transporter is required for cutin and wax secretion. *Plant Physiol.* **145**, 1345-1360.

- Peters, S., Mundree, S.G., Thomson, J.A., Farrant, J.M., and Keller, F.** (2007). Protection mechanisms in the resurrection plant *Xerophyta viscosa* (Baker): both sucrose and raffinose family oligosaccharides (RFOs) accumulate in leaves in response to water deficit. *J. Exp. Bot.* **58**, 1947-1956.
- Pighin, J.A., Zheng, H.Q., Balakshin, L.J., Goodman, I.P., Western, T.L., Jetter, R., Kunst, L., and Samuels, A.L.** (2004). Plant cuticular lipid export requires an ABC transporter. *Science* **306**, 702-704.
- Pinot, F., Salaun, J.P., Bosch, H., Lesot, A., Mioskowski, C., and Durst, F.** (1992). Omega-Hydroxylation of Z9-Octadecenoic, Z9, 10-Epoxystearic and 9,10-Dihydroxystearic Acids by Microsomal Cytochrome P450 Systems from *Vicia-Sativa*. *Biochem. Biophys. Res. Commun.* **184**, 183-193.
- Pluthero, F.G.** (1993). Rapid Purification of High-Activity Taq DNA-Polymerase. *Nucleic Acids Res.* **21**, 4850-4851.
- Poppenberger, B., Fujioka, S., Soeno, K., George, G.L., Vaistij, F.E., Hiranuma, S., Seto, H., Takatsuto, S., Adam, G., Yoshida, S., and Bowles, D.** (2005). The UGT73C5 of *Arabidopsis thaliana* glucosylates brassinosteroids. *Proc. Natl. Acad. Sci. U. S. A.* **102**, 15253-15258.
- Post-Beittenmiller, D.** (1998). The cloned *Eceriferum* genes of *Arabidopsis* and the corresponding Glossy genes in maize. *Plant Physiol. Biochem.* **36**, 157-166.
- Pruitt, R.E., Vielle-Calzada, J.P., Ploense, S.E., Grossniklaus, U., and Lolle, S.J.** (2000). FIDDLEHEAD, a gene required to suppress epidermal cell interactions in *Arabidopsis*, encodes a putative lipid biosynthetic enzyme. *Proc. Natl. Acad. Sci. U. S. A.* **97**, 1311-1316.
- Radmark, O., Shimizu, T., Jornvall, H., and Samuelsson, B.** (1984). Leukotriene-a-4 Hydrolase in Human-Leukocytes - Purification and Properties. *J. Biol. Chem.* **259**, 2339-2345.
- Rashotte, A.M., and Feldmann, K.A.** (1998). Correlations between epicuticular wax structures and chemical composition in *Arabidopsis thaliana*. *Int. J. Plant Sci.* **159**, 773-779.
- Riederer, M., and Schonherr, J.** (1988). Covalent Binding of Chemicals to Plant Cuticles - Quantitative-Determination of Epoxide Contents of Cutins. *Arch. Environ. Contam. Toxicol.* **17**, 21-25.
- Riederer, M., and Schreiber, L.** (2001). Protecting against water loss: analysis of the barrier properties of plant cuticles. *J. Exp. Bot.* **52**, 2023-2032.
- Rizzo, W.B., Lin, Z., and Carney, G.** (2001). Fatty aldehyde dehydrogenase: genomic structure, expression and mutation analysis in Sjogren-Larsson syndrome. *Chem.-Biol. Interact.* **130**, 297-307.
- Robatzek, S., and Somssich, I.E.** (2002). Targets of AtWRKY6 regulation during plant senescence and pathogen defense. *Genes Dev.* **16**, 1139-1149.
- Rosso, M.G., Li, Y., Strizhov, N., Reiss, B., Dekker, K., and Weisshaar, B.** (2003). An *Arabidopsis thaliana* T-DNA mutagenized population (GABI-Kat) for flanking sequence tag-based reverse genetics. *Plant Molecular Biology* **53**, 247-259.
- Rowland, O., Zheng, H.Q., Hepworth, S.R., Lam, P., Jetter, R., and Kunst, L.** (2006). CER4 encodes an alcohol-forming fatty acyl-coenzyme A reductase involved in cuticular wax production in *Arabidopsis*. *Plant Physiol.* **142**, 866-877.
- Sachettomartins, G., Fernandes, L.D., Felix, D.B., and Deoliveira, D.E.** (1995). Preferential Transcriptional Activity of a Glycine-Rich Protein Gene from *Arabidopsis-Thaliana* in Protoderm-Derived Cells. *Int. J. Plant Sci.* **156**, 460-470.

- Sambrook, J., and Russell, D.W.** (2001). *Molecular cloning: a laboratory manual*. (CSHL Press, New York).
- Sanchez-Fernandez, R., Davies, T.G.E., Coleman, J.O.D., and Rea, P.A.** (2001). The Arabidopsis thaliana ABC protein superfamily, a complete inventory. *J. Biol. Chem.* **276**, 30231-30244.
- Schnurr, J., Shockey, J., and Browse, J.** (2004). The acyl-CoA synthetase encoded by LACS2 is essential for normal cuticle development in Arabidopsis. *Plant Cell* **16**, 629-642.
- Schönherr, J.** (2000). Calcium chloride penetrates plant cuticles via aqueous pores. *Planta* **212**, 112-118.
- Schweizer, P., Felix, G., Buchala, A., Muller, C., and Metraux, J.P.** (1996a). Perception of free cutin monomers by plant cells. *Plant J.* **10**, 331-341.
- Schweizer, P., Jeanguenat, A., Whitacre, D., Metraux, J.P., and Mosinger, E.** (1996b). Induction of resistance in barley against *Erysiphe graminis f sp hordei* by free cutin monomers. *Physiol. Mol. Plant Pathol.* **49**, 103-120.
- Shevell, D.E., Kunkel, T., and Chua, N.H.** (2000). Cell wall alterations in the Arabidopsis emb30 mutant. *Plant Cell* **12**, 2047-2059.
- Shevell, D.E., Leu, W.M., Gillmor, C.S., Xia, G.X., Feldmann, K.A., and Chua, N.H.** (1994). Emb30 Is Essential for Normal-Cell Division, Cell Expansion, and Cell-Adhesion in Arabidopsis and Encodes a Protein That Has Similarity to Sec7. *Cell* **77**, 1051-1062.
- Shimizu, T., Radmark, O., and Samuelsson, B.** (1984). Enzyme with Dual Lipoxygenase Activities Catalyzes Leukotriene-A4 Synthesis from Arachidonic-Acid. *Proceedings of the National Academy of Sciences of the United States of America-Biological Sciences* **81**, 689-693.
- Sieber, P., Schorderet, M., Ryser, U., Buchala, A., Kolattukudy, P., Metraux, J.P., and Nawrath, C.** (2000). Transgenic Arabidopsis plants expressing a fungal cutinase show alterations in the structure and properties of the cuticle and postgenital organ fusions. *Plant Cell* **12**, 721-737.
- Siegel, B.A., and Verbeke, J.A.** (1989). Diffusible Factors Essential for Epidermal-Cell Redifferentiation in *Catharanthus-Roseus*. *Science* **244**, 580-582.
- Soberman, R.J., Sutyak, J.P., Okita, R.T., Wendelborn, D.F., Roberts, L.J., and Austen, K.F.** (1988). The Identification and Formation of 20-Aldehyde Leukotriene-B4. *J. Biol. Chem.* **263**, 7996-8002.
- Solovchenko, A., and Merzlyak, M.** (2003). Optical properties and contribution of cuticle to UV protection in plants: experiments with apple fruit. *Photochem. Photobiol. Sci.* **2**, 861-866.
- Sturaro, M., Hartings, H., Schmelzer, E., Velasco, R., Salamini, F., and Motto, M.** (2005). Cloning and characterization of GLOSSY1, a maize gene involved in cuticle membrane and wax production. *Plant Physiol.* **138**, 478-489.
- Suh, M.C., Samuels, A.L., Jetter, R., Kunst, L., Pollard, M., Ohlrogge, J., and Beisson, F.** (2005). Cuticular lipid composition, surface structure, and gene expression in Arabidopsis stem epidermis. *Plant Physiol.* **139**, 1649-1665.
- Sunkar, R., Bartels, D., and Kirch, H.H.** (2003). Overexpression of a stress-inducible aldehyde dehydrogenase gene from Arabidopsis thaliana in transgenic plants improves stress tolerance. *Plant J.* **35**, 452-464.
- Taji, T., Ohsumi, C., Seki, M., Iuchi, S., Yamaguchi-Shinozaki, K., and Shinozaki, K.** (2002). Important roles of drought- and cold-inducible genes for galactinol synthase in stress tolerance in Arabidopsis thaliana. *Plant Cell Physiol.* **43**, S233-S233.

- Tanaka, H., Watanabe, M., Watanabe, D., Tanaka, T., Machida, C., and Machida, Y.** (2002). ACR4, a putative receptor kinase gene of *Arabidopsis thaliana*, that is expressed in the outer cell layers of embryos and plants, is involved in proper embryogenesis. *Plant Cell Physiol.* **43**, 419-428.
- Tanaka, H., Onouchi, H., Kondo, M., Hara-Nishimura, I., Nishimura, M., Machida, C., and Machida, Y.** (2001). A subtilisin-like serine protease is required for epidermal surface formation in *Arabidopsis* embryos and juvenile plants. *Development* **128**, 4681-4689.
- Tanaka, T., Tanaka, H., Machida, C., Watanabe, M., and Machida, Y.** (2004). A new method for rapid visualization of defects in leaf cuticle reveals five intrinsic patterns of surface defects in *Arabidopsis*. *Plant J.* **37**, 139-146.
- Tephly, T.R., and Burchell, B.** (1990). Udp-Glucuronosyltransferases - a Family of Detoxifying Enzymes. *Trends in Pharmacological Sciences* **11**, 276-279.
- Todd, J., Post-Beittenmiller, D., and Jaworski, J.G.** (1999). KCS1 encodes a fatty acid elongase 3-ketoacyl-CoA synthase affecting wax biosynthesis in *Arabidopsis thaliana*. *Plant J.* **17**, 119-130.
- Trenkamp, S., Martin, W., and Tietjen, K.** (2004). Specific and differential inhibition of very-long-chain fatty acid elongases from *Arabidopsis thaliana* by different herbicides. *Proc. Natl. Acad. Sci. U. S. A.* **101**, 11903-11908.
- Villena, J.F., Dominguez, E., Stewart, D., and Heredia, A.** (1999). Characterization and biosynthesis of non-degradable polymers in plant cuticles. *Planta* **208**, 181-187.
- Vissenberg, K., Oyama, M., Osato, V., Yokoyama, R., Verbelen, J.P., and Nishitani, K.** (2005). Differential expression of AtXTH17, AtXTH18, AtXTH19 and AtXTH20 genes in *Arabidopsis* roots. Physiological roles in specification in cell wall construction. *Plant Cell Physiol.* **46**, 192-200.
- von Wettstein-Knowles, P.** (1982). Elongases and Epicuticular Wax Biosynthesis. *Physiologie Vegetale* **20**, 797-809.
- Watanabe, M., Tanaka, H., Watanabe, D., Machida, C., and Machida, Y.** (2004). The ACR4 receptor-like kinase is required for surface formation of epidermis-related tissues in *Arabidopsis thaliana*. *Plant J.* **39**, 298-308.
- Wellesen, K., Durst, F., Pinot, F., Benveniste, I., Nettesheim, K., Wisman, E., Steiner-Lange, S., Saedler, H., and Yephremov, A.** (2001). Functional analysis of the LACERATA gene of *Arabidopsis* provides evidence for different robes of fatty acid omega-hydroxylation in development. *Proc. Natl. Acad. Sci. U. S. A.* **98**, 9694-9699.
- Wilson, R.N., Heckman, J.W., and Somerville, C.R.** (1992). Gibberellin Is Required for Flowering in *Arabidopsis-Thaliana* under Short Days. *Plant Physiol.* **100**, 403-408.
- Wixtrom, R.N.a.H., B.D.** (1985). *Biochemical Pharmacology and Toxicology*, D. Zakim, and Vessey, D. A., ed (New York: Wiley).
- Wolfe, K.H., Gouy, M.L., Yang, Y.W., Sharp, P.M., and Li, W.H.** (1989). Date of the Monocot Dicot Divergence Estimated from Chloroplast DNA-Sequence Data. *Proc. Natl. Acad. Sci. U. S. A.* **86**, 6201-6205.
- Xiao, F.M., Goodwin, S.M., Xiao, Y.M., Sun, Z.Y., Baker, D., Tang, X.Y., Jenks, M.A., and Zhou, J.M.** (2004). *Arabidopsis* CYP86A2 represses *Pseudomonas syringae* type III genes and is required for cuticle development. *Embo J.* **23**, 2903-2913.
- Yamaguchi-Shinozaki, K., Koizumi, M., Urao, S., and Shinozaki, K.** (1992). Molecular Cloning and Characterization of 9 cDNAs for Genes That are Responsive to Desiccation in *Arabidopsis thaliana*: Sequence Analysis of One

- cDNA Clone That Encodes a Putative Transmembrane Channel Protein. *Plant Cell Physiol.* **33**, 217-224.
- Ye, S., Dhillon, S., Ke, X.Y., Collins, A.R., and Day, I.N.M.** (2001). An efficient procedure for genotyping single nucleotide polymorphisms. *Nucleic Acids Res.* **29**, art. no.-e88.
- Yephremov, A., and Schreiber, L.** (2005). The dark side of the cell wall: Molecular genetics of plant cuticle. *Plant Biosystems* **139**, 74-79.
- Yephremov, A., Wisman, E., Huijser, P., Huijser, C., Wellesen, K., and Saedler, H.** (1999). Characterization of the FIDDLEHEAD gene of Arabidopsis reveals a link between adhesion response and cell differentiation in the epidermis. *Plant Cell* **11**, 2187-2201.
- Yokoyama, R., and Nishitani, K.** (2001). A comprehensive expression analysis of all members of a gene family encoding cell-wall enzymes allowed us to predict cis-regulatory regions involved in cell-wall construction in specific organs of Arabidopsis. *Plant Cell Physiol.* **42**, 1025-1033.
- Yoshida, Y., Aoki, C., Iuchi, S., Nanjo, T., Seki, M., Sekiguchi, F., Yamaguchi-Shinozaki, K., and Shinozaki, K.** (2001). Characterization of four extensin genes in Arabidopsis thaliana by differential gene expression under stress and non-stress conditions. *DNA Res.* **8**, 115-122.
- Zhang, J.Y., Broeckling, C.D., Blancaflor, E.B., Sledge, M.K., Sumner, L.W., and Wang, Z.Y.** (2005). Overexpression of WXP1, a putative Medicago truncatula AP2 domain-containing transcription factor gene, increases cuticular wax accumulation and enhances drought tolerance in transgenic alfalfa (Medicago sativa). *Plant J.* **42**, 689-707.
- Zheng, H.Q., Rowland, O., and Kunst, L.** (2005). Disruptions of the Arabidopsis enoyl-CoA reductase gene reveal an essential role for very-long-chain fatty acid synthesis in cell expansion during plant morphogenesis. *Plant Cell* **17**, 1467-1481.
- Zhou, J.M., and Goldsbrough, P.B.** (1995). Structure, Organization and Expression of the Metallothionein Gene Family in Arabidopsis. *Mol. Gen. Genet.* **248**, 318-328.
- Zimmermann, P., Hirsch-Hoffmann, M., Hennig, L., and Genevestigator, G.W.** (2004). Arabidopsis microarray database and analysis toolbox (vol 136, pg 2621, 2004). *Plant Physiol.* **136**, 4335-4335.

8. Acknowledgments

I would like to thank Prof. Dr. Heinz Saedler for the opportunity to do a PhD in his department.

Thank you to my boss, “Sascha”, Dr. Alexander Yephremov, who supervised my work, taught me a lot about myself, cloning and writing.

Thank you to Prof. Dr. Lukas Schreiber, Dr. Benni Franke and all the “team of Bonn” for fruitful discussion, welcoming me in their lab and sharing their experience.

Thank you to Dr. Andrea Faust who was patient enough with “a forever kid” and with whom we had many laughs...

Thank you to Dr. Jose Reina who introduced me to the protein world and “did all his homework” during the preparation of this manuscript.

Thank you to Isa Will who help me a lot in the lab and taught me about order and clean records... even on tubes ☺.

Thank you to Roxana Teodor who knows about Microsoft Word and words.

I would also like to thank all the colleagues from the Saedler department who were there to lend me a hand... “Microarrays are small but give giant headaches”...

Thank you to Elmon Schmelzer and Rolf Hirtz for help, advice and many friendly “microscope hours”...

Thank you to Dr. Frank Pinot and Vincent Sauveplane for their friendly welcome, help and support...

Thank you to the gardeners who were always game and got the plants to play hide and sick and sometimes got them into fly bellies but, more regularly, took good care about the stars of this work.

Thank you to many other people particularly Marilyne Debieu who explain me all about “buler et phylosopher” (lazing around and “phylosophying”), Gudrun Böhmendorfer an other “Potter” and silence lover, Gaelle Rivory and Alex Kroll for some rich philosophical hours, and... to “three very special people”, who have always been present for me and will recognise themselves.

Well... still not over ☺...

Thank you to Lila Calmettes, Michelle Maruz, Angela Philet, Myfie Weiss, Agnes Tregaro, Aurelie Robert, Florence Hamon and Lydie Pellan...

9. Lebenslauf

Zur Person

Name: Derry (Frederique) Voisin

Geburtsdatum: März 1979

Ausbildung

September 1997-Shulabschluss: Abitur am „St Joseph“ Gymnasium in Loudeac, Frankreich.

Oktober 1997-Juni 1999: Diplôme d'Etudes Universitaires Generales (DEUG) an der „Catholique de l'ouest“ Universität in Guingamp, Frankreich.

Oktober 1999-Juni 2000: Bachelor in Molekular- und Zellbiologie (Schwerpunkt Genetik).an der „Claude Bernard Lyon 1“ Universität in Lyon, Frankreich.

→ **Juli-August 2000:** Industrie Praktikum bei Labofarm (Loudeac, Frankreich)

September 2000-Oktober 2003: Diplom- Biotechnologie an der „Ecole Supérieure de Biotechnologie de Strasbourg (ESBS)“ (Tri-Nationaler Studiengang) in Straßburg, Frankreich.

→ **Juli- August 2001:** Praktikum an der Albert-Ludwigs-Universität in Freiburg, Deutschland. Betreuer: Prof. C. Beck.

Auslandsstipendium vom DFJW (0904)

→ **Januar- September 2003:** Diplomarbeit am John Innes Center, U.K. Betreuer: Dr. David Rengel, Prof. Cathie Martin
Projekt: „Plastid and Cell differentiation in Arabidopsis thaliana: the DAG family“

Stipendium vom Conseil Régional D'Alsace (DO 305322).

September 2002-October 2003: Abschluss in Molekular-und Zellbiologie an der Louis Pasteur Universität in Straßburg, Frankreich.

Seit November 2003: Doktorarbeit in der Abteilung Molekulare Pflanzengenetik, Max-Planck-Institut für Züchtungsforschung in Köln, Deutschland.

Arbeitsgruppe: Dr. Alexander Yephremov

Betreuer: Prof. Heinz Saedler.

Stipendium: Marie Curie Early Stage Researcher Training.

Projekt: „ Biochemical and genetic responses in cuticular mutants“

10. Eidesstattliche Erklärung

Eidesstattliche Erklärung

Köln, 2007

Hiermit versichere ich, daß die von mir vorgelegte Dissertation selbständig angefertigt, die benutzten Quellen und Hilfsmittel vollständig angegeben und die Stellen der Arbeit- einschließlich Tabellen, Karten und Abbildungen-, die anderen Werken im Wortlaut oder dem Sinn nach entnommen sind, in jedem Einzelfall als Entlehnung kenntlich gemacht habe; daß diese Dissertation noch keiner anderen Fakultät oder Universität zur Prüfung vorgelegen hat; daß sie – abgesehen von unten angegebenen Teilpublikationen – noch nicht veröffentlicht worden ist sowie, daß ich eine solche Veröffentlichung vor Abschluß des Promotionsverfahrens nicht vornehmen werde.

Die Bestimmungen dieser Promotionsordnung sind mir bekannt. Die von mir vorgelegte Dissertation ist von Dr. Alexander Yephremov und Prof. Dr. Heinz Saedler betreut worden.